Cooperative Relaying and Resource Allocation in Future-Generation Cellular Networks

by

Xiaoxia Zhang

A thesis

presented to the University of Waterloo

in fulfillment of the

thesis requirement for the degree of

Doctor of Philosophy

in

Electrical and Computer Engineering

Waterloo, Ontario, Canada, 2015

Author's Declaration

I hereby declare that I am the sole author of this thesis. This is a true copy of the thesis, including any required final revisions, as accepted by my examiners.

I understand that my thesis may be made electronically available to the public.

Abstract

Driven by the significant consumer demand for reliable and high data rate communications, the future-generation cellular systems are expected to employ cutting-edge techniques to improve the service provisioning at substantially reduced costs. Cooperative relaying is one of the primary techniques due to its ability to improve the spectrum utilization by taking advantage of the broadcast nature of wireless signals. This dissertation studies the physical layer cooperative relaying technique and resource allocation schemes in the cooperative cellular networks to improve the spectrum and energy efficiency from the perspectives of downlink transmission, uplink transmission and device-to-device transmission, respectively.

For the downlink transmission, we consider an LTE-Advanced cooperative cellular network with the deployment of Type II in-band decode-and-forward relay stations (RSs) to enhance the cell-edge throughput and to extend the coverage area. This type of relays can better exploit the broadcast nature of wireless signals while improving the utilization of existing allocated spectral resources. For such a network, we propose joint orthogonal frequency division multiplexing (OFDM) subcarrier and power allocation schemes to optimize the downlink multi-user transmission efficiency. Firstly, an optimal power dividing method between eNB and RS is proposed to maximize the achievable rate on each subcarrier. Based on this result, we show that the optimal joint resource allocation scheme for maximizing the overall throughput is to allocate each subcarrier to the user with the best channel quality and to distribute power in a water-filling manner. Since the users' Quality of Service (QoS) provision is one of the major design objectives in cellular networks, we further formulate a lexicographical optimization problem to maximize the minimum rate of all users while improving the overall throughput. A sufficient condition for optimality is derived. Due to the complexity of searching for the optimal solution, we then propose an efficient, low-complexity suboptimal joint resource allocation algorithm, which

outperforms the existing suboptimal algorithms that simplify the joint design into separate allocation. Both theoretical and numerical analyses demonstrate that our proposed scheme can drastically improve the fairness as well as the overall throughput.

As the physical layer uplink transmission technology for LTE-Advanced cellular network is based on single carrier frequency division multiple access (SC-FDMA) with frequency domain equalization (FDE), this dissertation further studies the uplink achievable rate and power allocation to improve the uplink spectrum efficiency in the cellular network. Different from the downlink OFDM system, signals on all subcarriers in the SC-FDMA system are transmitted sequentially rather than in parallel, thus the user's achievable rate is not simply the summation of the rates on all allocated subcarriers. Moreover, each user equipment (UE) has its own transmission power constraint instead of a total power constraint at the base station in the downlink case. Therefore, the uplink resource allocation problem in the LTE-Advanced system is more challenging. To this end, we first derive the achievable rates of the SC-FDMA system with two commonly-used FDE techniques, zero-forcing (ZF) equalization and minimum mean square error (MMSE) equalization, based on the joint superposition coding for cooperative relaying. We then propose optimal power allocation schemes among subcarriers at both UE and RS to maximize the overall throughput of the system. Theoretical analysis and numerical results are provided to demonstrate a significant gain in the system throughput by our proposed power allocation schemes.

Besides the physical layer technology, the trend of improving energy efficiency in future cellular networks also motivates the network operators to continuously bring improvements in the entire network infrastructure. Such techniques include efficient base station (BS) redesign, opportunistic transmission such as device-to-device and cognitive radio communications. In the third part of this dissertation, we explore the potentials of employing cooperative relaying in a green device-to-device communication underlaying cellular net-

work to improve the energy efficiency and spectrum utilization of the system. As the green base station is powered by sustainable energy, the design objective is to enhance both sustainability and efficiency of the device-to-device communication. Specifically, we first propose optimal power adaptation schemes to maximize the network spectrum efficiency under two practical power constraints. We then take the dynamics of the charging and discharging processes of the energy buffer at the BS into consideration to ensure the network sustainability. To this end, the energy buffer is modeled as a G/D/1 queue where the input energy has a general distribution. Power allocation schemes are proposed based on the statistics of the energy buffer to further enhance the network efficiency and sustainability. Theoretical analysis and numerical results are presented to demonstrate that our proposed power allocation schemes can improve the network throughput while maintaining the network sustainability at a certain level.

Our analyses developed in this dissertation indicate that the cooperative transmission based on cooperative relaying can significantly improve the spectrum efficiency and energy efficiency of the cellular network for downlink transmission, uplink transmission and device-to-device communication. Our proposed cooperative relaying technique and resource allocation schemes can provide efficient solutions to practical design and optimization of future-generation cellular networks.

Acknowledgements

Most importantly, I would like to express my deep gratitude to my two supervisors: Dr. Xuemin (Sherman) Shen and Dr. Liang-Liang Xie, for their generous and insightful guidance, unconditional support and encouragement during my graduate studies at the University of Waterloo and throughout the complement of every detail in this thesis. They are not only advisors, but also role models of professionalism, integrity, respect and responsibility. I would like to thank them sincerely for everything I have achieved.

I would also like to thank Dr. Sagar Naik, Dr. Otman Basir and Dr. Grace Y. Yi, for serving on my dissertation committee and providing helpful suggestions to further improve the quality of this dissertation. A special appreciation goes to Dr. Alagan Anpalagan from Ryerson University for serving as an external examiner.

I am also grateful to Dr. Xiugang Wu, Dr. Xinsheng Zhou and all members in the Broadband Communications Research (BBCR) group. Especially, I wish to thank Dr. Rongxing Lu, Dr. Lin, X. Cai, Dr. Hao Liang, Dr. Tom Luan, Dr. Yongkang Liu, Dr. Zhongming Zhang, Dr. Qinghua Shen, Dr. Ning Zhang, Dr. Jian Qiao, Dr. Md. Shamsul Alam, Dr. Miao Wang, Dr. Amila P. K. Tharaperiya Gamage, Dr. Ning Lu, Kuan Zhang, Nan Cheng, Yong Zhou, Nan Chen, Jianbin Ni, Ran Zhang, Asmaa Abdallah, Qiang Ye, Chong Lou, Dr. Khadige Abboud, Yujie Tang, Sailesh Bharati, Miao He, and many others for all the valuable discussions and warm friendship.

Finally, I would like to thank my husband and my parents for their endless and unconditional love. Without their support, encouragement and understanding, it would be impossible to complete my graduate studies at the University of Waterloo.

Dedication

To my son, Terence.

Table of Contents

List of Tables

List of Figures

List of Abbreviations

3G Third Generation

3GPP Third Generation Partnership Project

AF Amplify-and-Forward

AWGN Additive White Gaussian Noise

BS Base Station

CDF Cumulative Distribution Function

CF Compress-and-Forward

CoMP Coordinated Multipoint

CP Cyclic Prefix

CSI Channel State Information

D2D Device-to-Device

DF Decode-and-Forward

DFT Discrete Fourier Transform

DL Downlink

eNB eNodeB

FDE Frequency Domain Equalization

IB In-Band

IDFT Inverse Discrete Fourier Transform

IMT-A International Mobile Telecommunications-Advanced

ISI Intersymbol Interference

KKT Kuhn-Tucker

LTE Long-Term Evolution

MAC Multiple Access Channel

MMSE Minimum Mean Square Error

MS Mobile Station

OFDM Orthogonal Frequency Division Multiplexing

OFDMA Orthogonal Frequency Division Multiple Access

OOB Out-of-Band

PAPR Peak-to-Average Power Ratio

QoS Quality of Service

RAN Radio Access Network

RS Relay Station

SC-FDMA Single Carrier Frequency Division Multiple Access

SNR Signal-to-Noise Ratio

UE User Equipment

UL Uplink

WLAN Wireless Local Area Networks

ZF Zero Forcing

Chapter 1

Introduction

The past several decades have witnessed enormous evolutions of communication systems, especially wireless communications. Due to the emerging technologies and improving QoS requirement, future-generation wireless communication systems are expected to meet even more challenging demands of high data rate and reliable multimedia communications. Thus, to develop a cost-effective network, employing state-of-the-art technical advances provides a practical yet efficient way to improve the network performance and QoS provisioning. In this chapter, an overview of next-generation cellular networks and some key innovative technologies are provided.

1.1 Future-Generation Cellular Systems

Third-generation (3G) wireless systems have now been deployed on a broad scale all over the world to provide high-speed downlink (DL) transmission and enhanced uplink (UL) transmission. However, user and operator requirements and expectations are continuously

evolving which forces the Third Generation Partnership Project (3GPP) to propose new air interface in order to ensure 3G's competitiveness in a long term. As a consequence, 3GPP has launched the Long-Term Evolution (LTE) standard of 3G for wireless high-speed data communication for mobile phones and data terminals at substantially reduced cost compared with current radio access technologies [1–3]. The primary goal of LTE is to increase the capacity and speed of wireless data networks using new digital signal processing (DSP) techniques and modulations.

Some of the targets and requirements for LTE standard include [4]:

- Peak data rates up to 100 Mbps for the downlink and 50 Mbps for the uplink.
- Average user throughput improved by factors 2 and 3 for uplink and downlink, respectively.
- Cell-edge user throughput improved by a factor 2 for uplink and downlink.
- Improved spectrum efficiency, targeting and improvement on the order of a factor of 3.
- Significantly reduced control and user plane latency.
- Reduced cost for operators and end users.
- Spectrum flexibility, enabling deployment in many different spectrum allocations.

In order to meet the above requirements, LTE Release 8 specifies that orthogonal frequency division multiplexing (OFDM) is the DL transmission scheme, and single-carrier frequency division multiple access (SC-FDMA) is the UL multiple access scheme. Besides, flexible bandwidth up to 20 MHz for each subchannel is allowed and a 15 kHz separation between two subcarriers should be guaranteed.

Currently, further enhancements are being studied to provide even more improvements to LTE Release 8 to meet or exceed the International Mobile Telecommunications-Advanced (IMT-A) requirements. These requirements facilitate future IMT-A systems to support peak data rates of 100 Mb/s and 1 Gb/s, respectively, in high-speed mobility environments (up to 350 km/h) and stationary and pedestrian environments (up to 10 km/h). The transmission bandwidth of IMT-A systems should be scalable and can change from 20 to 100 MHz, with downlink and uplink spectrum efficiencies in the ranges of [1.1, 15 b/s/Hz] and [0.7, 6.75 b/s/Hz], respectively.

To address the requirements and challenges of IMT-Advanced systems, 3GPP started its LTE-Advanced (also known as LTE Release 10) standardization process in 2009 as a major improvement of the LTE standard. LTE-Advanced targets at enhancing the existing LTE Release 8 standard and supporting much higher peak rates, higher throughput and coverage, and lower latencies, resulting in a better user experience. LTE-Advanced networks consider a series of new transmission technologies including carrier aggregation, advanced uplink and downlink spatial multiplexing, DL coordinated multipoint (CoMP) transmission, and heterogeneous networks with special emphasis on Type I and Type II relays [5–7].

1.2 Relays in 3GPP LTE-Advanced Systems

Cell edge performance is becoming increasingly important in future-generation cellular networks as cellular systems are provisioned to achieve almost-ubiquitous very high data rate coverage [8]. To this end, the deployment of relays is expected to be a cost-effective solution to extend the signal and service coverage and to enhance the overall throughput performance [9–12].

An LTE-Advanced relay is a device that can replicate signals and forward traffic between its two wireless interfaces under the LTE-Advanced air interface specification. In each macrocell, one or several relay stations (RSs) are deployed to help forward user information between neighboring user equipment (UE)/mobile station (MS) and the local evolutional NodeB (eNB)/base station (BS). The advantages of introducing relays in LTE-Advanced systems include:

- Achieving higher network throughput

  Cooperative communication with the help of relays can significantly improve the network throughput by taking advantage of the broadcast nature of wireless channels. The cooperative diversity can be achieved through sending multiple copies of a message. At the destination, instead of treating these signals as interference, the destination can combine and jointly decode the signals to achieve the diversity gain.

- Improving network reliability

  In the wireless environment, all signals suffer from attenuation and fading. In the traditional point-to-point cellular network, if the fading channel is severely degraded or blocked, the receiver is not able to decode the transmitted information, therefore continuous communication cannot be guaranteed. By transmitting various fading versions of a message, cooperative communication is an effective method to combat deep fading and make the network more reliable.

- Achieving larger coverage

  In the conventional centralized cellular network, the wireless coverage area of a base station is usually fixed due to the limitation of the available transmitting power at the base station. However, with cooperative relaying, a UE that is out of the traditional coverage area can thus be reached by means of multi-hoping.

- More efficient usage of energy resources

  In the wireless environment, signal strength attenuates with transmission distance. If the destination is relatively far away from the source, high transmitting power is required at the source for reliable transmission, which is difficult to realize in practical networks. With several intermediate nodes cooperating to transmit the message, a long-distance transmission breaks down to several shorter-range transmissions. Therefore, the energy resources can be utilized more efficiently, especially for the communications between spatially dispersed nodes.

There two types of relays being discussed in the context of 3GPP standards, Type I and Type II relays. A Type I relay creates its own physical cell and will be distinct from the primary base station cell. The UEs within the relay's cell range would receive and send reference signal and control messages directly from and to the relay. Therefore, the relay station appears as a Release 8 eNB to all UEs in its range. Typically, a Type I relay is employed to help a remote UE, which is located far away from an eNB, to access the eNB. Type I RSs mainly perform IP packet forwarding in the network layer (layer 3), and its main objective is to extend signal and service coverage. Type I relays are half-duplex, and are unable to transmit to the UEs and receive from the donor eNB simultaneously.

On the other hand, a Type II relay is a full-duplex relay which does not create a new cell. Type II RSs can help a local UE, which is located within the coverage of an eNB and has a direct communication link with the eNB, to improve its service quality and link capacity. So a Type II RS does not transmit the common reference signal or the control information, and it is transparent to all UEs within its coverage area and the UEs are not aware of its existence. Its main objective is to increase the overall system capacity by achieving multipath diversity and transmission gains for local UEs. With spatial separation, filtering, or enhanced interference cancellation, the full-duplex relays

require no specific resource partitioning [13].

The relays are connected to the radio access network (RAN) via a donor macrocell. Two types of backhaul connections are supported in LTE-Advanced: in-band (IB), where the eNB-relay link shares the same frequency bands with the direct eNB-UE transmission links within a cell, and out-of-band (OOB), where the eNB-relay link does not transmit in the same eNB-UE frequency bands.

In this dissertation, we focus on the in-band Type II relays since this type of relays can achieve cooperative transmission by exploiting the broadcast nature of wireless signals and improve the utilization of the existing allocated spectral resources.

1.2.1 Cooperative Relaying and Multi-hop Relaying

The benefits of cooperative communications with the help of relays have led to extensive research on relaying and forwarding. On whether the intermediate RSs cooperatively transmit with the source or not, two relaying schemes exist, i.e., cooperative relaying and multi-hop relaying.

Multi-hop relaying has originally been studied in the context of wireless ad hoc networks as a method to enable the network operation without the need of installing any fixed infrastructure. In recent years, the application of multi-hop transmission in centralized networks such as cellular networks and wireless local area networks (WLAN) has also drawn an upsurge of interest. A multi-hop transmission means that the communication between the source and the destination is carried out in multiple hops. At each hop, the RS receives the message from the immediate preceding node and broadcasts it to the downstream nodes within its transmission range. In this way, the destination can be found and the message can be forwarded successfully.

Multi-hop relaying has the same feature of cooperative relaying in the sense that they both break down a long-range transmission into several shorter-range transmissions by intermediate nodes functioning as relays. However, multi-hop relaying has fundamental differences from cooperative relaying.

In wireless environment, the destination node is capable of hearing all signals from the source and the relay nodes. For multi-hop relaying, the destination will only decode the signal from its immediate preceding node and treat all other signals as interference. To avoid the throughput decrease caused by high interference, in practical networks, extra radio bands or extra time periods are often required for intermediate nodes, which will cause more resource usage.

Essentially, all these signals carry the same information. A cooperative relay channel corresponds to the case where each intermediate relay node reconstructs and forwards the message based on signals received from all preceding nodes. It is obvious that the cooperative relaying can achieve higher spatial diversity compared with multi-hop relaying, because the former exploits the broadcast nature of wireless networks and utilizes the signals from all previous terminals.

1.2.2 Cooperative Protocols

The cooperative protocols can be categorized into three general classes: Amplify-and-Forward (AF), Decode-and-Forward (DF) and Compress-and-Forward (CF).

- Amplify-and-Forward (AF)

  AF relays simply amplify the received signals and transmits to the next hop. Besides the desired signal, it also amplifies and propagates the interference and noise from

the source-relay link. As the relay does not decode the message, the transmitted signal would cause interference to its own receiver as well. Therefore, extra resources such as frequency bands or time slots are needed at the AF relay for orthogonal transmission. The advantages of the AF relays include that AF relays have low costs and they are easier to implement.

- Decode-and-Forward (DF)

  If the relay node has the decoding capability, the received signal would first be decoded, then the relay node re-encodes and transmits to the next hop. With the DF protocol, noise can be completely eliminated, so the source and the relay are able to transmit in the same frequency band (channel) to improve the spectral efficiency. However, the coding/decoding processes for cooperation are usually needed which would increase the implementation cost.

- Compress-and-Forward (CF)

  The CF relays compress the received signal and transmit the compressed version to the next hop. Since the noise and interference from the previous hop cannot be avoided, CF is sometimes categorized with the AF strategy. The CF scheme is especially suitable for the situation where the channel between the source and the relay is worse than that between the source and the destination.

Unfortunately, there is no strategy that is always superior to others. Whether AF or DF can achieve higher rate depends on many factors including the network topology, the channel conditions, etc.

1.3 Motivation, Objectives and Contributions

Due to the ever growing user and operator requirement, improving the spectrum efficiency has always been a fundamental issue in cellular networks. Resource allocation is an efficient and effective method to improve the users' QoS by overcoming the limited availability of frequency spectrum, the total transmission power and the fading nature of the wireless channels. Traditionally, resource allocation has been studied broadly in various wireless networks to improve the utilization of existing allocated resources. However, considering the physical layer techniques and the unique features of cooperative relaying, resource allocation in future-generation cellular networks faces new challenges.

- Instead of simply amplifying and forwarding the received signal as a repeater, relays are expected to have more coding capability to achieve higher data rates in cellular networks. The resource scheduler in future-generation cellular networks with the deployment of relay stations needs to take into account the cooperative coding of the relay channel and redesign the resource allocation schemes accordingly.

- For broadband cellular network, the wireless channel encounters frequency-selective multipath fading, which leads to severe intersymbol interference (ISI) both in time and frequency impacting the service quality and data rates. To solve this issue, OFDM and SC-FDMA have been specified as the physical layer techniques to combat the ISI in LTE networks for downlink and uplink transmissions, respectively. OFDM and SC-FDMA are multicarrier transmission schemes where the broadband channel is divided into N narrowband orthogonal subchannels each operating at different subcarriers. The subcarriers can be dynamically allocated to users to exploit both multi-user diversity and frequency diversity at a finer granularity. Thus, subcarrier allocation has to be jointly considered with traditional power allocation to improve

the spectrum efficiency in the new context.

- Future-generation cellular networks envision ubiquitous mobile broadband access among all subscribed users. However, due to the attenuation of the received signal strength and the increase of interference from other eNBs or UEs, low signal-to-noise-ratio (SNR) at cell edge is expected. As a consequence, the QoS experienced by users at the cell edge could be severely degraded. Therefore, user fairness is also a significant performance metric for mobile users, besides the throughput improvement, for the resource allocation schemes.

- As several state-of-the-art physical layer technologies are employed in cellular networks to improve the spectrum efficiency, the resource allocation designed for one system cannot be applied directly to other systems since power and subcarrier requirements are usually different. For example, downlink OFDM system has a total power constraint and subcarriers can be dynamically assigned among users; however, uplink SC-FDMA system has individual power constraint and adjacent subcarrier requirement. As a result, the resource allocation schemes need to be adaptively designed to meet the specific requirements in different systems.

These fundamental challenges pose great difficulties for future-generation cellular network designers, and thus motivate us to propose new resource allocation schemes. Therefore, the objective of this dissertation is to incorporate the physical layer cooperative relaying technique in the cellular network and design separate resource allocation to improve the spectrum and energy efficiency.

The first part of this dissertation studies the adaptive joint subcarrier and power allocation for downlink LTE-Advanced relay systems. We focus on the in-band Type II full-duplex relay stations with decode-and-forward strategy, since this type of relays can

better exploit the broadcast nature of wireless signals while improving the utilization of existing allocated spectral resources. As OFDM divides the frequency band into orthogonal narrowband subchannels operating on different subcarriers, each subchannel can be viewed as a conventional relay channel where the eNB and the RS cooperate to transmit to the UE (destination). We first investigate the power allocation on each subcarrier and propose optimal power dividing schemes between the eNB and RS to maximize the relay channel's achievable rate. With the optimal power dividing schemes on each subcarrier, we then jointly allocate subcarrier and power in the multi-user OFDM network. In LTE-Advanced cellular networks, as the eNB needs to perform resource allocation in a rapidly changing environment, efficient joint resource allocation schemes with low computational cost are preferred, especially for cost-effective and delay-sensitive implementations. In this part, we first come up with an optimal joint subchannel and power allocation scheme to maximize the overall throughput. Then, user fairness is taken into consideration. A lexicographical optimization problem is formulated to guarantee the max-min fairness while improving the transmission efficiency and a sufficient condition of the optimal solution is provided. Due to the complexity of finding the optimal solution, we propose an efficient two-step joint resource allocation suboptimal algorithm with low computational complexity.

The main contributions of the first part of the dissertation are three-fold:

- The optimal power dividing schemes between the eNB and the RS can increase the transmission rate on each subcarrier. With this scheme, the cooperation between the eNB and the RS can be maximized to improve the transmission efficiency.
- In the multi-user OFDM networks, improving the fairness among users is usually at the expense of the reduced overall throughput. To tackle this issue, we formulate a novel lexicographical optimization problem where throughput will be optimized when maximum fairness is guaranteed.

- Due to the complexity of the optimal resource allocation, an efficient suboptimal joint allocation algorithm with low computational complexity is proposed. Compared with most two-step procedures, our suboptimal algorithm can effectively improve the minimum rate of all users as well as the average user rate.

The second part investigates the fundamental achievable rate and power allocation for the uplink communications in the LTE-Advanced network with the deployment of in-band decode-and-forward Type II full-duplex relay stations. The in-band relay allocates the same set of frequency subcarriers for cooperative transmission with each UE. Upon receiving a signal from UE, the relay first decodes it to eliminate the noise, then retransmits to the eNB in its own codes. With joint superposition coding at the source and the relay, higher rate can be achieved by improving the utilization of existing allocated spectral resources. The main contributions of this part include:

- Since SC-FDMA signals are no longer transmitted in parallel in the time domain, we revisit the joint superposition encoding and decoding processes for DF cooperative relaying in the frequency domain.

- We design ZF and MMSE equalizers at both RS and eNB taking into account the cooperative relay channels. Based on the proposed equalizers, the expressions of the achievable rate in the SC-FDMA relay system are derived.

- We propose optimal power allocation schemes among subcarriers at both UE and RS to maximize the overall throughput of the system.

In the third part, we consider a green device-to-device communication underlaying cellular network where the eNB is powered by sustainable energy. We aim at further improving the cellular network's throughput by exploiting the potential benefits of D2D and

cooperative relaying with green energy, while maintaining the network sustainability and guaranteeing users' QoS requirement. Cooperative communication is utilized to improve the transmission efficiency, and the eNB helps the D2D communication by relaying the source's signal to the destination. The cooperative eNB adopts the decode-and-forward protocol and transmits in the same channel with the source. We focus on designing efficient power allocation schemes and make the following contributions:

- Both green energy and wireless communication technologies are considered to provide an efficient transmission regime in a device-to-device communication underlaying cellular network, where a BS powered by sustainable energy is deployed in the network. To improve the network throughput, the green BS is equipped with cooperation devices to assist the communication between the source and the destination.

- We propose power allocation schemes to maximize the overall throughput under two practical types of power constraints depending on whether users are able to adjust their transmission power. Our proposed schemes can effectively improve the network throughput while ensuring that the energy harvested from the environment can sustain the wireless communication without any node outage.

- An analytical framework to model the dynamics of the green energy charging and discharging processes is presented. The energy buffer can be approximated as a G/D/1 queue where the energy charging process has a general distribution. The distribution of the buffer storage is derived which shed some light on the green network designs.

1.4 Outline

The remainder of this dissertation is organized in the following manner. Chapter 2 provides some background on the physical layer transmission and relaying techniques, as well as literature survey on resource allocation in the cellular networks. Downlink joint subcarrier and power allocation in LTE-Advanced relay network is presented in Chapter 3 and uplink achievable rate and resource allocation is presented in Chapter 4. Chapter 5 investigates the power allocation to maximize the sustainability and efficiency in green cellular networks. Finally, in Chapter 6, we provide some concluding remarks and future work.

Chapter 2

Background and Literature Review

This chapter first introduces the OFDM and SC-FDMA techniques for downlink and uplink transmissions, respectively. Then the capacity of single-user relay channel model is presented. After that, an overview and comparison of existing resource allocation schemes are provided.

2.1 Physical Layer Transmission Techniques in LTE Networks

To improve the spectrum efficiency and transmission rate, the physical layer techniques for LTE and LTE-A include OFDM as the downlink transmission scheme and SC-FDMA as the uplink multiple access scheme [14].

2.1.1 OFDM

In broadband applications, the wireless channel encounters frequency-selective multipath fading. The transmitted signal is scattered, diffracted and reflected, and reaches the antenna as an incoherent superposition of many signals each as a poorly synchronized echo component of the desired signal. This phenomenon leads to severe intersymbol interference (ISI) both in time and frequency impacting the service quality and data rates. To combat ISI, OFDM is an effective solution to realize a high performance physical layer and thus has been widely adopted by various wireless standards.

OFDM is based on the concept of multicarrier transmission. The idea is to divide the broadband channel into N narrowband subchannels each with a bandwidth much smaller than the coherence bandwidth of the channel. The high rate data stream is then split into N substreams of lower rate data which are modulated into N OFDM symbols and transmitted simultaneously on N orthogonal subcarriers. The low bandwidth of the subchannels along with the frequency spacing between them are necessary to have flat fading orthogonal subcarriers with approximately constant channel gain during each transmission block.

In particular, the transmitter and receiver structure of OFDM system is shown in Fig. 2.1. The sequence of N modulated symbols, $x_0, x_1, \ldots, x_{N-1}$, are converted into N parallel streams before takeing the N-point inverse discrete Fourier transform (IDFT). Then, the signals are converted into a serial stream before inserting the Cyclic Prefix (CP). Finally, the sequence is sent over the wireless channel. The OFDM demodulation reverses the above process. After converting the received signal back into the digital form, the CP is removed. Then the sequence is converted into a parallel of N data streams before performing the N-point discrete Fourier transform (DFT). At last, the sequence is transformed back to a serial stream.

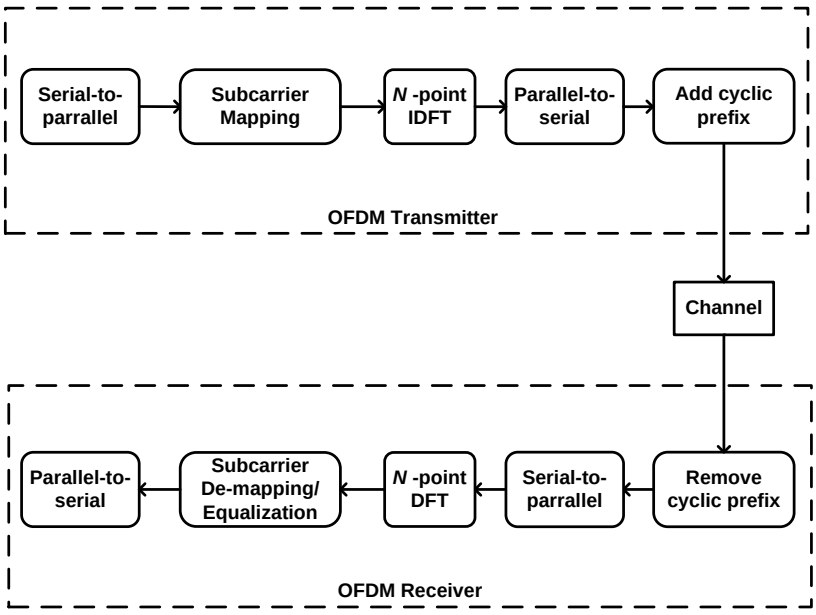

Figure 2.1: Transmitter and receiver structure in OFDM systems.

In this architecture, CP is simply a repetition of the last part of the preceding OFDM symbol, where the length of the CP exceed the channel delay spread. Therefore, ISI can be avoided by inserting the guard period between successive OFDM symbols.

2.1.2 SC-FDMA

Although OFDM can substantially reduce the intersymbol interference (ISI) and increase the data rate, a principal weakness is the high peak-to-average power ratio (PAPR), which would impose a heavy burden on the power amplifier of the transmitter, especially for the mobile terminals [15]. As a result, SC-FDMA is proposed as the uplink transmission technique to reduce the PAPR and make the mobile terminals more power-efficient. SC-FDMA can be viewed as a DFT precoded OFDMA, which is the multi-user version of

OFDM. SC-FDMA can achieve similar throughput performance and overall complexity with OFDMA, yet reduce the PAPR and transmitter cost due to its inherent single carrier nature. Unlike OFDMA, both transmission and detection of the signals are carried out in the time domain rather than in the frequency domain.

The block diagram of the general SC-FDMA transmitter and receiver structure is shown in Fig. 2.2. The sequence of the time-domain signals for transmission at user i is firstly transformed into frequency domain by the N_i-point DFT, then the sequence goes through the OFDMA processing. The decision is carried out in the time domain at the receiver after the N_i-point IDFT transforming the frequency-domain sequence into time domain.

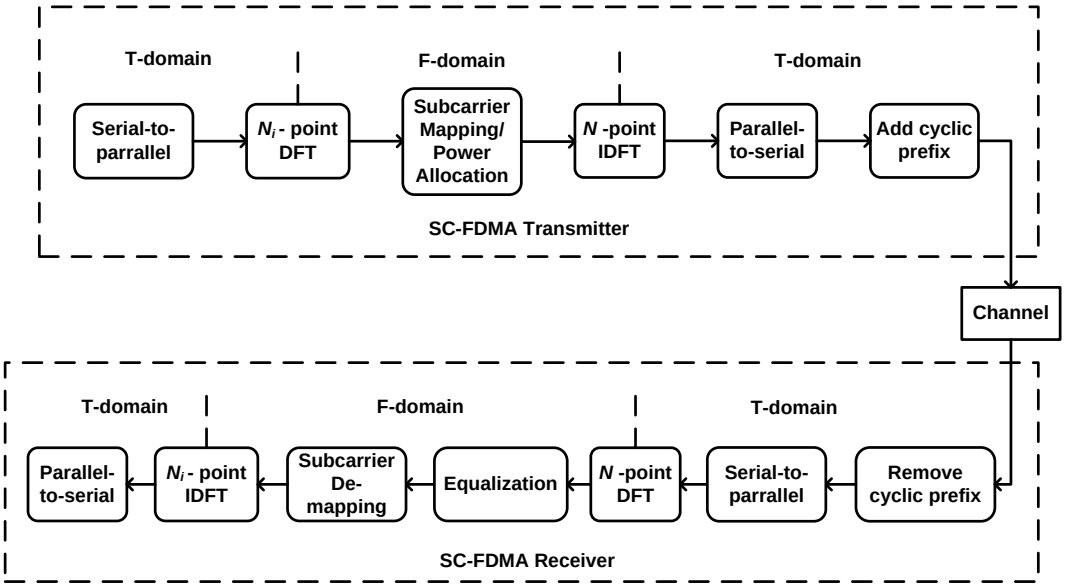

Figure 2.2: Transmitter and receiver structure in SC-FDMA systems.

2.2 Single-User Relay Channel

In this section, we review the relay channel model, which exploits the signal from the source node rather that simply treating it as interference, from an information theoretic perspective. The simplest discrete memoryless three-terminal relay channel is depicted in Fig. 2.3. In this channel, the source node $\boldsymbol{s}$ intends to send information to the destination node $\boldsymbol{d}$, which might be at a great distance from node $\boldsymbol{s}$ in many situations. The channel might suffer from severe attenuation such that any direct reliable communication at a high data rate is impossible. In this case, an intermediate relay node $\boldsymbol{r}$ can be deployed to relay the information from the source to the destination. With the help of the relay node, a single-hop and long-distance transmission can be replaced by a two-hop and shorter-range transmission. The presence of the intermediate node can significantly enhance the transmission performance by the two-phase communication: i) node $\boldsymbol{s}$ transmits to node $\boldsymbol{r}$, ii) node $\boldsymbol{r}$ transmits to the destination $\boldsymbol{d}$ along with node $\boldsymbol{s}$.

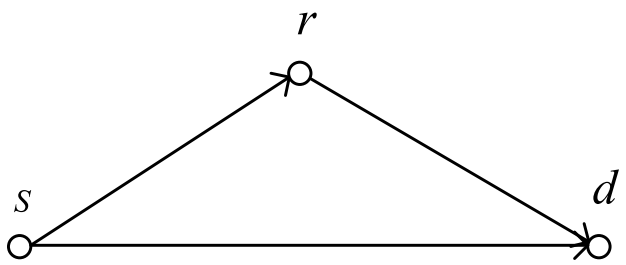

Figure 2.3: A single-user relay channel model.

The three-terminal relay channel was first proposed in [16], [17]. Two fundamental coding strategies for the relay are developed in [18]: decode-and-forward and amplify-and-forward. The difference between these two strategies relies on whether the relay node is able to decode or not. Unfortunately, whether one strategy is superior than the other depends on the network topology, channel conditions, etc. [19], [20]. In this dissertation,

we consider the scenario where the relay employs decode-and-forward strategy since in this case, the relay does not propagate the noise from the source-relay transmission.

The discrete memoryless relay channel with decode-and-forward strategy is modeled as

$$(\mathcal{X}_s \times \mathcal{X}_r,\ p(y_r, y_d|x_s, x_r),\ \mathcal{Y}_r \times \mathcal{Y}_d), \tag{2.1}$$

where x_s, y_d, y_r and x_r denote the input to the channel, the output of the channel, the observation by the relay and the input symbol chosen by the relay, respectively. $p(y_r, y_d|x_s, x_r)$ is the probability distribution on $\mathcal{Y}_r \times \mathcal{Y}_d$ for each (x_s, x_r).

The transmission block of a message W involves T transmission units. For $t = 1, 2, \ldots, T$, the source node sends $x_s(t) \in \mathcal{X}_s$ and the relay node sends $x_r(t) \in \mathcal{X}_r$. At the meantime, the relay receives $y_r(t) \in \mathcal{Y}_r$ and the destination receives $y_d(t) \in \mathcal{Y}_d$. Upon receiving signals from the source, the relay first decodes the message, then re-encodes and transmits it in the subsequent transmission block.

2.2.1 Upper and Lower Bounds on Channel Capacity

From the max-flow min-cut theorem [18, 21], the capacity C of any relay channel $(\mathcal{X}_s \times \mathcal{X}_r,\ p(y_r, y_d|x_s, x_r),\ \mathcal{Y}_r \times \mathcal{Y}_d)$ is bounded above by

$$C \leq \sup_{p(x_s, x_r)} \min\{I(X_s; Y_r, Y_d|X_r), I(X_s, X_r; Y_d)\}. \tag{2.2}$$

The first term in (2.2) upper bounds the rate for transmission from $\boldsymbol{s}$ to $\boldsymbol{r}$ and $\boldsymbol{d}$. The second term is the maximum information transferred from the two senders $\boldsymbol{s}$ and $\boldsymbol{r}$ to receiver $\boldsymbol{d}$.

When the relay node decodes and re-encodes the message, the following maximum achievable rate has been proved:

$$R = \max_{p(x_s, x_r)} \min\{I(X_s; Y_r|X_r), I(X_s, X_r; Y_d)\}, \tag{2.3}$$

where $I(X_s; Y_r|X_r)$ is the rate that the relay is able to decode (relay decoding rate), and $I(X_s, X_r; Y_d)$ is the rate that the destination can successfully decode the message (destination decoding rate).

If the relay receiver is better than the ultimate destination receiver in the sense that

$$p(y_r, y_d|x_s, x_r) = p(y_r|x_s, x_r)p(y_d|y_r, x_r), \tag{2.4}$$

the relay channel is physically degraded and the achievable rate in (2.3) is the capacity of the physically degraded relay channel.

2.2.2 Achievable Rate in the AWGN Environment

In this dissertation, we consider that all wireless channels are independent additive white Gaussian noise (AWGN) channels. Each transmission link is corrupted by a multiplicative fading gain coefficient in addition to an additive white Gaussian noise. The channel gain coefficients of the source-relay channel, the relay-destination channel and the source-destination channel are denoted by h_{sr}, h_{rd} and h_{sd} respectively. h_{sr}, h_{rd} and h_{sd} are independent complex random variables and the fading processes $h_{sr}(t)$, $h_{rd}(t)$ and $h_{sd}(t)$ are stationary and ergodic over time, where t is the time index. Assume the channel gain coefficients remain unchanged during each transmission unit.

Also, we assume that both the source and the relay have a maximum transmission power limitation. The transmitting power at the source node is bounded by

$$\frac{1}{S}\sum_{t=1}^{S} x_s^2(t) \leq P_s, \tag{2.5}$$

and the transmitting power constraint at the relay node is

$$\frac{1}{S}\sum_{t=1}^{S} x_r^2(t) \leq P_r. \tag{2.6}$$

We consider the full-duplex mode where the relays are able to receive and transmit simultaneously. With the DF strategy, the relay node first decodes the received signal, then transmits it along with the source in the subsequent time block. The received signals at the relay and at the destination are given by, respectively,

$$y_r(t) = h_{sr}x_s(t) + z_r(t), \tag{2.7}$$

and

$$y_d(t) = h_{sd}x_s(t) + h_{rd}x_r(t) + z_d(t), \tag{2.8}$$

where $z_r(t)$ and $z_d(t)$ are independent zero-mean Gaussian noises received at the relay node $\boldsymbol{r}$ and at the destination node $\boldsymbol{d}$ with variances both normalized to 1.

We consider consecutive transmissions including B blocks in total. At each transmission block, a message, w_b, $b = 1, \ldots, B$, is to be sent into the relay channel. The joint superposition encoding process for the relay channel at transmission block b consists of the generation of two independent code words: one code $\vec{x_0}$ containing the current block's message w_b and the other code $\vec{x_1}$ representing the previous block's message w_{b-1}. During the transmission block b, the relay node $\boldsymbol{r}$ only sends $\vec{x_1}$ containing message w_{b-1} with its maximum transmission power P_r. For the source node $\boldsymbol{s}$, it divides the total transmission power P_s into two parts, βP_s and $\bar{\beta}P_s$ with different purposes, where $\bar{\beta} = 1 - \beta$. βP_s is used for transmitting $\vec{x_0}$ and $\bar{\beta}P_s$ is devoted to cooperate with the relay for transmitting $\vec{x_1}$ to the destination. The code $\vec{x_s}$ sent by the source node is the superposition of two codes: $\vec{x_0}$ and $\vec{x_1}$, i.e.,

$$\begin{aligned} \vec{x_s} &= \sqrt{\beta}\vec{x_0} + \sqrt{\bar{\beta}}\vec{x_1}, \\ \vec{x_r} &= \vec{x_1}. \end{aligned} \tag{2.9}$$

Employing the joint superposition encoding and decoding, the following rate can be achieved for the single-user relay channel if all codes are generated according to Gaussian

distribution [18]:

$$
\begin{aligned}
R &= \max_{p(x_s,x_r)} \min \left\{ I\left(X_s; Y_r | X_r\right), I\left(X_s, X_r; Y_d\right) \right\} \\
&= \max_{0\le\beta\le 1} \min \left\{ \frac{1}{2}\log\left(1+|h_{sr}|^2\beta P_s\right), \right. \\
&\qquad \left. \frac{1}{2}\log\left(1+|h_{sd}|^2\beta P_s + (\sqrt{|h_{sd}|^2\bar{\beta}P_s}+\sqrt{|h_{rd}|^2 P_r})^2\right) \right\} \qquad (2.10) \\
&= \max_{0\le\beta\le 1} \min \left\{ \frac{1}{2}\log\left(1+|h_{sr}|^2\beta P_s\right), \right. \\
&\qquad \left. \frac{1}{2}\log\left(1+|h_{sd}|^2 P_s + |h_{rd}|^2 P_r + 2|h_{sd}||h_{rd}|\sqrt{\bar{\beta}P_s P_r}\right) \right\}.
\end{aligned}
$$

2.3 Related Works on Resource Allocation in Cellular Networks

Driven by the user demand of higher data rate communications, improving the network efficiency through resource allocation, especially power allocation, has attracted an upsurge of research interest for both downlink and uplink cellular networks.

In the traditional multi-user OFDM network, numerous subchannel and power allocation algorithms have been proposed. For example, [22] provides a sum capacity maximization scheme while [23, 24] propose algorithms to consider fairness of the system. [25–27] investigate resource allocation to balance both throughput and fairness by maximizing a utility function. These algorithms either iteratively search for the joint resource allocation or decompose the joint allocation into separate processes where a uniform power distribution is assumed when allocating subcarriers. Ideally, the subchannel and power allocation should be designed jointly since they are mutually dependent, especially when fairness needs to be considered.

Although resource allocation for multiuser OFDM transmission has been well studied in the literature, the optimality conditions and algorithms cannot be directly applied to the uplink case mainly for two reasons. Firstly, the capacity of the SC-FDMA system is not simply the summation of the capacity on each subcarriers as in OFDMA systems. Secondly, each UE has its own transmission power constraint instead of a total power constraint at the eNB in the downlink case. To this end, [28, 29] derive the single user transmission capacity of the SC-FDMA system with both ZF and MMSE equalization. [30] designs low-complexity subcarrier and power allocation schemes to improve the communication reliability.

Considering the unique features of the cooperative relay channels, recent studies have focused on the performance improvement and resource allocation to make efficient use of relays. Specifically, [31–34] have investigated the cooperative gain and power allocation schemes to improve the achievable rate. [35] studies the joint subcarrier, power and relay nodes allocation to maximize the transmission rate in the OFDMA system with AF relays. [36–41] study the joint OFDM subchannel and power allocation problem assuming the source and the relay transmit in two orthogonal channels. However, in terms of the in-band DF relay networks where the source and the relay occupy the same channel, few works have addressed the resource allocation issue.

For the uplink SC-FDMA system with relays, [42] studies the joint source power allocation and AF relay beamforming in multi-relay networks to improve the energy efficiency. [43] calculates the signal-to-noise ratio (SNR) and proposes relay selection in an opportunistic AF relay-assisted SC-FDMA system and [44] studies relay selection and subcarrier allocation for opportunistic DF relay-aided SC-FDMA systems assuming that the UE cannot communicate with the eNB directly. However, to the best of our knowledge, there is limited literature on the capacity analysis and power allocation for the SC-FDMA

system with cooperative decode-and-forward relays.

Chapter 3

Resource Allocation for Downlink OFDM System

In this chapter, we present the problem of the adaptive joint subcarrier and power allocation to improve the downlink transmission efficiency in an LTE-Advanced network with the deployment of in-band cooperative decode-and-forward relay stations.

3.1 System Model

The downlink cellular network structure considered in this chapter is shown in Fig. 3.1. In each LTE-Advanced cell, an eNB is installed in the center to serve several UEs. RSs with a smaller coverage area are deployed near the cell edge to improve the cell-edge users' throughput or to extend the cellular radio coverage. To simplify the problem, suppose no cooperation exists among adjacent RSs, so any user can only be served by its affiliated eNB or a single RS if possible.

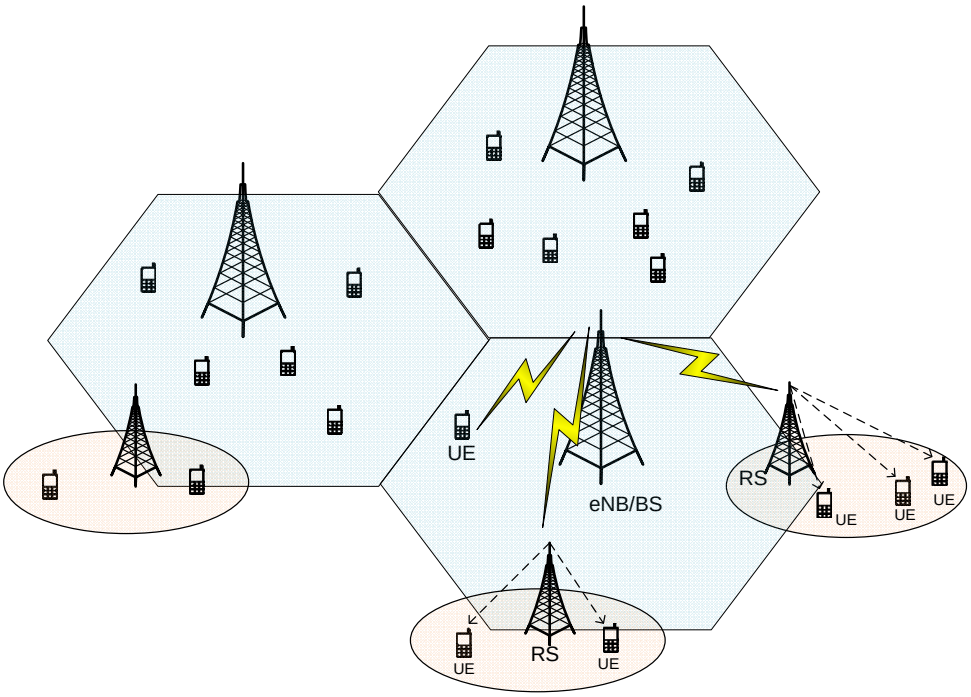

Figure 3.1: Downlink LTE-Advanced cellular network structure with the deployent of RSs.

In the downlink transmission, users receive signals from their serving eNB. If a user is also located within the relay's coverage range, the eNB can reach the user via two paths, which is modeled as the three-node cooperative relay channel. The desired downlink transmission is from the eNB to the user, while the affiliated RS aids the communication by capturing the signals sent from the eNB and forwarding them to the user. Upon receiving the signals, the relay decodes the original message and retransmits it in its own codes during the subsequent time slot. Two-hop transmissions are discussed in this chapter from a practical perspective. As the number of hops grows in the relay networks, the decoding complexity would be drastically increased [45].

In LTE-Advanced cellular systems, the downlink frequency domain transmission technique is OFDM where the available bandwidth B is divided into N orthogonal subchannels

operating at different subcarriers (tones) as shown in Fig. 3.2. Each subchannel has a bandwidth of B/N. The tones can be dynamically allocated to users to exploit both multi-user diversity and frequency diversity at a finer granularity.

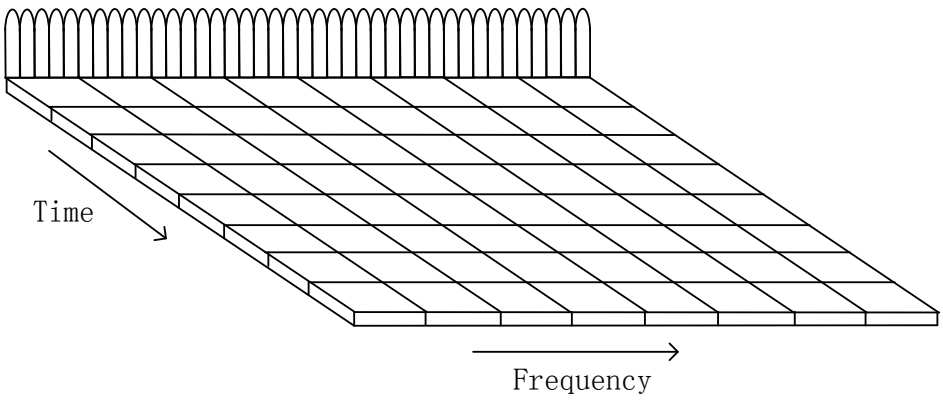

Figure 3.2: Time-frequency structure for downlink OFDM.

Let $\mathcal{M} = \{1, \ldots, M\}$ and $\mathcal{N} = \{1, \ldots, N\}$ denote the user set and the frequency-domain subchannel set, respectively. At the beginning of each time slot, the subchannels are allocated by the eNB and the transmission power can be dynamically adjusted at both eNB and RS to improve the transmission efficiency.

Suppose all wireless channels are independent AWGN channels where noise variances are normalized to 1. The channel gain coefficients for user k, $k \in \mathcal{M}$ on subchannel l, $l \in \mathcal{N}$ are denoted by $h_{sr}^{(k,l)}$, $h_{rd}^{(k,l)}$ and $h_{sd}^{(k,l)}$ representing the channel conditions of the eNB-RS, RS-UE and eNB-UE links, respectively. If a user is not within the RS coverage, there is only one direct transmission channel gain coefficient, $h_{sd}^{(k,l)}$. The channel state information is assumed to be known at both the transmitter and the receiver so that eNB can adaptively allocate the transmission power and subchannels according to the instantaneous channel state information.

The average transmitting power at the eNB and at the relay are bounded respectively by

$$\frac{1}{S}\sum_{t=1}^{S} x_s^2(t) \leq P_s$$
$$\frac{1}{S}\sum_{t=1}^{S} x_r^2(t) \leq P_r, \tag{3.1}$$

where x_s and x_r are signals transmitted from the eNB and from the RS, respectively, and t is the time index ranging from 1 to S as shown in Section 2.2.2. Suppose the power allocated to user k for transmission on the l^{th} subchannel at the eNB is $P_s^{(k,l)}$ and that at the relay station is represented by $P_r^{(k,l)}$. They must satisfy

$$\sum_{k,l} P_s^{(k,l)} \leq P_s$$
$$\sum_{k,l} P_r^{(k,l)} \leq P_r. \tag{3.2}$$

To indicate whether the l^{th} subcarrier is allocated to user k, we introduce a binary variable $\rho^{(k,l)}$:

$$\rho^{(k,l)} = \begin{cases} 1, & \text{the } l^{th} \text{ subchannel is allocated to user } k; \\ 0, & \text{otherwise.} \end{cases} \tag{3.3}$$

To avoid the interference, suppose each subchannel can only be allocated to one user during each transmission block.

As each subchannel has a bandwidth of B/N, based on (2.10), the maximum achievable rate of cooperative communication for user k in subchannel l averaged in the whole

transmission band in the AWGN environment is given by:

$$R^{(k,l)} = \max_{0\leq\beta^{(k,l)}\leq 1} \min \left\{ \frac{\rho^{(k,l)}}{N} \log\left(1 + \frac{|h_{sr}^{(k,l)}|^2 \beta^{(k,l)} P_s^{(k,l)}}{B/N}\right), \right.$$
$$\left. \frac{\rho^{(k,l)}}{N} \log\left(1 + \frac{|h_{sd}^{(k,l)}|^2 \beta^{(k,l)} P_s^{(k,l)}}{B/N} + \frac{\left(\sqrt{|h_{sd}^{(k,l)}|^2 \bar{\beta}^{(k,l)} P_s^{(k,l)}} + \sqrt{|h_{rd}^{(k,l)}|^2 P_r^{(k,l)}}\right)^2}{B/N}\right) \right\}, \tag{3.4}$$

where $\beta^{(k,l)} \in (0,1)$ is a coefficient determined by the source to adjust the portion of its transmission power used for cooperation with the relay in order to achieve the maximum rate. $\bar{\beta}^{(k,l)} = 1 - \beta^{(k,l)}$. For non-cooperative transmission, $P_r^{(k,l)} = 0$. The maximum transmission rate is the capacity of the direct eNB-UE link:

$$R^{(k,l)} = \frac{\rho^{(k,l)}}{N} \log\left(1 + \frac{|h_{sd}^{(k,l)}|^2 P_s^{(k,l)}}{B/N}\right). \tag{3.5}$$

Different from the power assignment problem which assumes each node has a unique power constraint, we focus on the fundamental performance limitation of the system with the existing allocated resources, e.g., bandwidth and total power. Our objective is to maximize the system's transmission efficiency; in other words, to find the minimum power needed to transmit a given amount of information at a certain rate under a bandwidth constraint. This is equivalent to finding the rate under a total power and bandwidth constraint [32]. Towards this end, we first investigate the joint OFDM subchannel and power allocation to maximize the sum rate of all users on all subchannels. Then we further consider fairness issue in the subsequent section. Specifically, the throughput maximization

problem can be formulated mathematically as:

$$\max_{P_s^{(k,l)},P_r^{(k,l)},\rho^{(k,l)}} \sum_{k\in\mathcal{M},l\in\mathcal{N}} R^{(k,l)}$$
$$\text{subject to } \sum_{k,l} P_s^{(k,l)} + \sum_{k,l} P_r^{(k,l)} \leq P_{total}$$
$$P_s^{(k,l)} \geq 0, \text{for all } k,\ l$$
$$P_r^{(k,l)} \geq 0, \text{for all } k,\ l$$
$$\rho^{(k,l)} \in \{0,1\}, \text{for all } k,\ l$$
$$\sum_{k\in\mathcal{M}} \rho^{(k,l)} \leq 1, \text{for all } l \tag{3.6}$$

where P_{total} is the total available power at the eNB and the RS.

Note that the optimal power and subchannel allocation are functions of the instantaneous channel gain coefficients. Since we assume the channel gain coefficients remain unchanged during each transmission block, the allocation $P_s^{(k,l)}(h_{sr}^{(k,l)}, h_{rd}^{(k,l)}, h_{sd}^{(k,l)})$, $P_r^{(k,l)}(h_{sr}^{(k,l)}, h_{rd}^{(k,l)}, h_{sd}^{(k,l)})$, and $\rho^{(k,l)}(h_{sr}^{(k,l)}, h_{rd}^{(k,l)}, h_{sd}^{(k,l)})$ can be simplified as $P_s^{(k,l)}$,$P_r^{(k,l)}$ and $\rho^{(k,l)}$ in the problem formulation.

Problem (3.6) can be categorized as a mixed integer nonlinear problem (MINLP) which is generally difficult to solve. However, considering the unique feature of the system that orthogonality exists among subcarriers and users, we propose a two-layer resource allocation scheme to solve (3.6). We first focus on the cooperative communication on a single subcarrier and derive the power dividing scheme between $P_s^{(k,l)}$ and $P_r^{(k,l)}$ to achieve the maximum rate in Section 3.2. With the optimal dividing scheme on each single subcarrier, the problem can be transformed to the traditional multi-user OFDM resource allocation problem. Then, we further consider the throughput maximization problem and minimum user rate maximization problem by proposing joint power and subchannel allocation schemes in Section 3.3.

3.2 Power Division for a Single-User Relay Channel

In this section, the first layer of the optimization problem is considered. Since the network can be viewed as the single-user relay channel on each subcarrier, our objective is to maximize the cooperation and the achievable rate for each subcarrier through power dividing between the eNB and the RS.

3.2.1 Problem Formulation

Without loss of generality, suppose the l^{th} subcarrier has been assigned to user k, $\rho^{(k,l)} = 1$. The first layer optimization problem can be written as:

$$\begin{aligned} &\max_{P_s^{(k,l)}, P_r^{(k,l)}} R^{(k,l)} \\ \text{subject to } &P_s^{(k,l)} + P_r^{(k,l)} \leq P^{(k,l)} \\ &P_s^{(k,l)} \geq 0, \\ &P_r^{(k,l)} \geq 0, \end{aligned} \tag{3.7}$$

where $P^{(k,l)}$ is the total transmission power assigned to this subchannel.

3.2.2 Power Allocation Schemes

To solve the above problem, for a limited total power consumption $P^{(k,l)}$, we need to decide the optimal $P_s^{(k,l)}$, $P_r^{(k,l)}$ and $\beta^{(k,l)}$ to maximize the achievable rate (3.4). Taking a closer look at (3.4) where $R^{(k,l)}$ is the minimum of two rates, the first rate is the eNB-RS channel capacity (relay decoding rate) and the second rate is the capacity of the multiple access channel (MAC) from eNB and RS to the UE (destination decoding rate). Since the highest

achievable rate is obtained when the relay decoding rate equals the destination decoding rate, the optimal power division scheme tries to balance these two rates by jointly designing $P_s^{(k,l)}$, $P_r^{(k,l)}$ and $\beta^{(k,l)}$. Depending on which rate is the bottleneck, there are two power dividing strategies that the source node can select [46]:

Depending on which rate is the bottleneck, there are two power dividing strategies that the source node can select [46]:

- If the destination decoding rate is the bottleneck, the source node can reduce $\beta^{(k,l)}$ until the relay decoding rate equals the destination decoding rate.
- If the relay decoding rate is the bottleneck, the source node will set $\beta^{(k,l)} = 1$.

Notice that when $\beta^{(k,l)} = 1$, the eNB and the relay will transmit independent codes. Therefore, the second case is also known as the "asynchronous case" while the first case is called the "synchronous case". The asynchronous case is more empirical to implement due to the reduction of coding complexity.

In the rest of the section, we will allocate $P_s^{(k,l)}$, $P_r^{(k,l)}$ and $\beta^{(k,l)}$ for both the synchronous case and the asynchronous case. However, with the optimal power allocation, whether synchronous case or asynchronous case achieves higher rate depends on the specific channel state information.

Synchronous Case

In this case, the destination decoding rate is the bottleneck, and $\beta^{(k,l)} \neq 1$. Denote $P_{s1}^{(k,l)} = \beta^{(k,l)} P_s^{(k,l)}$ and $P_{s2}^{(k,l)} = \bar{\beta}^{(k,l)} P_s^{(k,l)}$ as the two components of $P_s^{(k,l)}$. Since the signal received at the destination contains a combined strength, we first maximize the destination decoding rate with fixed total power for the multiple access (MAC) channel,

$P_0^{(k,l)}$, $P_0^{(k,l)} = P_{s_2}^{(k,l)} + P_r^{(k,l)}$. Then, we can allocate $P_{s_1}^{(k,l)}$ and $P_0^{(k,l)}$ under the total power constraint to achieve maximum rate.

The destination decoding rate is given by

$$\frac{1}{N}\log\left(1+\frac{|h_{sd}^{(k,l)}|^2\beta^{(k,l)}P_s^{(k,l)}}{B/N}+\frac{(\sqrt{|h_{sd}^{(k,l)}|^2\bar{\beta}^{(k,l)}P_s^{(k,l)}}+\sqrt{|h_{rd}^{(k,l)}|^2P_r^{(k,l)}}^2)}{B/N}\right), \tag{3.8}$$

which is equivalent to

$$\frac{1}{N}\log\left(1+\frac{|h_{sd}^{(k,l)}|^2P_{s_1}^{(k,l)}}{B/N}+\frac{(\sqrt{|h_{sd}^{(k,l)}|^2P_{s_2}^{(k,l)}}+\sqrt{|h_{rd}^{(k,l)}|^2P_r^{(k,l)}})^2}{B/N}\right). \tag{3.9}$$

With fixed $P_0^{(k,l)}$, it can be derived that the optimum power allocation between $P_{s_2}^{(k,l)}$ and $P_r^{(k,l)}$ is given by

$$\begin{aligned} P_{s_2}^{(k,l)} &= \frac{|h_{sd}^{(k,l)}|^2}{|h_{sd}^{(k,l)}|^2+|h_{rd}^{(k,l)}|^2}P_0^{(k,l)}, \\ P_r^{(k,l)} &= \frac{|h_{rd}^{(k,l)}|^2}{|h_{sd}^{(k,l)}|^2+|h_{rd}^{(k,l)}|^2}P_0^{(k,l)}, \end{aligned} \tag{3.10}$$

and the destination decoding rate becomes:

$$\frac{1}{N}\log\left(1+\frac{|h_{sd}^{(k,l)}|^2P_{s_1}^{(k,l)}+\left(|h_{sd}^{(k,l)}|^2+|h_{rd}^{(k,l)}|^2\right)P_0^{(k,l)}}{B/N}\right). \tag{3.11}$$

For the optimization problem (3.7), since the optimum of the achievable rate $R^{(k,l)}$ is attained when $P_{s_1}^{(k,l)}+P_0^{(k,l)} = P^{(k,l)}$ and when the relay decoding rate equals the destination decoding rate, i.e.,

$$\frac{1}{N}\log\left(1+\frac{|h_{sr}^{(k,l)}|^2P_{s_1}^{(k,l)}}{B/n}\right)=\frac{1}{N}\log\left(1+\frac{|h_{sd}^{(k,l)}|^2P_{s_1}^{(k,l)}+\left(|h_{sd}^{(k,l)}|^2+|h_{rd}^{(k,l)}|^2\right)P_0^{(k,l)}}{B/N}\right), \tag{3.12}$$

the optimization problem can be rewritten as:

$$\begin{aligned}
\max_{P_{s_1}^{(k,l)},P_0^{(k,l)}} \quad & \frac{1}{N}\log\left(1+\frac{|h_{sr}^{(k,l)}|^2 P_{s_1}^{(k,l)}}{B/N}\right) \\
\text{subject to } & P_{s_1}^{(k,l)} + P_0^{(k,l)} = P^{(k,l)} \\
& |h_{sr}^{(k,l)}|^2 P_{s_1}^{(k,l)} = |h_{sd}^{(k,l)}|^2 P_{s_1}^{(k,l)} + \left(|h_{sd}^{(k,l)}|^2 + |h_{rd}^{(k,l)}|^2\right) P_0^{(k,l)} \\
& P_s^{(k,l)} \geq 0 \\
& P_r^{(k,l)} \geq 0.
\end{aligned} \tag{3.13}$$

Actually, the constraints lead to only one feasible solution when $|h_{sr}^{(k,l)}| \geq |h_{sd}^{(k,l)}|$:

$$\begin{aligned}
P_{s_1}^{(k,l)} &= \frac{|h_{sd}^{(k,l)}|^2 + |h_{rd}^{(k,l)}|^2}{|h_{sr}^{(k,l)}|^2 + |h_{rd}^{(k,l)}|^2} P^{(k,l)}, \\
P_0^{(k,l)} &= \frac{|h_{sr}^{(k,l)}|^2 - |h_{sd}^{(k,l)}|^2}{|h_{sr}^{(k,l)}|^2 + |h_{rd}^{(k,l)}|^2} P^{(k,l)},
\end{aligned} \tag{3.14}$$

and the largest achievable rate is given by

$$R^{(k,l)} = \frac{1}{N}\log\left(1+\frac{|h_{sr}|^2\left(|h_{sd}|^2+|h_{rd}|^2\right)}{|h_{sr}|^2+|h_{rd}|^2}\cdot\frac{P^{(k,l)}}{B/N}\right). \tag{3.15}$$

Note that if $|h_{sr}^{(k,l)}| < |h_{sd}^{(k,l)}|$, the eNB-UE link has a better channel condition than the eNB-relay link. In this case, any direct transmission is more reliable than the cooperative transmission with the help of relays. When the relay obtains the channel state information, it first compares $|h_{sr}^{(k,l)}|$ with the channel condition of the direct transmission link to decide whether decode-and-forward needs to be performed to avoid any waste of the resources. In this scenario, the highest end user achievable rate (channel capacity) for non-cooperative transmission is

$$R^{(k,l)} = \frac{1}{N}\log\left(1+\frac{|h_{sd}^{(k,l)}|^2 P_s^{(k,l)}}{B/N}\right). \tag{3.16}$$

Asynchronous Case

In this case, the source and the relay employ independent codes, so that $\beta^{(k,l)} = 1$. By the same argument, the maximum achievable rate is obtained when the relay decoding rate equals the destination decoding rate. The optimization problem in this scenario can be formulated as:

$$\begin{aligned}
\max_{P_s^{(k,l)}, P_r^{(k,l)}} \quad & \frac{1}{N} \log \left(1 + \frac{|h_{sr}^{(k,l)}|^2 P_s^{(k,l)}}{B/N} \right) \\
\text{subject to} \quad & P_s^{(k,l)} + P_r^{(k,l)} = P^{(k,l)} \\
& |h_{sr}^{(k,l)}|^2 P_s^{(k,l)} = |h_{sd}^{(k,l)}|^2 P_s^{(k,l)} + |h_{rd}^{(k,l)}|^2 P_r^{(k,l)} \\
& P_s^{(k,l)} \geq 0 \\
& P_r^{(k,l)} \geq 0.
\end{aligned} \tag{3.17}$$

When $|h_{sr}^{(k,l)}| \geq |h_{sd}^{(k,l)}|$, the feasible region gives rise to the the following optimal power allocation:

$$\begin{aligned}
P_s^{(k,l)} &= \frac{|h_{rd}^{(k,l)}|^2}{|h_{sr}^{(k,l)}|^2 - |h_{sd}^{(k,l)}|^2 + |h_{rd}^{(k,l)}|^2} P^{(k,l)}, \\
P_r^{(k,l)} &= \frac{|h_{sr}^{(k,l)}|^2 - |h_{sd}^{(k,l)}|^2}{|h_{sr}^{(k,l)}|^2 - |h_{sd}^{(k,l)}|^2 + |h_{rd}^{(k,l)}|^2} P^{(k,l)},
\end{aligned} \tag{3.18}$$

and the largest achievable rate in this case is given by

$$R^{(k,l)} = \frac{1}{N} \log \left(1 + \frac{|h_{sr}^{(k,l)}|^2 |h_{rd}^{(k,l)}|^2}{|h_{sr}^{(k,l)}|^2 - |h_{sd}^{(k,l)}|^2 + |h_{rd}^{(k,l)}|^2} \cdot \frac{P^{(k,l)}}{B/n} \right). \tag{3.19}$$

3.3 Joint Power and Subchannel Allocation

With the optimal power dividing scheme between eNB and RS for a single-user relay channel on each subchannel, the optimization problem (3.6) can now be simplified to the

problem of jointly assigning subcarriers and power among all users in the network to attain the maximum overall throughput. In this section, two problems with different objectives are considered. We first investigate the subchannel and power allocation for throughput maximization problem and propose an optimal allocation algorithm. Then the fairness issue is further concerned as the second problem where our major target is to achieve maximum fairness among all users. Due to the complexity of the optimal solution, an efficient suboptimal algorithm with low computational cost is provided.

3.3.1 Throughput Maximization Problem

The simplified problem can be written as:

$$\begin{aligned} \max_{P^{(k,l)},\rho^{(k,l)}} & \sum_{k\in\mathcal{M},l\in\mathcal{N}} R^{(k,l)} \\ \text{subject to } & \sum_{k,l} P^{(k,l)} \leq P_{total} \\ & P^{(k,l)} \geq 0, \text{for all } k,\ l \\ & \rho^{(k,l)} \in \{0,1\}, \text{for all } k,\ l \\ & \sum_{k\in\mathcal{M}} \rho^{(k,l)} \leq 1, \text{for all } l. \end{aligned} \tag{3.20}$$

Define the unit power signal-to-noise ratio (SNR) for the single-user subchannel as:

$$H^{(k,l)} = \begin{cases} \frac{|h_{sr}^{(k,l)}|^2\left(|h_{sd}^{(k,l)}|^2+|h_{rd}^{(k,l)}|^2\right)}{\left(|h_{sr}^{(k,l)}|^2+|h_{rd}^{(k,l)}|^2\right)B/N}, & \text{the synchronous case,} \\ \frac{|h_{sr}^{(k,l)}|^2|h_{rd}^{(k,l)}|^2}{\left(|h_{sr}^{(k,l)}|^2-|h_{sd}^{(k,l)}|^2+|h_{rd}^{(k,l)}|^2\right)B/N}, & \text{the asynchronous case,} \\ \frac{|h_{sd}^{(k,l)}|^2}{B/N}, & \text{the non-cooperative case.} \end{cases} \tag{3.21}$$

Then the highest achievable rate for the relay channel has a unified expression similar

to the direct transmission capacity. $R^{(k,l)}$ can be written as

$$R^{(k,l)} = \frac{\rho^{(k,l)}}{N} \log\left(1 + H^{(k,l)} P^{(k,l)}\right). \tag{3.22}$$

Under the assumption that at most one user can be allocated on each subchannel (actually this assumption has been proved to be optimal in [22]), for any deterministic subchannel allocation, the multi-carrier transmission can be viewed as a Gaussian parallel channel with N independent channels coexisting in the network. For this type of network with a common power consumption constraint, the water-filling power allocation scheme has been proved to be optimal in terms of achieving the maximum overall throughput [21]. The fundamental spirit of water-filling is to allow higher transmitting power to be allocated to the channel with a better quality. For the subchannel allocation, it can be derived that assigning each subchannel to the user having the best channel quality is the optimal solution to the problem. In conclusion, the joint subchannel and power allocation scheme in terms of maximizing the overall throughput is shown in Theorem 1.

Theorem 1. *The optimal resource allocation scheme to the throughput maximization problem proceeds with the following steps:*

1. *For $l = 1, \ldots, N$, find a $k(l)$ satisfying $H^{(k(l),l)} \geq H^{(k',l)}$ for all $k' \in \mathcal{M}$. Assign subchannel l to user $k(l)$, i.e., set $\rho^{(k(l),l)} = 1$.*
2. *Allocate $P^{(k(l),l)} = \left(\lambda - \frac{1}{H^{(k(l),l)}}\right)^+$ as the transmitting power for user $k(l)$ at tone l. λ is the water-filling level that is chosen to satisfy the total power constraint $\sum_{k(l),l} P^{(k(l),l)} = P_{total}$.*

where $(\cdot)^+$ is defined as

$$(x)^+ = \begin{cases} x, & x \geq 0, \\ 0, & x < 0. \end{cases} \tag{3.23}$$

Proof. For any deterministic subchannel allocation $\{\rho^{(k,l)} : k \in \mathcal{M}, l \in \mathcal{N}\}$, we first show that the optimum throughput can be achieved by water-filling power allocation. To simplify the notations, denote the power allocated to subchannel l and the SNR on subchannel l by $P^{(l)}$ and $H^{(l)}$, respectively. The optimization problem can be written as

$$\begin{aligned} \max_{P^{(l)}} \ & \sum_l \frac{1}{N} \log\left(1 + H^{(l)} P^{(l)}\right) \\ \text{subject to } & \sum_l P^{(l)} \leq P_{total} \\ & P^{(l)} \geq 0. \end{aligned} \tag{3.24}$$

This standard convex optimization problem can be solved by the Lagrange multipliers. The details of the Lagrange multipliers method is shown as follows. Firstly, the optimization problem can be transformed to maximizing the following Lagrange function:

$$\mathcal{L}\left(P^{(1)}, \ldots, P^{(N)}\right) = \sum_l \frac{1}{N} \log\left(1 + H^{(l)} P^{(l)}\right) - \nu \left(\sum_l P^{(l)} - P_{total}\right). \tag{3.25}$$

where ν is the Lagrange multiplier coefficient. Then we differentiate (3.25) with respect to $P^{(l)}$, $l = 1, \ldots, N$ and set each derivative to 0 to obtain

$$\frac{\partial \mathcal{L}}{\partial P^{(l)}} = \frac{1}{N \ln 2} \cdot \frac{1}{1 + H^{(l)} P^{(l)}} - \nu = 0 \tag{3.26}$$

for $l = 1, \ldots, N$.

Therefore, the optimal power allocation is given by

$$P^{(l)} = \left(\lambda - \frac{1}{H^{(l)}}\right)^+, \tag{3.27}$$

and λ is chosen to satisfy

$$\sum \left(\lambda - \frac{1}{H^{(l)}}\right)^+ = P_{total}. \tag{3.28}$$

With the above optimal water-filling power allocation, we only need to prove that choosing the user with the highest SNR on each subchannel is the optimal subchannel allocation. To this end, we first divide the frequency subchannel set into two subsets: $V = \{l : P^{(l)} > 0\}$ and $V^C = \mathcal{N} \backslash V$. Let $|V|$ represent the cardinality of the set V. Thus,

$$\lambda = \frac{1}{|V|}(P_{total} + \sum_{l \in V} \frac{1}{H^{(l)}}). \tag{3.29}$$

The overall throughput can then be calculated as follows:

$$\begin{aligned} R_{total} &= \sum_{k \in \mathcal{M}, l \in \mathcal{N}} R^{(k,l)} \\ &= \frac{1}{N} \sum_{l \in V} \log \left(1 + H^{(l)} P^{(l)}\right) \\ &= \frac{1}{N} \sum_{l \in V} \log \left(H^{(l)} \lambda\right) \\ &= \frac{1}{N} \log \left(\lambda^{|V|} \cdot \prod_{l \in V} H^{(l)}\right). \end{aligned} \tag{3.30}$$

Taking derivative of R_{total} with respect to $H^{(l)},\ l \in V$ yields

$$\frac{\partial R_{total}}{\partial H^{(l)}} = \frac{1}{N \ln 2} \cdot \frac{\lambda - \frac{1}{H^{(l)}}}{\lambda \cdot H^{(l)}}. \tag{3.31}$$

For any $l \in V$, $\lambda - \frac{1}{H^{(l)}} > 0$, so $\frac{\partial R_{total}}{\partial H^{(l)}} > 0$. For those $l \in V^C$, $\frac{\partial R_{total}}{\partial H^{(l)}} = 0$. Therefore, the overall throughput is a monotonic non-decreasing function of the SNRs of all subchannels. Thus, the maximum overall throughput can be achieved when every subchannel is allocated to the user with the highest SNR. □

3.3.2 Fairness Concern

Although Theorem 1 can maximize the overall throughput, there is no minimum achievable rate guaranteed for each user. Especially, if there exists one user whose channel quality

outperforms all other users on every subchannel, all available subchannels and power would be assigned to this user. In this case, other users' transmission rate cannot be guaranteed.

As ensuring the mobile users' QoS requirements, e.g., a minimum transmission rate requirement, is one of the major design objectives in the cellular network, the subchannel and power allocation schemes should be adapted accordingly to meet these requirements. This issue has been addressed by some works, e.g., [23, 24]. However, most of these works only consider either achieving the absolute fairness or meeting each individual user's QoS requirement without any concern about the transmission efficiency of the entire system. Therefore, our research is to investigate both fairness and efficiency issue and try to come up with an improved resource allocation scheme to balance the transmission rates among different users in the network while maximizing the total throughput.

In this work, we adopt the fairness definition in [23] where the maximum fairness is achieved when all users have the same data rate. The maximum fairness can be obtained by solving the *max-min* problem to maximize the worst user's achievable rate. It is worth mentioning that the popular proportional fairness [24] can also be included in the *max-min* problem if a set of factors representing the weight of each user's rate is employed.

Different from [23] and most of the literatures where fairness is the only target, we propose a novel optimization problem where the overall throughput is also optimized when maximum fairness has been achieved. The two objectives have a hierarchical structure: the fairness objective has the highest priority to be optimized and among the feasible solutions, the overall throughput is further maximized.

The problem can be formulated as a lexicographic optimization problem:

$$\begin{aligned} \text{lex} \max_{P^{(k,l)},\rho^{(k,l)}} & \left(\min_k R_k, \sum_{k\in\mathcal{M}} R_k \right) \\ \text{subject to } & \sum_{k,l} P^{(k,l)} \leq P_{total} \\ & P^{(k,l)} \geq 0, \text{for all } k,\, l \\ & \rho^{(k,l)} \in \{0,1\}, \text{for all } k,\, l \\ & \sum_{k\in\mathcal{M}} \rho^{(k,l)} \leq 1, \text{for all } l, \end{aligned} \tag{3.32}$$

where R_k is the achievable rate for user k given by

$$R_k = \sum_{l\in\mathcal{N}} \frac{\rho^{(k,l)}}{N} \log\left(1 + H^{(k,l)} P^{(k,l)}\right). \tag{3.33}$$

To solve this problem, the subchannel and power allocation should be jointly designed. Whether a subchannel is assigned to a user or not depends on the user's rate which is controlled by the power allocated to this user. On the other hand, allocating power among subchannels depends on the channel condition of each subchannel which is decided by the subchannel allocation. In this work, we first try to find the optimal solution. Then as the eNB needs to allocate resources for the rapidly changing wireless channels, low-complexity suboptimal algorithms are preferred, especially for cost-effective and delay-sensitive implementations. Therefore, an efficient suboptimal algorithm is proposed as well.

Optimal Power and Subchannel Allocation

To solve this lexicographic maximization problem, a sufficient condition that the optimal joint power and subchannel allocation satisfies is described in the following theorem.

Theorem 2. *Let S_k denote the set of subchannels allocated to user k. $S_k^+ \subseteq S_k$ is the set containing only the subchannels associated with nonzero transmission power, i.e., $S_k^+ = \{l : \rho^{(k,l)} = 1$ and $P^{(k,l)} > 0\}$. The cardinality of S_k^+ is $|S_k^+|$. λ is the water-filling level. Thus the subchannel and power allocation is optimal for the lexicographic optimization problem (3.32) if it satisfies the following condition.*

$$H^{(S_1^+)}\lambda^{|S_1^+|} = H^{(S_2^+)}\lambda^{|S_2^+|} = \cdots = H^{(S_m^+)}\lambda^{|S_m^+|} \tag{3.34}$$

where

$$H^{(S_k^+)} = \prod_{l \in S_k^+} H^{(k,l)} \tag{3.35}$$

Proof. Since water-filling is always optimal for power allocation in spite of any subchannel assignment, in order to maximize the overall throughput, the power allocation should still follow a water-filling manner. Suppose that the water-filling level is λ which is a function of the channel gains on all subchannels. The achievable rate for user k can be derived as follows.

$$\begin{aligned} R_k &= \sum_{l \in S_k^+} \frac{1}{N} \log\left(1 + H^{(k,l)} P^{(k,l)}\right) \\ &= \sum_{l \in S_k^+} \frac{1}{N} \log\left(1 + H^{(k,l)}\left(\lambda - \frac{1}{H^{(k,l)}}\right)\right) \\ &= \sum_{l \in S_k^+} \frac{1}{N} \log\left(\lambda H^{(k,l)}\right) \\ &= \frac{1}{N} \log\left(H^{(S_k^+)}\lambda^{|S_k^+|}\right). \end{aligned} \tag{3.36}$$

Therefore, the ideal case is that $H^{(S_k^+)}\lambda^{|S_k^+|}$ is balanced to attain the same value for all users $k \in \mathcal{M}$. □

However, since λ is a function of all channel gains which will be determined by the subchannel assignment, it is very difficult to jointly allocate subchannels and power due to the computation complexity. Instead, most suboptimal solutions to the similar problem [23, 24] separate the joint allocation into two steps. Firstly, subchannels are allocated while assuming power is equally assigned in all subchannels. Then, based on the subchannel allocation, power distribution is optimized according to water-filling. In our work, we propose a joint suboptimal subchannel and power allocation algorithm where the subchannels are allocated based on the water-filling power distribution.

Suboptimal Power and Subchannel Allocation

The suboptimal resource allocation scheme contains two steps as well. We first allocate subchannels among all users while assuming power is distributed in water-filling manner with water-filling level λ. Then in the second step, λ can be decided based the subchannel allocation in the first step.

1. Suboptimal Subchannel Allocation Algorithm

   The first step only deals with the subchannel allocation scheme. Before proposing the subchannel allocation algorithm, we first introduce two new sets. Suppose $\mathcal{N}_s$ is the remaining subchannel set after each allocation. Initially, $\mathcal{N}_s = \mathcal{N}$. Moreover, define $\mathcal{M}_s$ as an ordered set containing all users $1, 2, \ldots, m$ where for any $i, j \in \mathcal{M}_s$, $i < j$ if and only if $H^{(S_i)} \leq H^{(S_j)}$. The suboptimal subchannel allocation process is summarized in the following algorithm.

   Note that compared with most suboptimal subchannel allocation algorithms assuming equal power distribution, Algorithm 1 reduces the complexity from $\mathcal{O}(MN)$ to $\mathcal{O}(N)$.

Algorithm 1 Suboptimal subchannel allocation algorithm with fairness concern

1: Initialize: $S_k = \emptyset$, $H^{(S_k)} = 1$ for all users $k = 1, 2, \ldots, M$. Let $\mathcal{N}_s = \mathcal{N}$ and $\mathcal{M}_s = \mathcal{M}$.

2: While $\mathcal{N}_s \neq \emptyset$, for $k = \mathcal{M}_s(1), \ldots, \mathcal{M}_s(M)$, find a subchannel $l(k) \in \mathcal{N}_s$ satisfying $H^{(k,l(k))} \geq H^{(k,l')}$ for all $l' \in \mathcal{N}_s$. Assign $l(k)$ to user k. Update $\mathcal{N}_s = \mathcal{N}_s - \{l(k)\}$ and $H^{(S_k)} = H^{(S_k)} \cdot H^{(k,l(k))}$.

3: Reorder the user set $\mathcal{M}_s$. Then go back to 2.

2. Optimal Power Allocation

After allocating the subchannels according to Algorithm 1, suppose the channel gain coefficient in each subchannel is $H^{(k,l)}$. According to the optimal water-filling power allocation, the power allocated in each subchannel is

$$P^{(k,l)} = \left(\lambda - \frac{1}{H^{(k,l)}}\right)^+ \tag{3.37}$$

and λ is chosen to satisfy the total power constraint $\sum P^{(k,l)} = P_{total}$.

3.4 Numerical Results

To evaluate the performance of our subchannel and power allocation schemes derived in the previous sections, the simulation results are presented in three parts. The first part depicts the achievable rates obtained by the power dividing schemes in the single-user relay channel. The second part demonstrates the superiority of the optimal joint subchannel and power allocation scheme for maximizing the overall throughput in a cellular network. The suboptimal allocation scheme to maximize the minimum rate of all users is evaluated in the third part. We assume that all wireless channels suffer from frequency selective fading and each subchannel experiences independent frequency flat fading.

3.4.1 Performance of Power Dividing Schemes for Single-User Relay Channel

To evaluate the performance of our optimal power dividing schemes derived in Section 3.2, we conduct simulations considering two specific network environments: Rayleigh fading environment and free space fading environment. In both environments, an achievable rate comparison is provided where the rates are derived with different power dividing schemes. Besides, in order to demonstrate the performance enhancement of introducing the relay station, we always set the capacity of non-cooperative transmission as a baseline for comparison.

1. Suppose all wireless channels suffer from independent Rayleigh fading. The average achievable rates are obtained employing the optimal power allocation (3.10), (3.14), and (3.18) for the synchronous case and the asynchronous case, respectively. The performance is compared with an equal power dividing scheme where the eNB and the RS transmit with the same power. The results are as shown in Fig. 3.3.

2. We consider the free space path loss model. Suppose each channel suffers from a signal strength attenuation which is proportional to some exponent of the transmission distance. For simplicity, in our simulation, the RS is located in the middle of the eNB and the mobile user. The path loss exponent normally ranges from 2 to 4 where 2 is adopted in our simulation. Fig. 3.4 depicts the rate comparison of our proposed schemes and the equal power allocation scheme.

In both network environments, transmission with the help of a relay station always outperforms the non-cooperative transmission in terms of achieving higher data rate, which demonstrates the benefit of deploying relay stations in cellular networks.

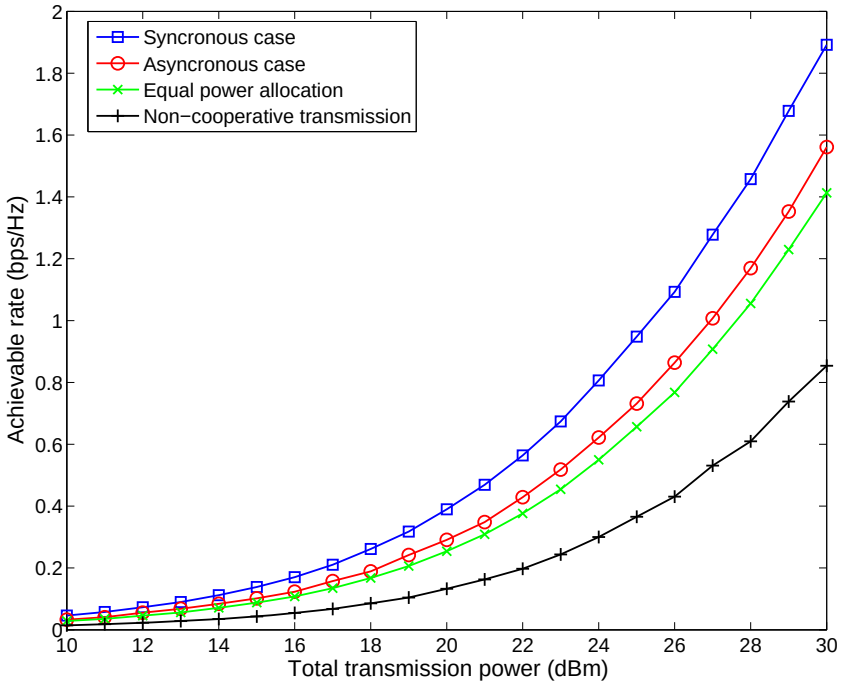

Figure 3.3: Comparison of single-user achievable rates in Rayleigh fading environment.

In terms of the comparison of the two cases, higher achievable rate can be obtained in synchronous case than in asynchronous case since the former one fully exploits the cooperation between the eNB and the relay in the coding process. However, synchronous case leads to high coding complexity which will increase the implementation cost significantly. Compared with the equal power dividing scheme, our optimal power dividing schemes achieve higher data rate in both asynchronous case and synchronous case.

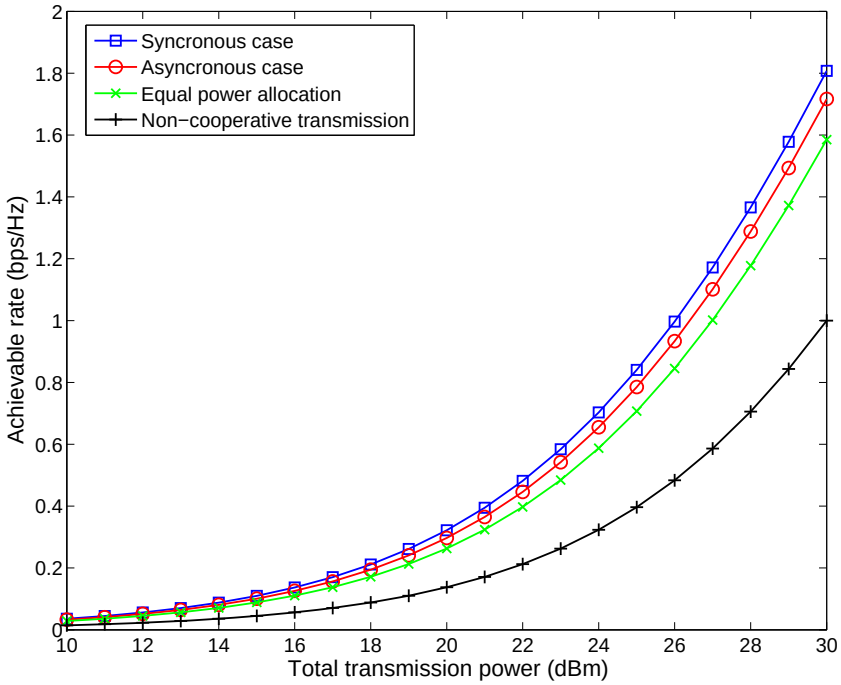

Figure 3.4: Comparison of single-user achievable rates in path loss environment.

3.4.2 Performance of Optimal Resource Allocation for Throughput Maximization

We consider an LTE-Advanced cellular network where the total available bandwidth is 20MHz and each subchannel has a bandwidth of 15kHz. On each frequency subcarrier, the wireless eNB-relay, relay-UE and eNB-UE channels are assumed to suffer from independent Rayleigh fading. Some simulation parameters are summarized in Table 3.1:

Fig. 3.5 shows the throughput per Hz using the optimal resource allocation scheme in Theorem 1 in the configured cellular cell. The throughput of the system is derived when the relay station operating in the synchronous case and the asynchronous case separately.

Table 3.1: Downlink cellular network simulation parameters.

Parameter	**Value**
Cellular layout	Hexagonal grid, 6 sectors per cell
Relay station layout	1 relay station per sector
Relay protocol	Decode-and-Forward
Transmission bandwidth	20MHz
Subcarrier separation	15kHz
Number of subcarriers in a resource block	12
Carrier frequency	2.7 GHz for downlink
Channel model	Frequency selective Rayleigh fading
UE distribution	Uniformly random
Number of UEs per sector	10
Total transmission power	80W

The performance is compared with the throughput of a system containing only direct transmissions. It is demonstrated that with the optimal resource allocation, the per Hz throughput is always increasing with the total available transmission power. With the help of a relay station, both the synchronous case and the asynchronous case outperform the direct transmission case.

To illustrate the superiority of our resource allocation scheme in Theorem 1, we further compare the throughput achieved by Theorem 1 with the following two resource allocation schemes:

1. The user with the best channel quality is picked on each subchannel and the power is distributed on the subchannels equally;

2. Both the subchannels and power are allocated equally among all users without any

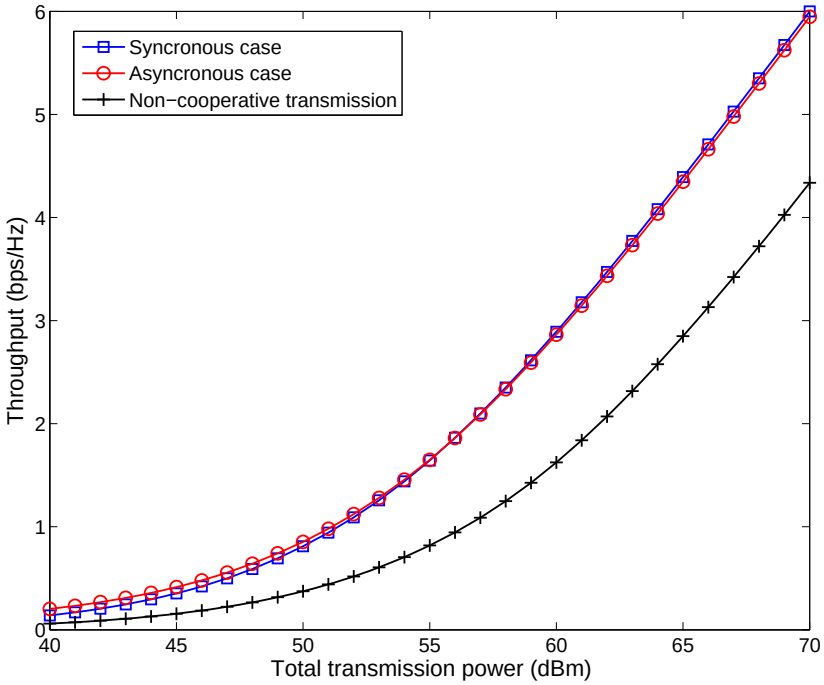

Figure 3.5: Overall throughput with optimal resource allocation scheme.

consideration of the channel conditions of each single user.

Fig. 3.6 illustrates the overall throughput comparison of these three schemes for synchronous relay station case and Fig. 3.7 depicts the same comparison when the relay station operates in the asynchronous mode. From these figures, it can be seen that the optimal resource allocation scheme achieves the highest throughput in both the synchronous case and the asynchronous case. Furthermore, scheme 1 outperforms scheme 2 since scheme 1 takes the variance of channel conditions into consideration as well.

Notice that in both figures, the throughput achieved by the optimal resource allocation scheme and that achieved by scheme 1 increase with the number of users. However, the

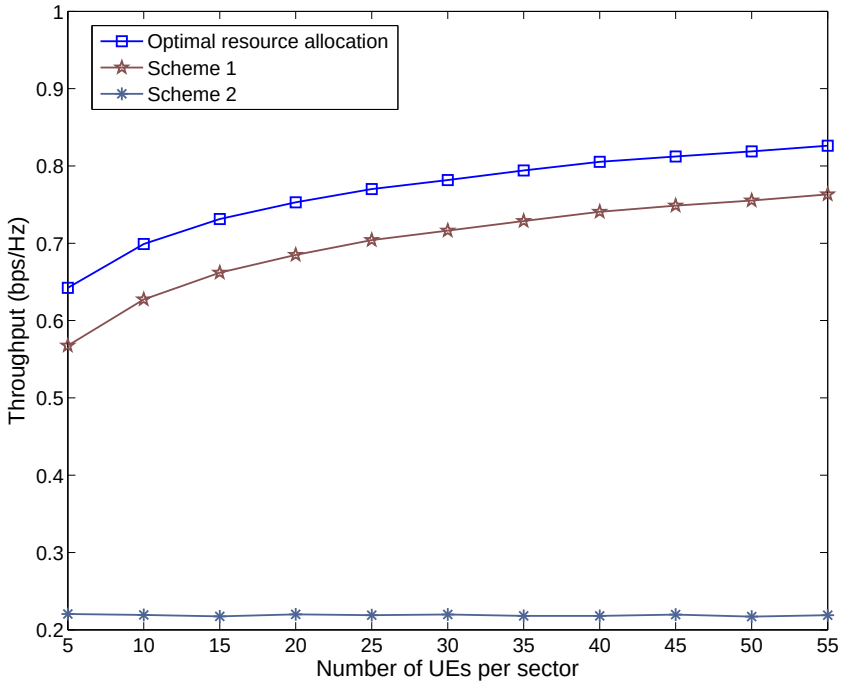

Figure 3.6: Comparison of overall throughput when RS operates in synchronous mode.

throughput achieved by scheme 2 remains almost unchanged when the number of users grows. This indicates that our allocation scheme and scheme 1 can better exploit the user diversity. As the number of users goes up, there is a higher chance that a user with better channel condition can be picked.

Fig. 3.8 depicts the rate distribution among users. We take one sector in a cellular cell where 10 users are served by the relay station as an example. It can be seen that although Theorem 1 has been proved to be optimal in terms of the overall throughput improvement of the system, the QoS requirement for each user has not been considered. In this figure, user #8 achieves almost 200% compared with user #3 which is not fair for users with poor channel conditions.

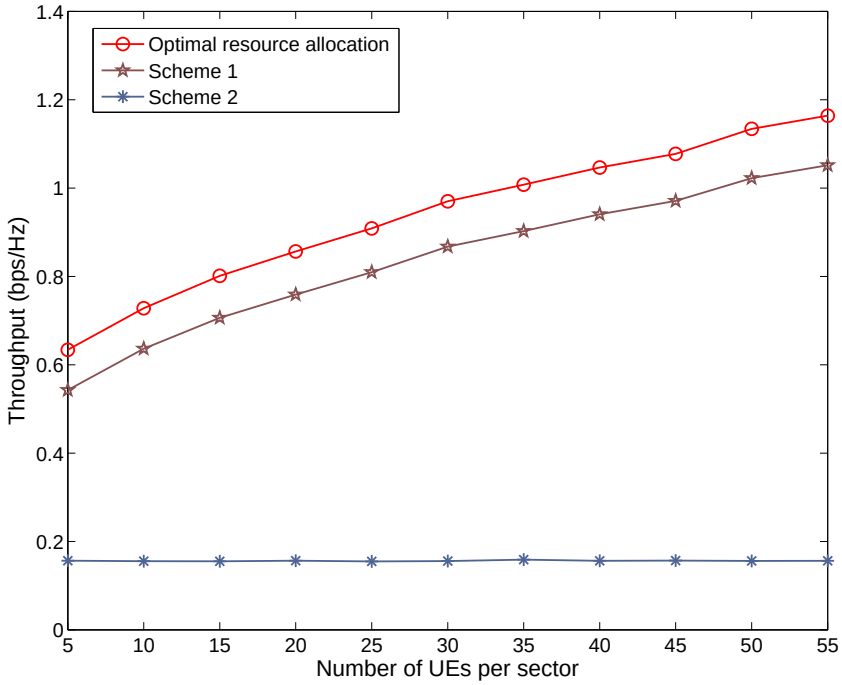

Figure 3.7: Comparison of overall throughput when RS operates in asynchronous mode.

3.4.3 Performance of Suboptimal Resource Allocation with Fairness Concern

In order to evaluate the performance of our proposed suboptimal subchannel and power allocation algorithm in improving fairness as well as the overall throughput, we compare both the minimum rate of all users and the average user rate achieved by our suboptimal algorithm with other suboptimal schemes. The total transmission power ranges from 30 to 50 dBm and assume that there are 30 users randomly distributed in each sector. The rest of the network parameters are unchanged. We only take the synchronous relay case as an example and similar results can be obtained in the asynchronous case.

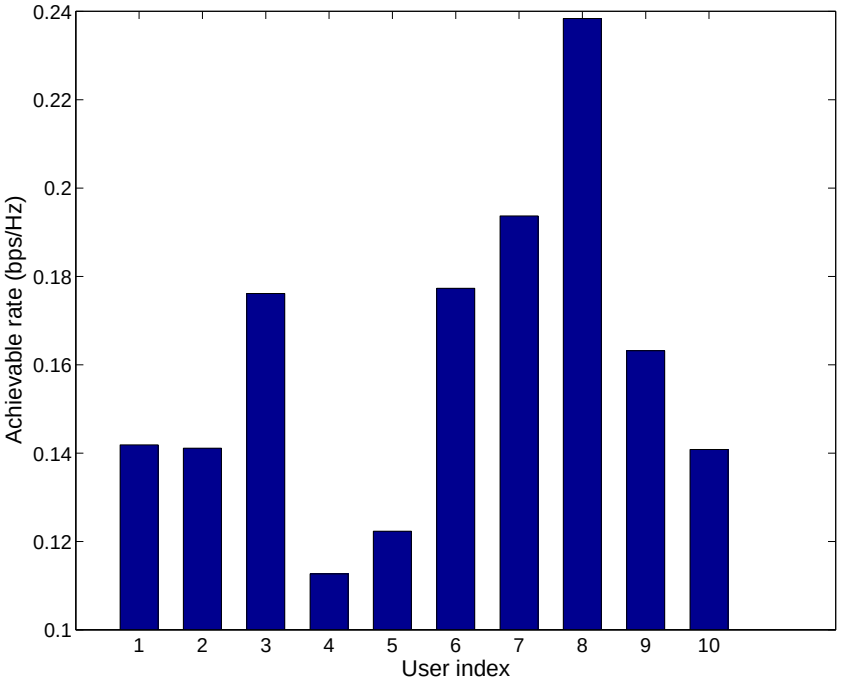

Figure 3.8: Rate distribution of 10 users.

We compare our proposed resource allocation scheme with the scheme which assumes equal power distribution while allocating subchannels [23,24] in Fig. 3.9. In the subchannel allocation step, the reference scheme assigns subchannels by assuming power is distributed equally; however, our proposed scheme is based on the optimal water-filling power allocation. In the power allocation step, all schemes employ the water-filling method. As a baseline for comparison, the optimal joint power and subchannel allocation scheme for throughput maximization is also depicted.

Fig. 3.9(a) shows the minimum rate of all users obtained by the three schemes. It can be seen that our proposed scheme can increase the minimum rate of all users drastically. Employing the optimal throughput maximization scheme, it is possible that some users

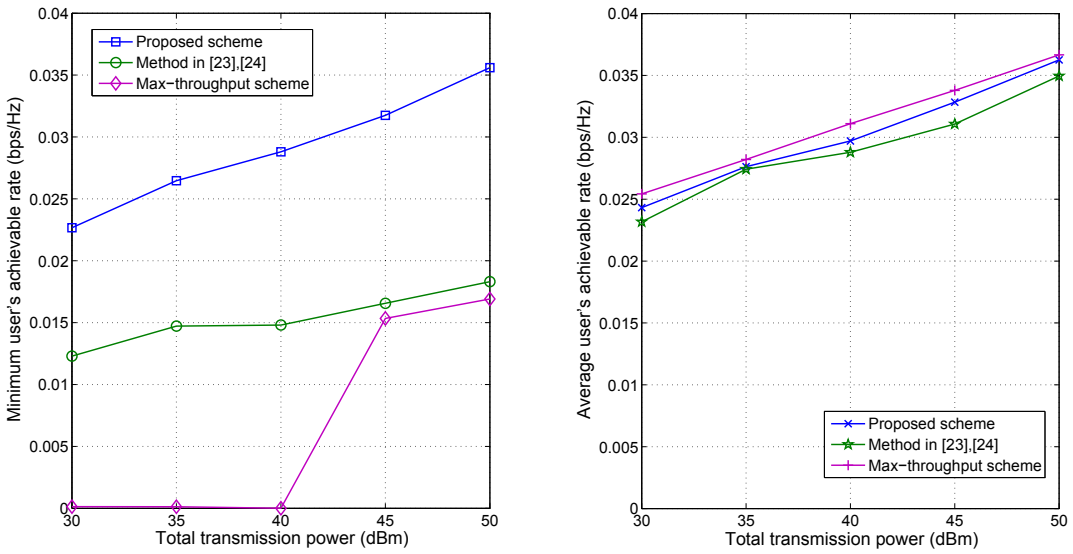

(a) (b)

Figure 3.9: Comparison of minimum rate of all users and average user rates.

could not have any chance to transmit at all.

In terms of the average user rate which is shown in Fig. 3.9(b), the optimal throughput maximization scheme can always outperform other schemes. All the three schemes achieve similar rates since in each scheme, the subchannel allocation tends to pick a user with good channel quality.

3.5 Summary

In this chapter, we have investigated the downlink resource allocation to improve the transmission efficiency in an LTE-Advanced cellular system where relays are installed. Instead of simply amplifying and forwarding the received signal, relays are expected to have more

coding capability to achieve higher data rates. We focus on the In-Band Type II decode-and-forward relays where the source and the relay transmit in the same frequency band (channel). An optimal subcarrier and power allocation scheme is proposed to maximize the overall throughput. Then we consider the fairness issue and come up with a two-step suboptimal algorithm that jointly allocate subcarrier and power to maximize the minimum rate of all users while improving the system throughput. Numerical results indicate that our proposed algorithm can improve the minimum rate of all users by about 80% compared with the reference scheme. Furthermore, in terms of the overall throughput, our scheme can achieve about 90% of the maximum throughput while the reference obtains around 84%.

Chapter 4

Achievable Rate and Power Allocation for Uplink SC-FDMA System

In this chapter, we investigate the fundamental achievable rate and power allocation for the uplink communications in the LTE-Advanced network with the deployment of in-band cooperative decode-and-forward relay stations.

4.1 System Model

The uplink cooperative communication framework in the LTE-Advanced network is shown in Fig. 4.1. In each cell, an eNB is located in the center where a set of UEs intend to connect to the eNB simultaneously for uplink transmission. Near the cell edge, several dedicated Type II in-band decode-and-forward relay stations are installed to assist the communication

and improve the transmission rate for the users within the RS's communication range. We consider that the interference can be avoided by proper interference coordination among neighboring RSs, e.g., through careful carrier selection enabled by carrier aggregation in LTE-Advanced networks.

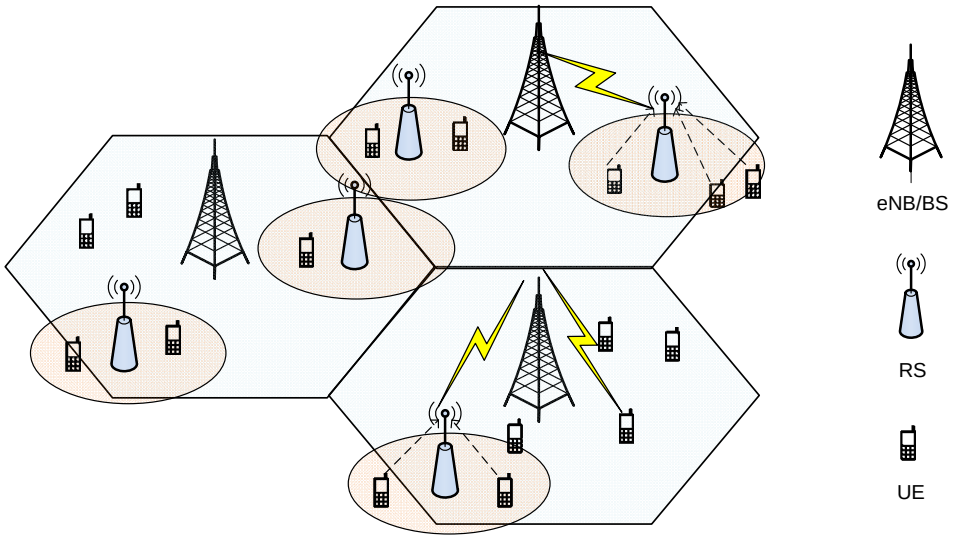

Figure 4.1: Uplink transmission with the deployment of RSs in an LTE-Advanced network.

Each UE within the RS's coverage area broadcasts its transmission signals to both its affiliated eNB and the RS. The RS aids the communication in the sense that it first decodes the received signals from the UE, then forwards the message to the eNB in its own codes, which forms a three-node cooperative relay channel. Therefore, the eNB receives the superposition of the signals from two paths, the direct UE-eNB transmission link and the relay transmission link. Similar to the downlink case, we only focus on two-hop communications due to the drastic increase of the coding complexity associated with multiple hops [45].

The system model consists of one eNB, one RS and a set of M users, denoted by $\mathcal{M} = \{1, \ldots, M\}$, transmitting to the eNB with the help of the RS. The total available

bandwidth B is divided into N orthogonal subcarriers indexed by $\mathcal{N} = \{1, \ldots, N\}$, where each subcarrier has a bandwidth of B/N. $\mathcal{N}_i \subset \mathcal{N}$ is the set of subcarriers occupied by user i for the uplink transmission. The number of subcarriers in $\mathcal{N}_i$ is denoted by N_i. Since LTE systems employ localized SC-FDMA as the uplink transmission technology, subcarriers assigned to a user need to be adjacent to each other [47]. Besides, each subcarrier can only be allocated to at most one user, i.e., $\mathcal{N}_i \bigcup \mathcal{N}_j = \emptyset$, for $i, j \in \mathcal{M}, i \neq j$.

Consider that all wireless channels are independent and suffer from frequency selective fading and AWGN. As the bandwidth of a single subcarrier is narrow, signals on each subcarrier experience frequency flat fading. The channel gain coefficients for user i, $i \in \mathcal{M}$ on subcarrier k, $k \in \mathcal{N}_i$ are denoted by $h_{s_i r}^{(k)}$, $h_{rd}^{(k)}$ and $h_{s_i d}^{(k)}$ representing the channel conditions of the UE-RS, RS-eNB and UE-eNB links, respectively. The corresponding frequency response are denoted by $H_{s_i r}^{(k)}$, $H_{rd}^{(k)}$ and $H_{s_i d}^{(k)}$. Based on the received pilot signals, we assume that RS has perfect knowledge of the channel state information (CSI) of the UE-RS link and eNB has the perfect knowledge of the CSI of all links in order to perform equalization and decoding. Based on the CSI, the resource scheduler located at the eNB allocates subcarriers and transmission power for both the UE and the RS. The decision is then fedback to the SC-FDMA transmitter scheduler at the UE and the RS for subcarrier mapping and power allocation.

4.2 Signal Representations in the SC-FDMA Relay System

The block diagram of the SC-FDMA transmitter and receiver structure for transmission of user i's signals is shown in Fig. 4.2.

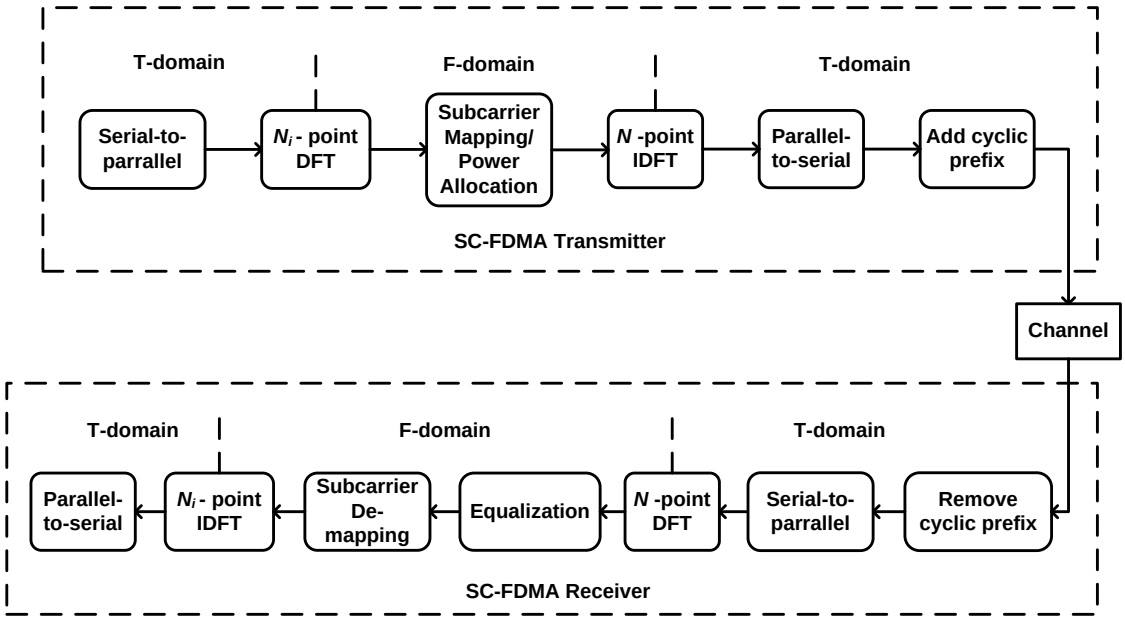

Figure 4.2: Transmitter and receiver structure for user i in SC-FDMA systems.

SC-FDMA is also referred to as DFT-spread OFDMA. The sequence of the time-domain signals for transmission at user i is firstly transformed into frequency domain by the N_i-point DFT, then the sequence goes through the OFDMA processing. The decision is carried out in the time domain at the receiver after the N_i-point IDFT transforming the frequency-domain sequence into time domain.

4.2.1 Transmitted Signals at UE

The input to the transmitter at user i is a sequence of N_i time-domain symbols $\{x_{s_i}(u),\ u = 1, \ldots, N_i\}$. After the N_i-point DFT, it is transformed into a sequence of frequency-domain symbols $\{X_{s_i}(v),\ v = 1, \ldots, N_i\}$. The frequency-domain scheduler then maps these symbols on a set of N_i active subcarriers selected from a total number of N subcarriers, and

allocates the transmission power for each subcarrier. Assume the power allocated to subcarrier k for transmission at user i is $P_{s_i}^{(k)}$, which needs to satisfy a total power constraint:

$$\sum_{k \in \mathcal{N}_i} P_{s_i}^{(k)} \leq P_{s_i}, \tag{4.1}$$

where P_{s_i} is the total available transmission power at user i.

After the subcarrier mapping and power allocation, the frequency-domain signal on subcarrier k is denoted by $X_{s_i}^{(k)},\ k \in \mathcal{N}_i$. $X_{s_i}^{(k)}$ is then transformed back into time domain by the N-point inverse DFT (IDFT) before transmitting to the channel.

4.2.2 Received and Transmitted Signals at the RS

The sequence of the time domain signals received at the RS is first transformed into the frequency domain by the N-point DFT. Denote $Y_r^{(k)},\ k \in \mathcal{N}_i$ as the frequency-domain representation of the received signal on subcarrier k at the RS, which is given by

$$Y_r^{(k)} = H_{s_i r}^{(k)} X_{s_i}^{(k)} + W_r^{(k)}, \tag{4.2}$$

where $W_r^{(k)}$ with variance σ_r^2 is the DFT of the additive white Gaussian noise received at the RS.

The frequency domain equalization technique is utilized at the RS in order to mitigate the frequency selective fading effect induced by the wireless propagation channel. Then the sequence is transformed back to the time domain, denoted by $y_r(u),\ u = 1, \ldots, N_i$, for decoding, and the decoded message will be encoded and transmitted in the subsequent transmission block.

Upon receiving the signals from the users, the full-duplex RS transmits a sequence, $x_r(u),\ u = 1, \ldots, N_i$, to the SC-FDMA transmitter for cooperative transmission of user

i's message. The same set of subcarriers $\mathcal{N}_i$ is selected at the RS for the transmission of user i's message. The frequency domain representation of the transmitted signal on the kth subcarrier is $X_r^{(k)}, k \in \mathcal{N}_i$, and the power allocated to the kth subcarrier is $P_r^{(k)}$, which satisfies:

$$\sum_{k \in \mathcal{N}} P_r^{(k)} \leq P_r, \tag{4.3}$$

where P_r is the total transmission power at the RS.

4.2.3 Received Signals at the eNB

The received signal at the eNB on subcarrier k is the superposition of the signal from the user and the signal from the RS, i.e.,

$$Y_d^{(k)} = H_{s_i d}^{(k)} X_{s_i}^{(k)} + H_{rd}^{(k)} X_r^{(k)} + W_d^{(k)}, \tag{4.4}$$

where $W_d^{(k)}$ is the additive white Gaussian noise received at the eNB on subcarrier k, and the variance is given by σ_d^2.

The corresponding time domain symbols after the transformation for decision is denoted by the vector $y_d(u),\ u = 1, \ldots, N_i$.

4.3 Achievable Rates of the SC-FDMA Relay System

To avoid propagating noise and to improve the transmission rate, the decode-and-forward RS is deployed to cooperate with the UE to transmit the signals to the eNB. The achievable rate in the AWGN channel is attained by the joint superposition coding which maximizes the cooperation between the source and the relay. In this section, we consider the joint superposition coding with equalization techniques in the SC-FDMA system and derive the expressions of the achievable rate for ZF and MMSE equalization, respectively.

4.3.1 Joint Encoding

As shown in Section 2.2.2, the joint superposition encoding process of the relay channel consists of a consecutive B blocks of transmission, indexed by $b = 1, \ldots, B$. In each transmission block, two independent code words, $\vec{x_0}$ and $\vec{x_1}$ containing N_i i.i.d. random variables, are employed. RS transmits $\vec{x_1}$ with its full transmission power while UE transmits a superposition of $\vec{x_0}$ and $\vec{x_1}$ to achieve the cooperation, i.e.,

$$\begin{aligned} \vec{x_{s_i}} &= \sqrt{\beta}\vec{x_0} + \sqrt{\bar{\beta}}\vec{x_1}, \\ \vec{x_r} &= \vec{x_1}, \end{aligned} \tag{4.5}$$

where $0 \leq \beta \leq 1$ is the power dividing parameter and $\bar{\beta} = 1 - \beta$.

After transforming the codes into frequency domain and performing subcarrier mapping and power allocation by the transmitter, the symbols transmitted on the kth subcarrier at the UE and RS are given by

$$\begin{aligned} X_{s_i}^{(k)} &= \sqrt{P_{s_i}^{(k)}}(\sqrt{\beta}X_0^{(k)} + \sqrt{\bar{\beta}}X_1^{(k)}), \\ X_r^{(k)} &= \sqrt{P_r^{(k)}}X_1^{(k)}, \end{aligned} \tag{4.6}$$

where $X_0^{(k)}$ and $X_1^{(k)}$ are the frequency domain representations of $\vec{x_0}$ and $\vec{x_1}$ on the kth subcarrier, respectively.

4.3.2 Decoding at the RS

At the end of each transmission block, the relay receives (in the frequency domain):

$$\begin{aligned} Y_r^{(k)} &= H_{s_i r}^{(k)} X_{s_i}^{(k)} + W_r^{(k)} \\ &= \sqrt{\beta P_{s_i}^{(k)}} H_{s_i r}^{(k)} X_0^{(k)} + \sqrt{\bar{\beta} P_{s_i}^{(k)}} H_{s_i r}^{(k)} X_1^{(k)} + W_r^{(k)}. \end{aligned} \tag{4.7}$$

To eliminate the intersymbol interference and achieve similar performance of OFDMA with the same overall complexity, frequency domain equalization is performed before the signals are transformed and decoded in the time domain. ZF and MMSE are the two commonly used frequency domain equalization techniques in the SC-FDMA system. ZF equalization can completely eliminate the ISI with a simple structure. However, it degrades the system performance due to noise enhancement. Superior performance can be achieved using the MMSE equalization [48, 49]. In the following, the achievable rate of the SC-FDMA relay system is derived for both ZF and MMSE equalization techniques.

ZF equalization

If zero-forcing equalization technique is employed at the receiver of RS, the output signal of the equalizer on subcarrier k is given by

$$\begin{aligned} Z_r^{(k)} =& \frac{Y_r^{(k)}}{\sqrt{\beta P_{s_i}^{(k)}} H_{s_i r}^{(k)}} \\ =& X_0^{(k)} + \sqrt{\bar{\beta}/\beta} X_1^{(k)} + \frac{W_r^{(k)}}{\sqrt{\beta P_{s_i}^{(k)}} H_{s_i r}^{(k)}}. \end{aligned} \tag{4.8}$$

The decoding process is carried out in the time domain. After the subcarrier de-mapping and IDFT, the uth element of the time-domain sequence $\vec{z_r}$ is given by

$$\begin{aligned} z_r(u) &= \frac{1}{\sqrt{N_i}} \sum_{k=1}^{N_i} Z_r^{(k)} e^{j2\pi ku/N_i} \\ &= x_0(u) + \sqrt{\bar{\beta}/\beta} \cdot x_1(u) + \frac{1}{\sqrt{N_i}} \sum_k \frac{W_r^{(k)}}{\sqrt{\beta P_{s_i}^{(k)}} H_{s_i r}^{(k)}} e^{j2\pi ku/N_i}. \end{aligned} \tag{4.9}$$

Since $\vec{x_1}$ is the RS's transmitted symbol in the current transmission block, the unknown information in this channel is $\vec{x_0}$. Therefore, at the end of the transmission block b, the RS

needs to decode $\vec{x_0}$ and w_b, where w_b will be re-encoded and transmitted in the subsequent transmission block by the RS. The maximum achievable rate for the RS to decode $\mathbf{x}_0$ is given by

$$\begin{aligned} R_r^{\mathrm{ZF}} =& I(X_0; Z_r|X_1) \\ =& C\bigg(\Big(\frac{1}{N_i}\sum_k \frac{\sigma_r^2}{\beta P_{s_i}^{(k)}|H_{s_ir}^{(k)}|^2}\Big)^{-1}\bigg), \end{aligned} \tag{4.10}$$

where $C(x) = \log_2(1+x)$.

MMSE equalization

Unlike ZF equalization, MMSE equalization technique also suppresses noise, thus it can achieve higher transmission rate. The output of an MMSE equalizer on the kth subcarrier is given by

$$\begin{aligned} Z_r^{(k)} &= \frac{\sqrt{\beta P_{s_i}^{(k)}} H_{s_ir}^{(k)^*}}{\beta P_{s_i}^{(k)}|H_{s_ir}^{(k)}|^2 + \sigma_r^2} Y_r^{(k)} \\ &= \frac{\beta P_{s_i}^{(k)}|H_{s_ir}^{(k)}|^2}{\beta P_{s_i}^{(k)}|H_{s_ir}^{(k)}|^2 + \sigma_r^2} X_0^{(k)} + \frac{\sqrt{\beta\bar{\beta}} P_{s_i}^{(k)}|H_{s_ir}^{(k)}|^2}{\beta P_{s_i}^{(k)}|H_{s_ir}^{(k)}|^2 + \sigma_r^2} X_1^{(k)} + \frac{\sqrt{\beta P_{s_i}^{(k)}} H_{s_ir}^{(k)^*}}{\beta P_{s_i}^{(k)}|H_{s_ir}^{(k)}|^2 + \sigma_r^2} W_r^{(k)}. \end{aligned} \tag{4.11}$$

The uth element of the time-domain sequence $\vec{z_r}$ is given by

$$\begin{aligned} z_r(u) =& \frac{1}{\sqrt{N_i}} \sum_k \frac{\beta P_{s_i}^{(k)}|H_{s_ir}^{(k)}|^2}{\beta P_{s_i}^{(k)}|H_{s_ir}^{(k)}|^2 + \sigma_r^2} X_0^{(k)} e^{j2\pi ku/N_i} \\ &+ \frac{1}{\sqrt{N_i}} \sum_k \frac{\sqrt{\beta\bar{\beta}} P_{s_i}^{(k)}|H_{s_ir}^{(k)}|^2}{\beta P_{s_i}^{(k)}|H_{s_ir}^{(k)}|^2 + \sigma_r^2} X_1^{(k)} e^{j2\pi ku/N_i} \\ &+ \frac{1}{\sqrt{N_i}} \sum_k \frac{\sqrt{\beta P_{s_i}^{(k)}} H_{s_ir}^{(k)^*}}{\beta P_{s_i}^{(k)}|H_{s_ir}^{(k)}|^2 + \sigma_r^2} W_r^{(k)} e^{j2\pi ku/N_i}. \end{aligned} \tag{4.12}$$

Let

$$\lambda = \frac{1}{N_i}\sum_k \frac{\beta P_{s_i}^{(k)}|H_{s_i r}^{(k)}|^2}{\beta P_{s_i}^{(k)}|H_{s_i r}^{(k)}|^2 + \sigma_r^2}. \tag{4.13}$$

To decode $\vec{x_0}$, the achievable rate is then given by

$$\begin{aligned} R_r^{\text{MMSE}} &= C\Big(\frac{\lambda^2}{\lambda - \lambda^2}\Big) \\ &= C\left(\frac{\frac{1}{N_i}\sum_k \frac{\beta P_{s_i}^{(k)}|H_{s_i r}^{(k)}|^2}{\beta P_{s_i}^{(k)}|H_{s_i r}^{(k)}|^2+\sigma_r^2}}{1 - \frac{1}{N_i}\sum_k \frac{\beta P_{s_i}^{(k)}|H_{s_i r}^{(k)}|^2}{\beta P_{s_i}^{(k)}|H_{s_i r}^{(k)}|^2+\sigma_r^2}}\right) \\ &= C\left(\left[\Big(\frac{1}{N_i}\sum_k \frac{\beta P_{s_i}^{(k)}|H_{s_i r}^{(k)}|^2}{\beta P_{s_i}^{(k)}|H_{s_i r}^{(k)}|^2 + \sigma_r^2}\Big)^{-1} - 1\right]^{-1}\right). \end{aligned} \tag{4.14}$$

4.3.3 Decoding at the eNB

On the kth subcarrier, the destination eNB receives the superposition of the UE signal and the relay signal, i.e.,

$$\begin{aligned} Y_d^{(k)} &= H_{s_i d}^{(k)} X_{s_i}^{(k)} + H_{rd}^{(k)} X_r^{(k)} + W_d^{(k)} \\ &= \sqrt{\beta P_{s_i}^{(k)}} H_{s_i d}^{(k)} X_0^{(k)} + W_d^{(k)} + \left(\sqrt{\bar{\beta} P_{s_i}^{(k)}} H_{s_i d}^{(k)} + \sqrt{P_r^{(k)}} H_{rd}^{(k)}\right) X_1^{(k)}. \end{aligned} \tag{4.15}$$

At the end of transmission block b, the eNB decodes the previous block's message w_{b-1} in two steps based on the received signals of block b and $b-1$. Denote the time domain symbol for decoding as z_d. First, $\vec{x_1}$ from block b is decoded at rate $R_{d1} = I(X_1; Z_d)$ while treating $\vec{x_0}$ as noise. Then based on the decoded $\vec{x_1}$, $\vec{x_0}$ from block $b-1$ and w_{b-1} are decoded at rate $R_d = I(X_0; Z_d|X_1) + R_{d1} = I(X_0, X_1; Z_d)$. The structure of the equalization and decoding process at the eNB in the SC-FDMA system is shown in Fig. 4.3.

At the receiver during each transmission block, the frequency-domain sequence after the N-point DFT goes into two parallel equalizers. The first equalizer is designed to equalize

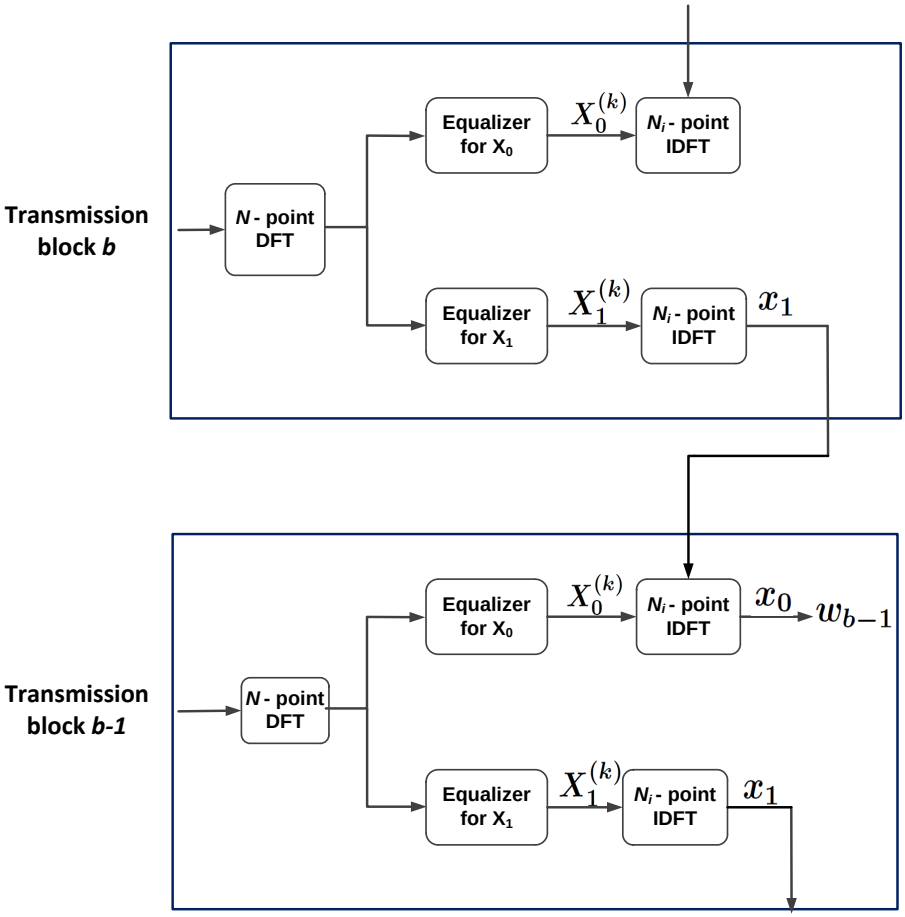

Figure 4.3: Equalization and decoding process at the eNB.

$X_1^{(k)}$ and the second equalizer is for $X_0^{(k)}$ equalization. Combined with the decoded $\vec{x_1}$ from block b, the joint decoding process in block $b-1$ is able to decode $\vec{x_0}$ and w_{b-1}.

ZF equalization

The output signal of a ZF equalizer to equalize $X_1^{(k)}$ is given by

$$\begin{aligned} Z_{d1}^{(k)} &= \frac{Y_d^{(k)}}{\sqrt{\bar{\beta}P_{s_i}^{(k)}}H_{s_id}^{(k)} + \sqrt{P_r^{(k)}}H_{rd}^{(k)}} \\ &= X_1^{(k)} + \frac{\sqrt{\beta P_{s_i}^{(k)}}H_{s_id}^{(k)}}{\sqrt{\bar{\beta}P_{s_i}^{(k)}}H_{s_id}^{(k)} + \sqrt{P_r^{(k)}}H_{rd}^{(k)}}X_0^{(k)} + \frac{1}{\sqrt{\bar{\beta}P_{s_i}^{(k)}}H_{s_id}^{(k)} + \sqrt{P_r^{(k)}}H_{rd}^{(k)}}W_d^{(k)}. \end{aligned} \tag{4.16}$$

Therefore, the uth element of the time domain signal $\vec{z_{d1}}$ is the IDFT of $Z_{d1}^{(k)}$, which is given by

$$\begin{aligned} z_{d1}(u) = x_1(u) &+ \mathrm{IDFT}\left(\frac{\sqrt{\beta P_{s_i}^{(k)}}H_{s_id}^{(k)}}{\sqrt{\bar{\beta}P_{s_i}^{(k)}}H_{s_id}^{(k)} + \sqrt{P_r^{(k)}}H_{rd}^{(k)}}X_0^{(k)}\right) \\ &+ \mathrm{IDFT}\left(\frac{1}{\sqrt{\bar{\beta}P_{s_i}^{(k)}}H_{s_id}^{(k)} + \sqrt{P_r^{(k)}}H_{rd}^{(k)}}W_d^{(k)}\right). \end{aligned} \tag{4.17}$$

The maximum achievable rate for the eNB to decode $\vec{x_1}$ is thus given by

$$\begin{aligned} R_{d1}^{\mathrm{ZF}} &= I(X_1; Z_{d1}) \\ &= C\left(\left(\frac{1}{N_i}\sum_k \frac{\beta P_{s_i}^{(k)}|H_{s_id}^{(k)}|^2 + \sigma_d^2}{\left|\sqrt{\bar{\beta}P_{s_i}^{(k)}}H_{s_id}^{(k)} + \sqrt{P_r^{(k)}}H_{rd}^{(k)}\right|^2}\right)^{-1}\right). \end{aligned} \tag{4.18}$$

Then, we decode $\vec{x_0}$ and the message w_{b-1}. The output signal of the equalizer for $X_0^{(k)}$ on the kth subcarrier is given by

$$\begin{aligned} Z_{d2}^{(k)} &= \frac{Y_d^{(k)}}{\sqrt{\beta P_{s_i}^{(k)}}H_{s_id}^{(k)}} \\ &= X_0^{(k)} + \frac{1}{\sqrt{\beta P_{s_i}^{(k)}}H_{s_id}^{(k)}}W_d^{(k)} + \frac{\sqrt{\bar{\beta}P_{s_i}^{(k)}}H_{s_id}^{(k)} + \sqrt{P_r^{(k)}}H_{rd}^{(k)}}{\sqrt{\beta P_{s_i}^{(k)}}H_{s_id}^{(k)}}X_1^{(k)}. \end{aligned} \tag{4.19}$$

The uth element of the time domain signal after the IDFT can be written as

$$z_{d2}(u) = x_0(u) + \mathrm{IDFT}\left(\frac{1}{\sqrt{\beta P_{s_i}^{(k)}} H_{s_i d}^{(k)}} W_d^{(k)}\right) + \mathrm{IDFT}\left(\frac{\sqrt{\bar{\beta} P_{s_i}^{(k)}} H_{s_i d}^{(k)} + \sqrt{P_r^{(k)}} H_{rd}^{(k)}}{\sqrt{\beta P_{s_i}^{(k)}} H_{s_i d}^{(k)}} X_1^{(k)}\right). \tag{4.20}$$

Then, the total achievable rate for the destination to decode $\vec{x_0}$ and w_{b-1} with ZF equalization is given by

$$\begin{aligned} R_d^{\mathrm{ZF}} &= I(X_0; Z_{d2}|X_1) + R_{d1}^{\mathrm{ZF}} \\ &= C\left(\left(\frac{1}{N_i}\sum_k \frac{\sigma_d^2}{\beta P_{s_i}^{(k)} |H_{s_i d}^{(k)}|^2}\right)^{-1}\right) + C\left(\left(\frac{1}{N_i}\sum_k \frac{\beta P_{s_i}^{(k)} |H_{s_i d}^{(k)}|^2 + \sigma_d^2}{\left|\sqrt{\bar{\beta} P_{s_i}^{(k)}} H_{s_i d}^{(k)} + \sqrt{P_r^{(k)}} H_{rd}^{(k)}\right|^2}\right)^{-1}\right). \end{aligned} \tag{4.21}$$

MMSE equalization

If MMSE equalization is employed at the receiver, the output signal of the equalizer for $X_1^{(k)}$ is given by

$$\begin{aligned} Z_{d1}^{(k)} =& \frac{\left(\sqrt{\bar{\beta} P_{s_i}^{(k)}} H_{s_i d}^{(k)} + \sqrt{P_r^{(k)}} H_{rd}^{(k)}\right)^*}{\left|\sqrt{\bar{\beta} P_{s_i}^{(k)}} H_{s_i d}^{(k)} + \sqrt{P_r^{(k)}} H_{rd}^{(k)}\right|^2 + \sigma_d^2} Y_d^{(k)} \\ =& \frac{\left|\sqrt{\bar{\beta} P_{s_i}^{(k)}} H_{s_i d}^{(k)} + \sqrt{P_r^{(k)}} H_{rd}^{(k)}\right|^2}{\left|\sqrt{\bar{\beta} P_{s_i}^{(k)}} H_{s_i d}^{(k)} + \sqrt{P_r^{(k)}} H_{rd}^{(k)}\right|^2 + \sigma_d^2} X_1^{(k)} \\ &+ \frac{\sqrt{\beta P_{s_i}^{(k)}} H_{s_i d}^{(k)} \left(\sqrt{\bar{\beta} P_{s_i}^{(k)}} H_{s_i d}^{(k)} + \sqrt{P_r^{(k)}} H_{rd}^{(k)}\right)^*}{\left|\sqrt{\bar{\beta} P_{s_i}^{(k)}} H_{s_i d}^{(k)} + \sqrt{P_r^{(k)}} H_{rd}^{(k)}\right|^2 + \sigma_d^2} X_0^{(k)} \\ &+ \frac{\left(\sqrt{\bar{\beta} P_{s_i}^{(k)}} H_{s_i d}^{(k)} + \sqrt{P_r^{(k)}} H_{rd}^{(k)}\right)^*}{\left|\sqrt{\bar{\beta} P_{s_i}^{(k)}} H_{s_i d}^{(k)} + \sqrt{P_r^{(k)}} H_{rd}^{(k)}\right|^2 + \sigma_d^2} W_d^{(k)}. \end{aligned} \tag{4.22}$$

By the same argument, the signal is then transformed into the time domain by the IDFT for decision. Let

$$\lambda_1 = \frac{1}{N_i}\sum_k \frac{\left|\sqrt{\bar{\beta}P_{s_i}^{(k)}}H_{s_id}^{(k)} + \sqrt{P_r^{(k)}}H_{rd}^{(k)}\right|^2}{\left|\sqrt{\bar{\beta}P_{s_i}^{(k)}}H_{s_id}^{(k)} + \sqrt{P_r^{(k)}}H_{rd}^{(k)}\right|^2 + \sigma_d^2}. \tag{4.23}$$

The decoding rate for $\vec{x_1}$ at the eNB is thus given by

$$\begin{aligned} R_{d1}^{\text{MMSE}} &= C\left(\frac{\lambda_1}{1-\lambda_1}\right) \\ &= C\left(\left[\left(\frac{1}{N_i}\sum_k \frac{\left|\sqrt{\bar{\beta}P_{s_i}^{(k)}}H_{s_id}^{(k)} + \sqrt{P_r^{(k)}}H_{rd}^{(k)}\right|^2}{\left|\sqrt{\bar{\beta}P_{s_i}^{(k)}}H_{s_id}^{(k)} + \sqrt{P_r^{(k)}}H_{rd}^{(k)}\right|^2 + \sigma_d^2}\right)^{-1} - 1\right]^{-1}\right). \end{aligned} \tag{4.24}$$

The output signal of the MMSE equalizer for $X_0^{(k)}$ is given by

$$\begin{aligned} Z_{d2}^{(k)} &= \frac{\sqrt{\beta P_{s_i}^{(k)}}H_{s_id}^{(k)^*}}{\beta P_{s_i}^{(k)}|H_{s_id}^{(k)}|^2 + \sigma_d^2}Y_d^{(k)} \\ &= \frac{\beta P_{s_i}^{(k)}|H_{s_id}^{(k)}|^2}{\beta P_{s_i}^{(k)}|H_{s_id}^{(k)}|^2 + \sigma_d^2}X_0^{(k)} + \frac{\sqrt{\beta P_{s_i}^{(k)}}H_{s_id}^{(k)^*}}{\beta P_{s_i}^{(k)}|H_{s_id}^{(k)}|^2 + \sigma_d^2}W_d^{(k)} \\ &+ \frac{\sqrt{\beta P_{s_i}^{(k)}}H_{s_id}^{(k)^*}\left(\sqrt{\bar{\beta}P_{s_i}^{(k)}}H_{s_id}^{(k)} + \sqrt{P_r^{(k)}}H_{rd}^{(k)}\right)}{\beta P_{s_i}^{(k)}|H_{s_id}^{(k)}|^2 + \sigma_d^2}X_1^{(k)}. \end{aligned} \tag{4.25}$$

Denote λ_2 as

$$\lambda_2 = \frac{1}{N_i}\sum_k \frac{\beta P_{s_i}^{(k)}|H_{s_id}^{(k)}|^2}{\beta P_{s_i}^{(k)}|H_{s_id}^{(k)}|^2 + \sigma_d^2}. \tag{4.26}$$

The maximum achievable rate for decoding $\vec{x_0}$ and w_{b-1} at the eNB with MMSE equal-

ization can be calculated as

$$
\begin{aligned}
R_d^{\mathrm{MMSE}} &= C\left(\frac{\lambda_2}{1-\lambda_2}\right) + R_{d1}^{\mathrm{MMSE}} \\
&= C\left(\left[\left(\frac{1}{N_i}\sum_k \frac{\beta P_{s_i}^{(k)}|H_{s_id}^{(k)}|^2}{\beta P_{s_i}^{(k)}|H_{s_id}^{(k)}|^2+\sigma_d^2}\right)^{-1}-1\right]^{-1}\right)+ \\
&C\left(\left[\left(\frac{1}{N_i}\sum_k \frac{\left|\sqrt{\bar{\beta}P_{s_i}^{(k)}}H_{s_id}^{(k)}+\sqrt{P_r^{(k)}}H_{rd}^{(k)}\right|^2}{\left|\sqrt{\bar{\beta}P_{s_i}^{(k)}}H_{s_id}^{(k)}+\sqrt{P_r^{(k)}}H_{rd}^{(k)}\right|^2+\sigma_d^2}\right)^{-1}-1\right]^{-1}\right).
\end{aligned} \tag{4.27}
$$

4.3.4 Achievable Rates

The maximum achievable rate for user i to transmit in the SC-FDMA system with the help of a relay station is the minimum of the RS decoding rate and the eNB decoding rate. If ZF equalization technique is utilized, the achievable rate for user i's transmission is given by

$$
R_i^{\mathrm{ZF}} = \max_{0<\beta<1} \min\left\{R_r^{\mathrm{ZF}}, R_d^{\mathrm{ZF}}\right\}, \tag{4.28}
$$

and the achievable rate with MMSE equalization technique is

$$
R_i^{\mathrm{MMSE}} = \max_{0<\beta<1} \min\left\{R_r^{\mathrm{MMSE}}, R_d^{\mathrm{MMSE}}\right\}. \tag{4.29}
$$

4.4 Power Allocation for Throughput Maximization

Based on the achievable rate of the SC-FDMA relay system derived in the previous section, we allocate transmission power among the subcarriers at both UE and RS to maximize the cooperation gain and the overall throughput of the system.

The problem can be modeled mathematically as the following optimization problem:

$$\begin{aligned} \max_{P_{s_i}^{(k)}, P_r^{(k)}} & \sum_{i \in \mathcal{M}} R_i \\ \text{subject to } & \sum_{k \in \mathcal{N}_i} P_{s_i}^{(k)} \leq P_{s_i}, \forall i \in \mathcal{M} \\ & \sum_{k \in \mathcal{N}} P_r^{(k)} \leq P_r \\ & P_{s_i}^{(k)} \geq 0, \text{for all } k, \, i \\ & P_r^{(k)} \geq 0, \text{for all } k. \end{aligned} \tag{4.30}$$

The objective is to maximize the summation of the uplink achievable rates of all users in the network. For uplink transmission, each user has its individual power constraint. The relay's transmission power on all subcarriers satisfy a total power constraint.

Since (4.30) is a max-min problem, generally it is very difficult to solve. However, as each user occupies an exclusive set of subcarriers and has individual power constraint, this problem can be decomposed into a two-layer power allocation problem. We first maximize the achievable rate of a single user through allocating power among its assigned subcarriers at both UE and RS assuming a fixed power constraint at the RS for the user, i.e.,

$$\begin{aligned} \max_{P_{s_i}^{(k)}, P_r^{(k)}} & R_i \\ \text{subject to } & \sum_{k \in \mathcal{N}_i} P_{s_i}^{(k)} \leq P_{s_i} \\ & \sum_{k \in \mathcal{N}_i} P_r^{(k)} \leq P_{r_i} \\ & P_{s_i}^{(k)} \geq 0, \text{for all } k \\ & P_r^{(k)} \geq 0, \text{for all } k. \end{aligned} \tag{4.31}$$

In (4.31), the total power available for relaying user i's information at the RS is denoted as P_{r_i}. In the second subproblem, the RS distributes its total available transmission power among all users to maximize the overall throughput, i.e.,

$$\begin{aligned} &\max_{P_{r_i}} \sum_{i\in\mathcal{M}} R_i \\ \text{subject to } &\sum_{i\in\mathcal{M}} P_{r_i} \leq P_r \\ &P_{r_i} \geq 0, \text{for all } i. \end{aligned} \tag{4.32}$$

In the following, we consider the uplink SC-FDMA system employing ZF and MMSE equalization techniques separately and solve the two-layer optimization problem accordingly.

4.4.1 Power Allocation with ZF Equalization

The objective is to solve the two-layer optimization problem when a ZF equalization is utilized. In the uplink communication systems, the function and transmission power of the transmitters are normally both very limited. To simplify the transmitter design, we focus on the asynchronous relaying case with the power dividing parameter $\beta = 1$, i.e., the source and the relay use independent codes.

In the asynchronous case, the single user's uplink achievable rate can be written as:

$$\begin{aligned} R_i^{\text{ZF}} = \min \Bigg\{ & C\Bigg(\Big(\frac{1}{N_i}\sum_k \frac{\sigma_r^2}{P_{s_i}^{(k)}|H_{s_ir}^{(k)}|^2}\Big)^{-1}\Bigg), \\ & C\Bigg(\Big(\frac{1}{N_i}\sum_k \frac{P_{s_i}^{(k)}|H_{s_id}^{(k)}|^2+\sigma_d^2}{P_r^{(k)}|H_{rd}^{(k)}|^2}\Big)^{-1}\Bigg) + C\Bigg(\Big(\frac{1}{N_i}\sum_k \frac{\sigma_d^2}{P_{s_i}^{(k)}|H_{s_id}^{(k)}|^2}\Big)^{-1}\Bigg)\Bigg\}, \end{aligned} \tag{4.33}$$

where the first term denotes the relay decoding rate and the second term represents the eNB decoding rate.

Consider that in the uplink communications, the transmission power at the relay station is normally much greater than the available power at the mobile terminal, i.e., $P_r^{(k)} >> P_{s_i}^{(k)}$, which means that the relay decoding rate is the bottleneck of the achievable rate for user i. Since the relay decoding rate only depends on the allocated user transmission power, (4.31) can be solved in two steps. First, we try to find the optimal power allocation among the assigned subcarriers at the UE to maximize the relay decoding rate, thus to maximize the upper bound of user i's achievable rate. Then, the optimal allocation of RS transmission power on each subcarrier can be determined to ensure that this upper bound is achievable.

To find the optimal power allocation at the UE, it is equivalent to solve the following optimization problem:

$$\begin{aligned} \min_{P_{s_i}^{(k)}} & \sum_{k\in\mathcal{N}_i} \frac{\sigma_r^2}{P_{s_i}^{(k)}|H_{s_ir}^{(k)}|^2} \\ \text{subject to } & \sum_{k\in\mathcal{N}_i} P_{s_i}^{(k)} \le P_{s_i} \\ & P_{s_i}^{(k)} \ge 0. \end{aligned} \tag{4.34}$$

Since (4.34) is a convex optimization problem, the Kuhn-Tucker condition (KKT condition) characterizes the necessary and sufficient condition that the optimal solution needs to satisfy. The Lagrangian can be written as

$$\mathcal{L} = \sum_{k\in\mathcal{N}_i} \frac{\sigma_r^2}{P_{s_i}^{(k)}|H_{s_ir}^{(k)}|^2} + \lambda\Big(\sum_{k\in\mathcal{N}_i} P_{s_i}^{(k)} - P_{s_i}\Big), \tag{4.35}$$

and the KKT condition is given by

$$\frac{\partial\mathcal{L}}{\partial P_{s_i}^{(k)}} = \lambda - \frac{\sigma_r^2}{|H_{s_ir}^{(k)}|^2}\frac{1}{{P_{s_i}^{(k)}}^2} = 0, \tag{4.36}$$

where λ is chosen to satisfy the UE's transmission power constraint $\sum_{k\in\mathcal{N}_i} P_{s_i}^{(k)} \le P_{s_i}$.

Solving (4.36), the optimal $P_{s_i}^{(k)*}$ is given by

$$P_{s_i}^{(k)*} = \frac{P_{s_i}}{|H_{s_i r}^{(k)}| \cdot \sum_{k \in \mathcal{N}_i} |H_{s_i r}^{(k)}|^{-1}}. \tag{4.37}$$

Then, the optimal $P_r^{(k)*}$ should maximize the eNB decoding rate with $P_{s_i}^{(k)*}$ given in (4.37). Specifically, $P_r^{(k)*}$ can be obtained by the KKT condition with the following Lagrangian:

$$\mathcal{L} = \sum_{k \in \mathcal{N}_i} \frac{P_{s_i}^{(k)} |H_{s_i d}^{(k)}|^2 + \sigma_d^2}{P_r^{(k)} |H_{rd}^{(k)}|^2} + \mu \Big(\sum_{k \in \mathcal{N}_i} P_r^{(k)} - P_{r_i} \Big). \tag{4.38}$$

The KKT condition is given by

$$\frac{\partial \mathcal{L}}{\partial P_r^{(k)}} = \mu - \frac{P_{s_i}^{(k)} |H_{s_i d}^{(k)}|^2 + \sigma_d^2}{P_r^{(k)} |H_{rd}^{(k)}|^2} \cdot \frac{1}{{P_r^{(k)}}^2} = 0, \tag{4.39}$$

where μ is chosen to satisfy the RS power constraint $\sum_{k \in \mathcal{N}_i} P_r^{(k)} \leq P_{r_i}$.

Solving (4.39), the optimal $P_r^{(k)*}$ is given by

$$P_r^{(k)*} = \frac{P_{r_i}}{\sum_{k \in \mathcal{N}_i} \frac{\sqrt{P_{s_i}^{(k)*} |H_{s_i d}^{(k)}|^2 + \sigma_d^2}}{|H_{rd}^{(k)}|}} \cdot \frac{\sqrt{P_{s_i}^{(k)*} |H_{s_i d}^{(k)}|^2 + \sigma_d^2}}{|H_{rd}^{(k)}|}. \tag{4.40}$$

To solve subproblem (4.32), we need to allocate the RS transmission power among users to maximize the overall throughput of the system. Consider that the available transmission power at the RS is sufficient enough compared with the total power at the UE, and the eNB decoding rate increases with P_{r_i} while the RS decoding rate remains unchanged. The optimal $P_{r_i}^*$ is the smallest value that can make the eNB decoding rate equal the RS decoding rate, thus the upper bound of each user's achievable rate can be achieved.

Therefore, the optimal RS transmission power for relaying user i's information $P_{r_i}^*$ can be attained by solving the following equation:

$$C\left(\left(\frac{1}{N_i}\sum_k \frac{P_{s_i}^{(k)*}|H_{s_id}^{(k)}|^2+\sigma_d^2}{P_r^{(k)*}|H_{rd}^{(k)}|^2}\right)^{-1}\right)$$
$$= C\left(\left(\frac{1}{N_i}\sum_k \frac{\sigma_r^2}{P_{s_i}^{(k)*}|H_{s_ir}^{(k)}|^2}\right)^{-1}\right) - C\left(\left(\frac{1}{N_i}\sum_k \frac{\sigma_d^2}{P_{s_i}^{(k)*}|H_{s_id}^{(k)}|^2}\right)^{-1}\right). \quad (4.41)$$

4.4.2 Power Allocation with MMSE Equalization

The single user's achievable rate in the asynchronous relaying case when MMSE equalization technique is employed is given by

$$R_i^{\text{MMSE}} = \min\left\{C\left(\left[\left(\frac{1}{N_i}\sum_k \frac{P_{s_i}^{(k)}|H_{s_ir}^{(k)}|^2}{P_{s_i}^{(k)}|H_{s_ir}^{(k)}|^2+\sigma_r^2}\right)^{-1}-1\right]^{-1}\right),\right.$$
$$\left. C\left(\left[\left(\frac{1}{N_i}\sum_k \frac{P_r^{(k)}|H_{rd}^{(k)}|^2}{P_r^{(k)}|H_{rd}^{(k)}|^2+\sigma_d^2}\right)^{-1}-1\right]^{-1}\right)+C\left(\left[\left(\frac{1}{N_i}\sum_k \frac{P_{s_i}^{(k)}|H_{s_id}^{(k)}|^2}{P_{s_i}^{(k)}|H_{s_id}^{(k)}|^2+\sigma_d^2}\right)^{-1}-1\right]^{-1}\right)\right\}. \quad (4.42)$$

When $P_r^{(k)} >> P_{s_i}^{(k)}$, the relay decoding rate is the bottleneck of (4.42). To find the optimal user transmission power allocation to maximize the relay decoding rate, we first solve the following optimization problem:

$$\max_{P_{s_i}^{(k)}} \sum_{k\in\mathcal{N}_i} \frac{P_{s_i}^{(k)}|H_{s_ir}^{(k)}|^2}{P_{s_i}^{(k)}|H_{s_ir}^{(k)}|^2+\sigma_r^2}$$
$$\text{subject to} \sum_{k\in\mathcal{N}_i} P_{s_i}^{(k)} \le P_{s_i}$$
$$P_{s_i}^{(k)} \ge 0. \quad (4.43)$$

(4.43) is also a convex optimization problem and can be solved by the KKT condition.

The Lagrangian is given by

$$\mathcal{L} = \sum_{k\in\mathcal{N}_i} \frac{P_{s_i}^{(k)}|H_{s_ir}^{(k)}|^2}{P_{s_i}^{(k)}|H_{s_ir}^{(k)}|^2 + \sigma_r^2} - \lambda\Big(\sum_{k\in\mathcal{N}_i} P_{s_i}^{(k)} - P_{s_i}\Big), \tag{4.44}$$

and the KKT condition is given by

$$\frac{\partial\mathcal{L}}{\partial P_{s_i}^{(k)}} = \frac{|H_{s_ir}^{(k)}|^2\sigma_r^2}{\Big(P_{s_i}^{(k)}|H_{s_ir}^{(k)}|^2 + \sigma_r^2\Big)^2} - \lambda = 0, \tag{4.45}$$

where λ is determined by the transmission power constraint at user i, i.e., $\sum_{k\in\mathcal{N}_i} P_{s_i}^{(k)} \leq P_{s_i}$.

Hence the optimal $P_{s_i}^{(k)*}$ is a water-filling solution given by

$$P_{s_i}^{(k)*} = \left(\frac{\sigma_r}{|H_{s_ir}^{(k)}|\sqrt{\lambda}} - \frac{\sigma_r^2}{|H_{s_ir}^{(k)}|^2}\right)^+, \tag{4.46}$$

where function $(\cdot)^+$ is defined as

$$(x)^+ = \begin{cases} x, & \text{if } x \geq 0; \\ 0, & \text{if } x < 0. \end{cases} \tag{4.47}$$

The optimal power allocated to subcarrier k at the RS, $P_r^{(k)*}$, needs to maximize the eNB decoding rate with $P_{s_i}^{(k)*}$ given in (4.46). $P_r^{(k)*}$ can be obtained by the KKT condition. The Lagrangian is given by

$$\mathcal{L} = \sum_{k\in\mathcal{N}_i} \frac{P_r^{(k)}|H_{rd}^{(k)}|^2}{P_r^{(k)}|H_{rd}^{(k)}|^2 + \sigma_d^2} - \mu\Big(\sum_{k\in\mathcal{N}_i} P_r^{(k)} - P_{r_i}\Big). \tag{4.48}$$

The KKT condition can be written as

$$\frac{\partial\mathcal{L}}{\partial P_r^{(k)}} = \frac{|H_{rd}^{(k)}|^2\sigma_d^2}{\Big(P_r^{(k)}|H_{rd}^{(k)}|^2 + \sigma_d^2\Big)^2} - \mu = 0, \tag{4.49}$$

where μ is chosen to satisfy the transmission power constraint at the RS, i.e., $\sum_{k\in\mathcal{N}_i} P_r^{(k)} \leq P_{r_i}$.

The optimal $P_r^{(k)*}$ is also a water-filling solution given by

$$P_r^{(k)*} = \left(\frac{\sigma_d}{|H_{rd}^{(k)}|\sqrt{\mu}} - \frac{\sigma_d^2}{|H_{rd}^{(k)}|^2} \right)^+. \tag{4.50}$$

To maximize the overall throughput of the system, the optimal RS transmission power allocated for relaying user i's message, $P_{r_i}^*$, is the smallest value that can achieve the upper bound of user i's achievable rate. Specifically, $P_{r_i}^*$ makes the user i's RS decoding rate equal the eNB decoding rate and thus can be obtained by solving the following equation:

$$\begin{aligned} & C\left(\left[\left(\frac{1}{N_i} \sum_k \frac{P_r^{(k)*}|H_{rd}^{(k)}|^2}{P_r^{(k)*}|H_{rd}^{(k)}|^2 + \sigma_d^2} \right)^{-1} - 1 \right]^{-1} \right) \\ =& C\left(\left[\left(\frac{1}{N_i} \sum_k \frac{P_{s_i}^{(k)*}|H_{s_ir}^{(k)}|^2}{P_{s_i}^{(k)*}|H_{s_ir}^{(k)}|^2 + \sigma_r^2} \right)^{-1} - 1 \right]^{-1} \right) - C\left(\left[\left(\frac{1}{N_i} \sum_k \frac{P_{s_i}^{(k)*}|H_{s_id}^{(k)}|^2}{P_{s_i}^{(k)*}|H_{s_id}^{(k)}|^2 + \sigma_d^2} \right)^{-1} - 1 \right]^{-1} \right). \end{aligned} \tag{4.51}$$

4.5 Numerical Results

To verify the derived uplink achievable rates and evaluate the performance of the proposed power allocation schemes in SC-FDMA system, we present our numerical results considering practical network scenarios.

We consider that all wireless channels suffer from independent frequency selective fading and each subcarrier is subject to frequency flat Rayleigh fading. In our simulation, a typical urban area propagation model with 9 paths specified in [50] is employed, and the parameters are listed in Table 4.1.

Fig. 4.4 shows the RS decoding rate and the eNB decoding rate derived with different values of the power dividing parameter β for both ZF equalization and MMSE equalization in a single user SC-FDMA system. The uplink user equipment is allocated with one

Table 4.1: Relative power of the delay profile.

Delay (μs)	0.0	0.05	0.12	0.2	0.23	0.5	1.6	2.3	5.0
Power (dB)	-1.0	-1.0	-1.0	0.0	0.0	0.0	-3.0	-5.0	-7.0

resource block, i.e., 12 consecutive subcarriers, for transmission. The transmission power is 15dBm at both UE and RS, and is equally assigned to all allocated subcarriers. The noise variance received at the RS on each subcarrier is normalized to 1, and the noise variance at the eNB is 2.

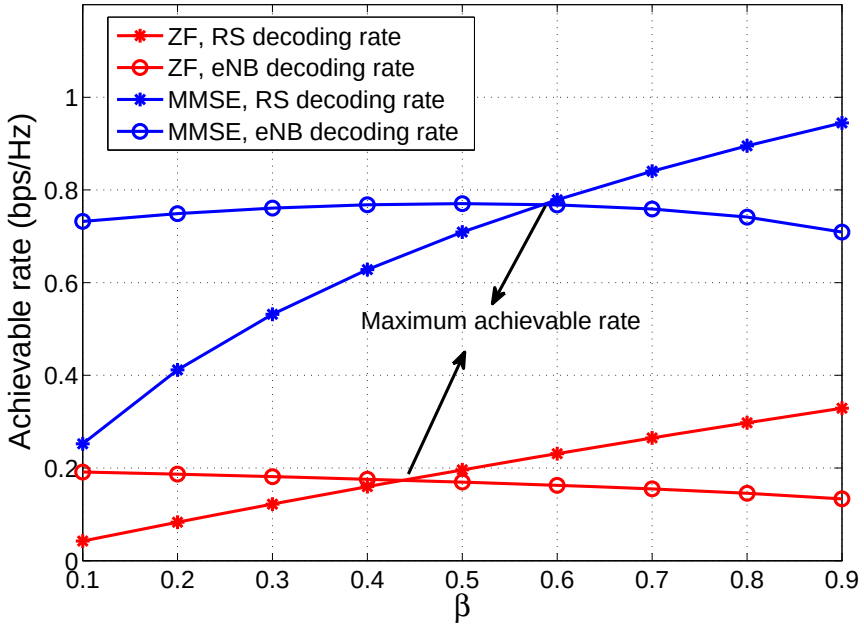

Figure 4.4: RS decoding rate and eNB decoding rate with ZF and MMSE equalization.

It can be seen that MMSE equalization generally achieves higher rate than ZF equalization due to noise suppression. The user's achievable rate is the minimum of its RS decoding rate and eNB decoding rate. The maximum achievable rate is achieved with the

optimal power dividing parameter which ensures that the user's RS decoding rate equals its eNB decoding rate.

Fig. 4.5 shows the maximum achievable rate of a single user in both OFDMA and SC-FDMA systems with MMSE and ZF equalization techniques. We compare the derived achievable rate of the decode-and-forward relay channel with the single user's capacity of the direct transmission without the help of RSs. The single user's achievable rate of the relay channel in OFDMA networks is calculated based on equation (4) in [51]. The capacity of the SC-FDMA system is determined according to equation (9) and (12) for ZF equalization and MMSE equalization, respectively. The total transmission power at the UE and RS ranges from 20dBm to 30dBm for the relaying case while the UE power matches the total transmission power for the direct transmission case in order to conduct a fair comparison. The transmission power is equally distributed on all subcarriers in both cases. The rest of the simulation parameters remain unchanged.

In Fig. 4.5, it can be seen that the spectrum efficiency of both SC-FDMA and OFDMA systems with and without relay stations increases with the total transmission power. In wireless environment, OFDMA achieves higher rate than SC-FDMA due to the parallel transmission structure of OFDMA signals. Fig. 4.5 also shows that the cooperative transmission with the help of a decode-and-forward relay can significantly improve the user rate compared with non-cooperative transmission, which demonstrates the benefits of deploying relay stations in the cellular network.

To evaluate the performance of our proposed power allocation schemes for both ZF and MMSE equalization, we first compare the single user's achievable rate achieved by our proposed power allocation schemes with an equal power allocation scheme, which is most commonly employed for deriving capacity and resource allocation schemes [28, 29] as shown in Fig. 4.6. The equal power allocation scheme assigns the transmission power at

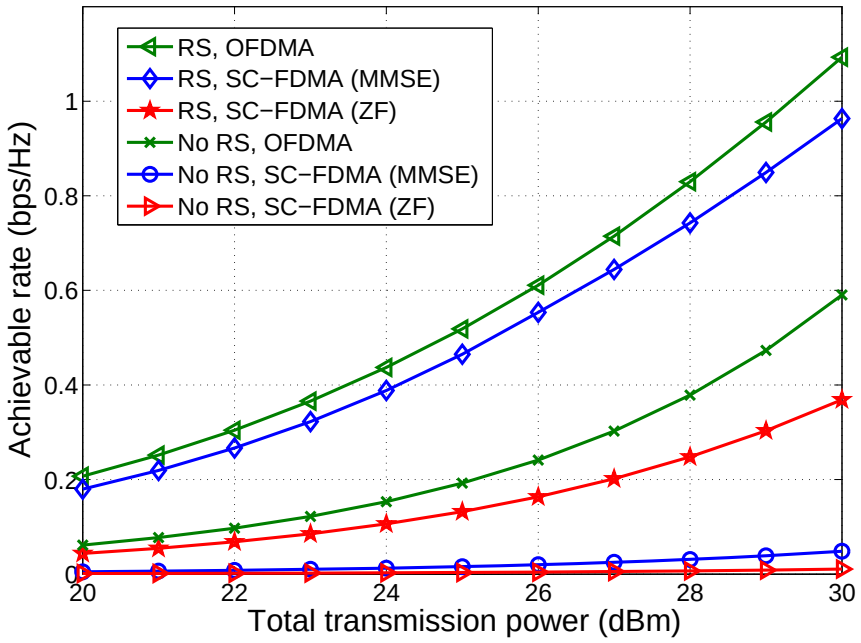

Figure 4.5: Rate comparison of SC-FDMA and OFDMA relay systems.

both UE and RS equally to all subcarriers. Consider that the transmission power at the UE is 25dBm and the transmission power at the RS for each user is fixed and ranges from 30dBm to 45dBm.

It can be seen that our proposed power allocation schemes can improve the single user's achievable rate for both ZF and MMSE equalization compared with the equal power allocation scheme. As the RS's transmission power increases, the eNB decoding rate rises accordingly while the RS decoding rate remains unchanged. Thus, the single user's achievable rate reaches an upper bound, which is determined by the RS decoding rate.

Fig. 4.7 compares the overall throughput of our proposed power allocation schemes and the equal power allocation scheme in the uplink transmission of a cellular network. The RS's total available transmission power is 50dBm, which would be allocated among

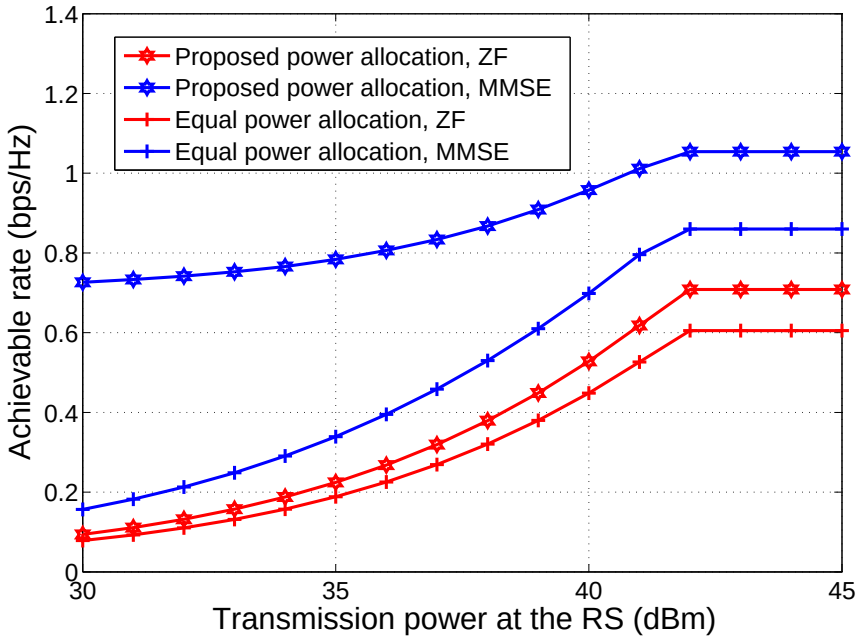

Figure 4.6: Comparison of single-user uplink achievable rates.

all users according to (4.41) and (4.51). Some simulation parameters are summarized in Table 4.2:

As the transmission bandwidth is sufficient since each user occupies only one resource block, the throughput achieved by our proposed power allocation schemes and equal power allocation scheme increases with the number of users for both ZF and MMSE equalization. It can be seen that our proposed power allocation schemes outperform the equal power allocation scheme drastically, especially in the MMSE equalization scenario. The ZF equalization shows a poor noise performance and the improvement is relatively limited as the noise contributions of highly attenuated subchannels are rather large, which limits the overall system performance.

Table 4.2: Uplink cellular network simulation parameters.

Parameter	**Value**
Cellular layout	Hexagonal grid, 6 sectors per cell
Relay station layout	1 relay station per sector
Relay protocol	Decode-and-Forward
Transmission bandwidth	20MHz
Subcarrier separation	15kHz
♯ of subcarriers in a resource block	12
Carrier frequency	2GHz for uplink
Channel model	Frequency selective Rayleigh fading
UE distribution	Uniformly random
UE transmission power	25dBm
RS transmission power	50dBm

4.6 Summary

In this chapter, we have studied the uplink cooperative transmission with Type II in-band decode-and-forward relays and power allocation to improve the transmission efficiency in an uplink LTE-Advanced cellular system. As SC-FDMA is the physical layer technique for the LTE-Advanced system, the capacity and resource allocation schemes for the downlink OFDMA system cannot be applied directly to the SC-FDMA system. Therefore, we have first studied the joint superposition coding and derived the expressions of the achievable rate of an uplink SC-FDMA system with both ZF and MMSE equalization. We then have proposed optimal power allocation schemes to maximize the overall throughput of the system.

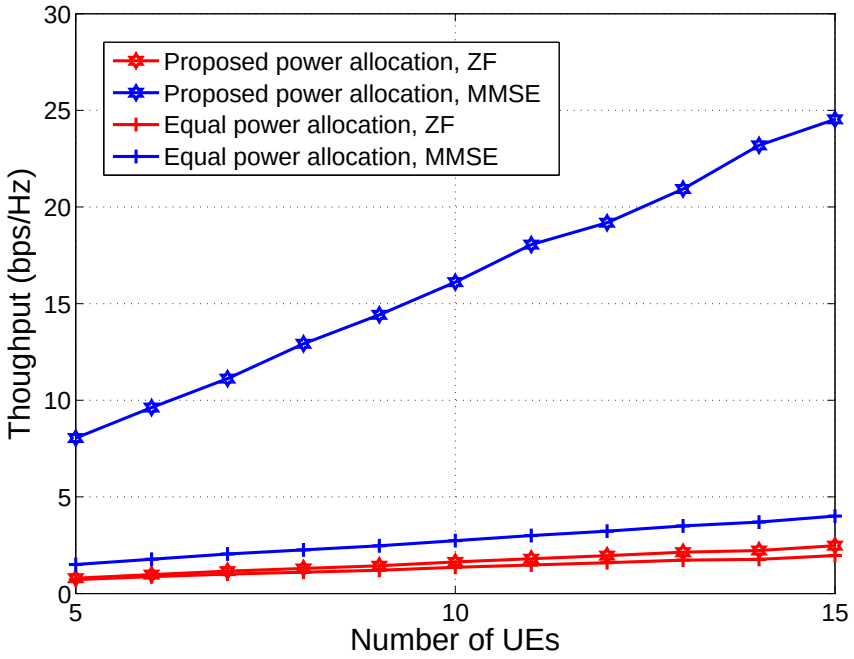

Figure 4.7: Comparison of the overall throughput in an uplink cellular network.

Chapter 5

Optimizing Network Sustainability and Efficiency in Green Cellular Networks

In this chapter, we study the resource allocation in a device-to-device communication underlaying green cellular network to improve the cellular network's throughput while maintaining the network sustainability and guaranteeing users' QoS requirement.

5.1 System Configuration

5.1.1 Green Cellular Network

With astronomical escalation of mobile terminals, the cellular industry has unprecedented growth of data traffic requirement, which leads to enormous energy consumption. In 2011,

more than 4 million base stations have been deployed to provide services for mobile users, causing an extremely high energy consumption of 25MWh per year in average [52]. Among the devices of cellular networks, the base stations (BSs) occupy almost 60% of the whole network's energy consumption [53], and more than 90% of peak energy is consumed even when a BS is idle [54]. Nowadays, the energy cost of cellular networks has become a significant portion of the operational expenditure with the increase of energy price. For example, the operation cost of a BS powered by electrical grid is approximately 3000 US dollars per year, and the cost may be ten times more if BSs are powered by diesel power generators in the rural area [52]. The rising energy costs and carbon footprint of operating cellular networks is motivating the standardization authorities and network operators to continuously explore future technologies in order to bring improvements in the entire network infrastructure.

To provide sustainable and clean power, eco-friendly green energy, e.g., solar, wind and hydro, is emerging as a popular substitute of traditional energy. Combining the advances of wireless technology with green energy, green base stations, i.e., base stations powered by green energy, are anticipated to be widely deployed to construct the future-generation cellular networks. In traditional electricity grid based cellular networks, the base stations are generally powered by limited yet stable resources, e.g., coal, petroleum and natural gas. The most critical research issue in this field is to maximize the energy efficiency, such that the energy utilization can be improved. However, unlike traditional energy, green energy highly depends on its location, local weather and time, which is naturally sustainable and highly dynamic. For example, the harvested energy by solar panels has a world of difference in daytime and night within the same day, which also varies at different locations depending on the intensity of solar radiation. The dynamic capability and availability of green energy may cause intermittent power support for green base stations, which have

shifted the fundamental design criterion and the main performance metric of green cellular networks from energy efficiency to energy sustainability. Therefore, how to efficiently allocate harvested energy to ensure the network sustainability and fulfill the explosively increasing user demand has become an essential research issue.

5.1.2 Device-to-Device Communication

As energy consumption is a critical concern in future-generation cellular networks, one of the schemes that is being considered to offload the cellular traffic and to improve user experience and resource utilization is the device-to-device communications, which is a feature appeared in LTE Release 12. LTE D2D communication is in a peer to peer manner, which does not use the cellular network infrastructure, but enables LTE based devices to communicate directly with one another when they are in close proximity. This form of communication is used where direct communication is needed within a small area.

Direct communications between devices can provide several benefits to users in various applications when the devices are in close proximity:

- Improved spectrum reuse and system throughput

  If the D2D link is far away from active cellular users, the D2D communication link could reuse the licensed spectrum in LTE network. Therefore, the spectrum utilization and the system throughput could be improved.

- Improved reliability

  Since LTE D2D communication does not rely on cellular infrastructure, devices are able to communicate locally with each other to provide high reliability communications, especially if the LTE network has failed.

- Offloading in cellular networks

  D2D communications allow large volumes of data to be transferred from one device to another over short distances and using a direct connection. This form of D2D link could transfer data without overloading the cellular network.

- Improved energy efficiency

  D2D communication could reduce the energy consumption of the base station and improve the energy utilization of the entire network by employing lower transmission power level as the distance of the communication is shorter.

5.1.3 Network Model

In this chapter, we combine both green technology and D2D communications to improve the spectrum and energy efficiency in the cellular network. Specifically, we consider a device-to-device communication underlaying cellular network as shown in Fig. 5.1. The network consists of a set of wireless users and a single BS, where all the users are located within the transmission range of the BS. The wireless channels of cellular network and D2D communication are orthogonal with each other, thus the interference between cellular network and D2D communication is ignorable. Wireless users can communicate with each other by either cellular network through the BS or by direct data transmission through device-to-device communication. As the BS occupies almost 60% energy consumption of the whole network, a green BS, i.e., a BS powered by renewable energy, is equipped in the network. Since the renewable energy is by nature intermittent and variable, the BS is associated with a rechargeable battery with large capacity to buffer the dynamically charged energy and to provide a constant power output. To ensure the network connectivity, a back up energy source, such as power grid or battery is also available at the BS to provide

temporary power supply in some extreme cases when the harvested renewable energy is unable to support reliable communication.

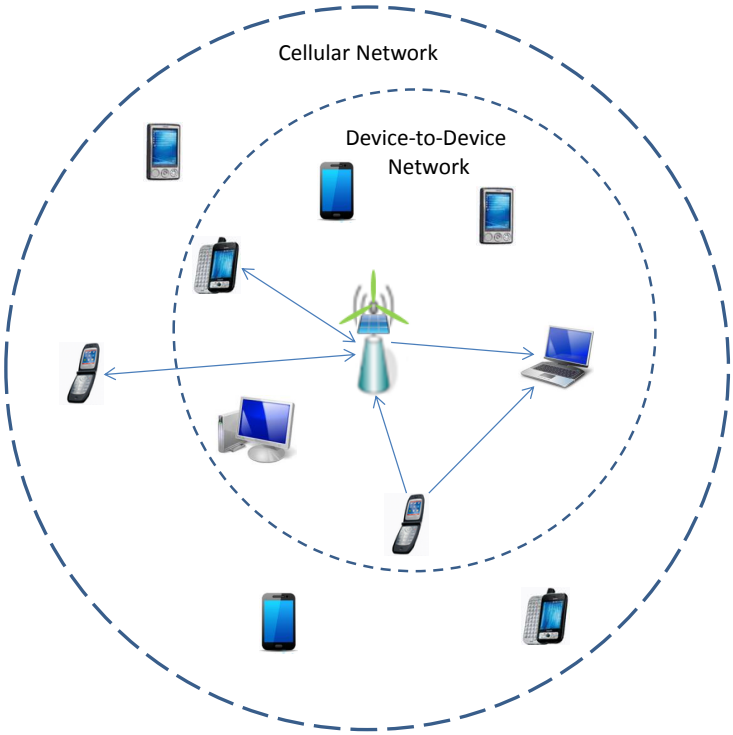

Figure 5.1: A green device-to-device communication underlaying cellular network.

For device-to-device communication in the network, each mobile user can communicate with all other users within the network, and has the same time period for transmission. As the D2D communication is orthogonal to cellular radio, we consider that the green BS functions as a relay in the D2D network and is capable of cooperation to further improve the D2D transmission rate. In this chapter, we also adopt the DF protocol at the BS to better exploit the broadcast nature of wireless signals, so that the source and the relay are able to transmit at the same time and on the same frequency band to improve the spectrum efficiency.

In order to maintain fairness, each user has the same time period T for data transmission, which is scheduled by the BS through Time Division Multiple Access (TDMA) in a synchronized manner. During each time period, only one source-destination pair, i.e., one communication channel is permitted for transmission in the network. Suppose there are m pairs in the network, represented by $\mathcal{M} = \{1, \ldots, m\}$. Let i be the current active channel, $i = 1, \ldots, m$. The source node, destination node and the BS for channel i are denoted as s_i and d_i and r, respectively. As only one source-destination pair is allowed to transmit, each transmission channel in this network forms a three-terminal relay channel. To avoid the confusion, in the rest of this chapter, the term "BS" and "relay node" will be used interchangeably.

In the D2D network, assume that all wireless channels are independent AWGN channels. The channel gain coefficients are denoted by $h_{s_i r}$, $h_{r d_i}$ and $h_{s_i d_i}$ representing the channel conditions for the source-BS, BS-destination and source-destination channels, respectively. The channel gain coefficients can be obtained through a feedback channel in cellular networks. Here, we assume that these coefficients can be estimated accurately at the BS. The variances of independent Gaussian noises received at the relay node r and at the destination node d_i are both normalized to 1.

Suppose the transmitting power at the source node is bounded by

$$\frac{1}{S}\sum_{t=1}^{S} x_{s_i}^2(t) \leq P_s^{(i)}, \tag{5.1}$$

and the transmitting power constraint for the relay node when channel i is active is

$$\frac{1}{S}\sum_{t=1}^{S} x_r^2(t) \leq P_r^{(i)}. \tag{5.2}$$

As shown in Section 2.2.2, when channel i is active, the highest achievable rate of the

relay channel is given by

$$
\begin{aligned}
R^{(i)} &= \max_{p(x_{s_i},x_r)} \min\{I(X_{s_i};Y_r|X_r), I(X_{s_i},X_r;Y_{d_i})\} \\
&= \max_{0\le\beta\le 1} \min\left\{ \frac{1}{2}\log\left(1+|h_{s_ir}|^2\beta P_s^{(i)}\right), \right. \\
&\quad \left. \frac{1}{2}\log\left(1+|h_{s_id_i}|^2\beta P_s^{(i)} + \left(\sqrt{|h_{s_id_i}|^2\bar{\beta}P_s^{(i)}} + \sqrt{|h_{rd_i}|^2 P_r^{(i)}}\right)^2\right)\right\}. \qquad (5.3)
\end{aligned}
$$

5.2 Rate Maximization

As each single user's achievable rate can be improved by optimally adapting the transmission power, in this section, we consider two types of power constraints, depending on whether wireless users are capable of adjusting their transmission power, and present the optimal power adaptation schemes and the maximum single link's achievable rates separately.

- Both wireless users and BS can adopt different power levels for data transmission. We aim to maximize the transmission efficiency, i.e., to maximize the overall transmission rate of the channel under a total power constraint.
- Only BS is able to adjust its power level and all wireless users transmit with a fixed power. In this scenario, we will derive the optimal transmission power at the BS in terms of maximizing the transmission rate.

5.2.1 Rate Maximization under a Total Power Constraint

The objective is to allocate $P_s^{(i)}$ and $P_r^{(i)}$ under a total power consumption constraint $P_{tot}^{(i)}$, which is the maximum available transmission power for channel i. The problem can be

formulated as the following optimization problem:

$$\begin{aligned} \max_{P_s^{(i)}, P_r^{(i)}} \quad & R^{(i)} \\ \text{subject to} \quad & P_s^{(i)} + P_r^{(i)} \leq P_{tot}^{(i)} \\ & P_s^{(i)} \geq 0 \\ & P_r^{(i)} \geq 0. \end{aligned} \tag{5.4}$$

The rate maximization problem under a total power constraint is similar to the power dividing problem in a single-user relay channel shown in (3.7). As the detailed process of solving this problem have been derived in Section 3.2, in this subsection, we only provide the optimal power adaptation schemes and the maximum single link's achievable rate.

Synchronous Case

In this case, the destination decoding rate is the bottleneck, and $\beta < 1$. Denote $P_{s_1}^{(i)} = \beta P_s^{(i)}$ and $P_{s_2}^{(i)} = \bar{\beta} P_s^{(i)}$ as the two components of $P_s^{(i)}$. Following the same argument in Section 3.2, the optimal power adaptation scheme when $|h_{s_i d_i}| \leq |h_{s_i r}|$ is given by

$$\begin{aligned} P_{s_1}^{(i)} &= \frac{|h_{s_i d_i}|^2 + |h_{r d_i}|^2}{|h_{s_i r}|^2 + |h_{r d_i}|^2} P_{tot}^{(i)}, \\ P_{s_2}^{(i)} &= \frac{|h_{s_i d_i}|^2 (|h_{s_i r}|^2 - |h_{s_i d_i}|^2)}{(|h_{s_i d_i}|^2 + |h_{r d_i}|^2)(|h_{s_i r}|^2 + |h_{r d_i}|^2)} P_{tot}^{(i)}, \\ P_r^{(i)} &= \frac{|h_{r d_i}|^2 (|h_{s_i r}|^2 - |h_{s_i d_i}|^2)}{(|h_{s_i d_i}|^2 + |h_{r d_i}|^2)(|h_{s_i r}|^2 + |h_{r d_i}|^2)} P_{tot}^{(i)}. \end{aligned} \tag{5.5}$$

With the optimal power adaptation scheme, the maximum single link's achievable rate in the synchronous case is given by

$$R_{sync}^{(i)} = \frac{1}{2} \log \left(1 + \frac{|h_{s_i r}|^2 (|h_{s_i d_i}|^2 + |h_{r d_i}|^2)}{|h_{s_i r}|^2 + |h_{r d_i}|^2} \cdot P_{tot}^{(i)} \right). \tag{5.6}$$

If $|h_{s_i d_i}| > |h_{s_i r}|$, the source-destination channel has a better channel condition. In this case, the BS does not help the source-destination transmission to avoid the waste of resources, and the highest end user rate (channel capacity) for non-cooperative transmission is

$$R_{dir}^{(i)} = \frac{1}{2} \log \left(1 + |h_{s_i d_i}|^2 P_s^{(i)}\right). \tag{5.7}$$

Asynchronous Case

The source and the relay employ independent codes, so that $\beta = 1$. When $|h_{s_i d_i}| \leq |h_{s_i r}|$, the following power adaptation scheme is optimal:

$$\begin{aligned} P_s^{(i)} =& \frac{|h_{rd_i}|^2}{|h_{s_i r}|^2 - |h_{s_i d_i}|^2 + |h_{rd_i}|^2} P_{tot}^{(i)}, \\ P_r^{(i)} =& \frac{|h_{s_i r}|^2 - |h_{s_i d_i}|^2}{|h_{s_i r}|^2 - |h_{s_i d_i}|^2 + |h_{rd_i}|^2} P_{tot}^{(i)}, \end{aligned} \tag{5.8}$$

and the maximum single link's achievable rate in the asynchronous case is given by

$$R_{asyn}^{(i)} = \frac{1}{2} \log \left(1 + \frac{|h_{s_i r}|^2 |h_{rd_i}|^2}{|h_{s_i r}|^2 - |h_{s_i d_i}|^2 + |h_{rd_i}|^2} \cdot P_{tot}^{(i)}\right). \tag{5.9}$$

Remark 1. *The optimal cooperation strategy and power adaptation scheme to maximize the achievable rate depends on the channel conditions and the locations of the users. For example, in the AWGN environment with path loss, if BS is closer to the source, the power allocation for the synchronous case achieves higher rate; otherwise, the power allocation scheme for the asynchronous case achieves higher rate.*

5.2.2 Rate Maximization under BS Power Constraint

Suppose all users have a fixed transmission power $P_s^{(i)} = P_s$ and only BS can adjust its power level based on the harvested energy and the QoS requirement. Then, the rate

maximization problem under BS power constraint is formulated as:

$$\begin{aligned} &\max_{P_r^{(i)}} R^{(i)} \\ &\text{subject to } P_s^{(i)} = P_s \\ &P_r^{(i)} \leq P_r, \end{aligned} \tag{5.10}$$

where P_r is the maximum transmission power at the BS.

Intuitively, the achievable rate $R^{(i)}$ always improves with the BS transmission power. However, since the relay decoding rate is independent of $P_r^{(i)}$, in this problem, we are interested in how $R^{(i)}$ changes with BS transmission power $P_r^{(i)}$. When the power level at the BS is known, the source node will adapt its transmission power accordingly by choosing proper β to maximize the achievable rate.

As shown in Section 5.2.1, when $|h_{s_i d_i}| > |h_{s_i r}|$, the source transmits to the destination directly. Therefore, we only discuss the power adaptation scheme for the source and the BS to maximize the achievable rate when $|h_{s_i d_i}| \leq |h_{s_i r}|$.

In the synchronous case, the relay decoding rate is the dominant one, so the source node will choose $0 < \beta < 1$ to balance the relay decoding rate and the destination decoding rate. In this case, $R^{(i)}$ increases with $P_r^{(i)}$, so the maximum is achieved when $P_r^{(i)} = P_r$. In the asynchronous case, the relay decoding rate will become the bottleneck, so $\beta = 1$.

Synchronous Case

In this case, the maximum rate is achieved when $P_r^{(i)} = P_r$ and

$$|h_{s_i r}|^2 \beta P_s = |h_{s_i d_i}|^2 \beta P_s + \left(\sqrt{|h_{s_i d_i}|^2 \bar{\beta} P_s} + \sqrt{|h_{r d_i}|^2 P_r} \right)^2. \tag{5.11}$$

Solving (5.11) for β, we can get

$$\beta = \frac{|h_{s_i d_i}|^2 |h_{rd_i}|^2}{|h_{s_i r}|^4 P_s} \cdot \left(\sqrt{\frac{|h_{s_i r}|^2 P_s - |h_{rd_i}|^2 P_r}{|h_{rd_i}|^2}} + \sqrt{\frac{(|h_{s_i r}|^2 - |h_{s_i d_i}|^2) P_r}{|h_{s_i d_i}|^2}} \right)^2. \tag{5.12}$$

The condition for this case to happen is

$$P_r < \frac{|h_{s_i r}|^2 - |h_{s_i d_i}|^2}{|h_{rd_i}|^2} P_s. \tag{5.13}$$

Therefore, the maximum rate is given by

$$R_{sync}^{(i)} = \frac{1}{2} \log \left(1 + \frac{|h_{s_i d_i}|^2 |h_{rd_i}|^2}{|h_{s_i r}|^2} \cdot \left(\sqrt{\frac{|h_{s_i r}|^2 P_s - |h_{rd_i}|^2 P_r}{|h_{rd_i}|^2}} + \sqrt{\frac{(|h_{s_i r}|^2 - |h_{s_i d_i}|^2) P_r}{|h_{s_i d_i}|^2}} \right)^2 \right). \tag{5.14}$$

Asynchronous Case

When $P_r \geq \frac{|h_{s_i r}|^2 - |h_{s_i d_i}|^2}{|h_{rd_i}|^2} P_s$, $\beta = 1$. Since the bottleneck is the relay decoding rate, improving $P_r^{(i)}$ cannot increase the achievable rate. In this case, the maximum transmission rate is a constant given by

$$R_{asyn}^{(i)} = \frac{1}{2} \log \left(1 + |h_{s_i r}|^2 P_s \right), \tag{5.15}$$

and the optimal transmission power at the BS is given by

$$P_r^{(i)} = \frac{|h_{s_i r}|^2 - |h_{s_i d_i}|^2}{|h_{rd_i}|^2} P_s. \tag{5.16}$$

In conclusion, depending on the BS's power output as well as its location, the maximum achievable rate for the optimization problem (5.10) is given by

$$R^{(i)} = \begin{cases} \frac{1}{2} \log \left(1 + \frac{|h_{s_i d_i}|^2 |h_{rd_i}|^2}{|h_{s_i r}|^2} \cdot \left(\sqrt{\frac{|h_{s_i r}|^2 P_s - |h_{rd_i}|^2 P_r}{|h_{rd_i}|^2}} + \sqrt{\frac{(|h_{s_i r}|^2 - |h_{s_i d_i}|^2) P_r}{|h_{s_i d_i}|^2}} \right)^2 \right), \\ \qquad\qquad \text{if } P_r < \frac{|h_{s_i r}|^2 - |h_{s_i d_i}|^2}{|h_{rd_i}|^2} P_s; \\ \frac{1}{2} \log \left(1 + |h_{s_i r}|^2 P_s \right), \qquad \text{if } P_r \geq \frac{|h_{s_i r}|^2 - |h_{s_i d_i}|^2}{|h_{rd_i}|^2} P_s. \end{cases} \tag{5.17}$$

5.3 Power Allocation Considering Energy Buffer Dynamics

In green cellular network, the BS is equipped with a rechargeable energy battery to store and release the harvested renewable energy. In this section, we take the dynamic energy charging/discharging processes into consideration to allocate the maximum power output $P_r^{(i)}$ for each channel i.

5.3.1 Energy Buffer Model

Since the renewable energy is intrinsically intermittent, the charging process is a stochastic process. Denote $N(t)$ as the total harvested energy over time $[0, t]$. $N(t)$ is non-decreasing and its corresponding charging rate is $\lambda(t)$. Considering the intermittency of the renewable energy sources, we assume that the charging rate changes over time and the charging process is described as a non-homogeneous random process in this chapter. As the transmission time for each channel is relatively short compared with the process, the charging rate of the process during channel i's transmission can be approximated as a constant $\lambda^{(i)}$.

The harvested energy at the BS is consumed for signal processing, coding and forwarding the information to the destination. The total transmission energy when channel i is active can be calculated by

$$E^{(i)} = P_r^{(i)} T, \tag{5.18}$$

where T is the transmission time for channel i.

Suppose the energy used for signal processing and coding is a constant E_0 for all time periods. Denote $V(t)$ as the total energy discharged over $[0, t]$. Then

$$V(t) = \frac{E_0 t}{T} + \int_0^t P_r(s) ds, \tag{5.19}$$

where $P_r(s) = P_r^{(i)}$ when channel i is active at time s. The discharging rate of channel i is thus a constant given by

$$\mu^{(i)} = P_r^{(i)} + E_0/T. \tag{5.20}$$

Denote C as the battery capacity, which is assumed to be large enough to store the energy harvested within a time period. Then the energy stored in the buffer at time t is given by

$$Q(t) = \min[\max[N(t) - V(t), 0], C]. \tag{5.21}$$

Define $D(Q_0^{(i)})$ as the energy depletion time of the energy buffer with initial buffer length $Q_0^{(i)}$,

$$D(Q_0^{(i)}) = \inf(t \geq 0 | Q(t) = 0, Q(0) = Q_0^{(i)}), \tag{5.22}$$

where $\inf\{t \in \mathcal{T}\}$ denotes the infimum of set $\mathcal{T}$.

Our objective is to design maximum transmission power for each channel while preventing the device-to-device communication network from battery energy depletion. Specifically, we intend to avoid energy buffer vacancy during each transmission period by deciding the transmission power at the beginning of the period.

To achieve this goal, we investigate the relationship between the energy depletion time of the energy buffer $D(Q_0^{(i)})$ and the discharging rate $\mu^{(i)}$. Let $f_D(t; Q_0^{(i)})$ denote the probability density function of the energy depletion time. Based on the start up delay analysis in [55], we have

$$f_D(t; Q_0^{(i)}) = -\frac{d}{dt} \int_0^\infty p^Q(q, t) dq, \tag{5.23}$$

where $p^Q(q, t)$ is the probability density function of the buffer energy storage $Q(t)$ at time t.

In the following, we intend to obtain $p^Q(q,t)$, which is denoted as

$$p^Q(q,t) = \mathrm{E}[\delta(q - Q(t))], \tag{5.24}$$

where $\mathrm{E}[\cdot]$ calculates the expectation of the input function.

During each transmission period, the energy buffer has a random input and a constant rate output. Without loss of generality, suppose the arrival process during channel i's transmission is a random process with a general distribution. Thus, the temporal evolution of the energy buffer during a small time interval Δ can be described by

$$dQ(t) = Q(t+\Delta) - Q(t) = \eta(\Delta) - \mu^{(i)}\Delta, \tag{5.25}$$

where $\eta(\Delta) = N(t+\Delta) - N(t)$ denotes the the summation of energy charged during Δ.

The charging process with a general distribution can be approximated as a Wiener process with a drift [56, 57]. The drift during channel i's transmission is at rate $\lambda^{(i)}$. The variance of the charging process $\nu^{(i)}$ is determined by the Wiener process. In a Wiener process, the increment within a time duration Δ is normally distributed with zero mean and a variance, which is linearly proportional to the time duration Δ [58]. As a result, let $\nu^{(i)} = 2\gamma\Delta$, where 2γ is a scaling factor determined by the specific charging technology. The probability density function for $\eta(\Delta) = x + \lambda^{(i)}\Delta$ is given by

$$p^\eta(x,\Delta) = \frac{1}{\sqrt{4\pi\Delta\gamma}} e^{-(x-\lambda^{(i)}\Delta)^2/(4\Delta\gamma)}. \tag{5.26}$$

Since the analysis of probability density function with a constant drift rate is complex, to facilitate analysis, we adopt the techniques in [59] to obtain $p^Q(q,t)$ through Fourier transform. Let $\mathcal{F}\{u(x)\}$ denote the Fourier transform of a function $u(x)$, we have

$$\mathcal{F}\{u(x)\} := \hat{u}_\xi = \int_{-\infty}^{\infty} u(x) e^{-j\xi x} dx, \tag{5.27}$$

where $\hat{u}_\xi$ is the transformed function, and ξ is the transform variable. The Fourier transform of the probability density function is a characteristic function of the random variable. Thus, the Fourier transform preserves all the random variable's statistic information. This feature guarantees the accuracy of our analysis.

Let $\hat{p}_\xi^Q(t)$ and $\hat{p}_\xi^\eta(\Delta)$ denote the Fourier transform of $p^Q(q,t)$ and $p^\eta(x,\Delta)$, respectively. Perform Fourier transform on (5.25) and take $\Delta \to 0$, we get

$$\frac{\partial}{\partial t}\hat{p}_\xi^Q(t) = \mu^{(i)}\mathcal{F}\{\frac{\partial}{\partial q}p^Q(q,t)\} + \hat{p}_\xi^Q(t)\phi_\xi, \tag{5.28}$$

where

$$\phi_\xi = \lim_{\Delta\to 0}\frac{1}{\Delta}[\hat{p}_\xi^\eta(\Delta) - 1]. \tag{5.29}$$

To get $\hat{p}_\xi^\eta(\Delta)$ in (5.29), we perform Fourier transform on the probability density function $p^\eta(x,\Delta)$, which is given by (5.26), and obtain

$$\hat{p}_\xi^\eta(\Delta) = e^{-\gamma\Delta\xi^2}e^{-j\xi\lambda^{(i)}}. \tag{5.30}$$

Thus, ϕ_ξ is given by

$$\phi_\xi = -\gamma\xi^2 - j\xi\lambda^{(i)}. \tag{5.31}$$

Based on the time derivative property of Fourier transform, (5.28) could be further reformed as

$$\begin{aligned}\frac{\partial}{\partial t}\hat{p}_\xi^Q(t) &= j\xi\mu^{(i)}\hat{p}_\xi^Q(t) + \hat{p}_\xi^Q(t)\phi_\xi \\ &= (j\xi\mu^{(i)} + \phi_\xi)\hat{p}_\xi^Q(t).\end{aligned} \tag{5.32}$$

To solve this first order ordinary differential equation (5.32), we need to determine initial values. The initial condition of (5.32) could be obtained at time $t = 0$. At time $t = 0$, the energy buffer length is $Q_0^{(i)}$, namely $p^Q(q = Q_0^{(i)}, 0) = 1$. The Fourier transform

of this condition is $\hat{p}_{\xi}^{Q}(0) = e^{-j\xi Q_0^{(i)}}$. With this initial condition and (5.31), the solution to (5.32) can be obtained as

$$\hat{p}_{\xi}^{Q}(t) = e^{-j\xi Q_0^{(i)}} e^{(j\xi(\mu^{(i)}-\lambda^{(i)})-\gamma\xi^2)t}. \tag{5.33}$$

Finally, $p^{Q}(q,t)$ can be obtained by performing the inverse Fourier transform on (5.33). Replacing $p^{Q}(q,t)$ in (5.23), the probability density function of the energy depletion time with initial buffer length $Q_0^{(i)}$ is given by

$$f_D(t; Q_0^{(i)}) = \frac{Q_0^{(i)}}{\sqrt{4\gamma\pi t^3}} \exp\left\{-\frac{(Q_0^{(i)} + (\lambda^{(i)} - \mu^{(i)})t)^2}{4\gamma t}\right\}. \tag{5.34}$$

5.3.2 Power Allocation Schemes

We have modeled the energy buffer and provided the probability density function of energy depletion time in the previous subsection. Based on our theoretical analysis, in this subsection, we design power allocation schemes to maximize the transmission efficiency while ensuring the network sustainability. Assume that the initial energy storage in the buffer and the statistical parameters of the charging process can be estimated and are available at the beginning of each transmission period. The BS can adjust the discharging rate by choosing transmission power $P_r^{(i)}$ during channel i's transmission period. The objective of our power allocation scheme is to maximize each individual channel's transmission rate while maintaining the sustainability of the network at a certain level. We still consider two different network scenarios depending on whether users are able to adjust the transmission power. In the first network scenario, both the BS and users can adjust transmission power. Thus, our scheme can allocate power for both the BS and user to improve the transmission efficiency. Then, we consider the case where users cannot adjust their transmission power due to equipment constraints, which means that only the BS can choose various power

levels for data transmission. In the following, we present the transmission power allocation frameworks under both total power constraint and BS power constraint cases.

Power Allocation under Total Power Constraint

We first consider the situation that both the BS and users can adjust their transmission power levels. In the proposed network scenario, since improving the transmission rate is at the expense of consuming more transmission power, the communication network may not be sustainable over time due to power depletion. To tackle this issue, our design objective is to improve the transmission efficiency of each channel while maintaining the whole network's sustainability. Our proposed scheme allocates both BS transmission power and user transmission power on a slot-by-slot basis.

At the beginning of channel i's transmission period, the remaining energy in the buffer is $Q_0^{(i)}$. In order to maintain the network sustainability, the maximum transmission power $P_r^{(i)*}$ for the BS on channel i is determined by numerically solving the following equation:

$$E[D(Q_0^{(i)})] = T + \delta, \tag{5.35}$$

where δ denotes a constant to guarantee the sustainability of green wireless networks. δ is decided according to the tolerance level of the transmission or the available volume of backup energy. If there is sufficient backup energy or the transmission has high tolerance level, i.e., the network tolerates a high transmission latency like data transmission, δ can be set to a small value. If the available volume of the backup energy is not enough and the transmission does not tolerate a high transmission latency, such as voice/video, a large δ is chosen.

Based on our analysis in Section 5.3.1, the expectation of the depletion time can be

calculated by

$$E[D(Q_0^{(i)})] = \int_0^{\infty} \frac{Q_0^{(i)}}{\sqrt{4\gamma\pi t}} \exp\left\{-\frac{(Q_0^{(i)} + (\lambda^{(i)} - (P_r^{(i)} + E_0/T))t)^2}{4\gamma t}\right\} dt. \tag{5.36}$$

Then, we can obtain the optimal P_s to maximize the transmission efficiency based on the value of $P_r^{(i)^*}$. In the total power constraint case, the user is able to adjust its own transmission power to cooperate with the BS to improve the transmission efficiency. Based on (5.5) in Section 5.2.1, in the synchronous case, the optimal transmission power for the user is given by

$$P_s^{(i)^*} = \frac{|h_{s_i d_i}|^2(|h_{s_i d_i}|^2 + |h_{rd_i}|^2) + |h_{rd_i}|^2(|h_{s_i r}|^2 + |h_{rd_i}|^2)}{|h_{s_i d_i}|^2(|h_{s_i r}|^2 - |h_{s_i d_i}|^2)} P_r^{(i)^*}. \tag{5.37}$$

In the asynchronous case, according to (5.8), the optimal user transmission power is given by

$$P_s^{(i)^*} = \frac{|h_{rd_i}|^2}{|h_{s_i r}|^2 - |h_{s_i d_i}|^2} P_r^{(i)^*}. \tag{5.38}$$

Power Allocation under BS Power Constraint

We further consider the case that users can not adjust their transmission power level due to the device constraints. In this case, users transmit with fixed power while the BS adapts its transmission power to meet our design objective.

According to (5.17), the maximum rate for the optimization problem (5.10) is achieved when $P_r^{(i)} = P_r$ if $P_r < \frac{|h_{s_i r}|^2 - |h_{s_i d_i}|^2}{|h_{rd_i}|^2} P_s$, and $P_r^{(i)} = \frac{|h_{s_i r}|^2 - |h_{s_i d_i}|^2}{|h_{rd_i}|^2} P_s$ if $P_r \geq \frac{|h_{s_i r}|^2 - |h_{s_i d_i}|^2}{|h_{rd_i}|^2} P_s$.

Therefore, the power allocation scheme performs as follows: at the beginning of channel i's transmission period, based on the remaining buffer energy $Q_0^{(i)}$, the BS first calculates a transmission power $P_r^{(i)^*}$ such that

$$E[D(Q_0^{(i)})] = T + \delta, \tag{5.39}$$

which is the same as the first step of the power allocation scheme in the total power constraint case.

Then, the BS compares $P_r^{(i)^*}$ with $\min\{P_r, \frac{|h_{s_i r}|^2 - |h_{s_i d_i}|^2}{|h_{r d_i}|^2} P_s\}$ and chooses the minimum of the two values as the optimal transmission power.

5.4 Numerical Results

In this section, we provide some numerical results to evaluate our power allocation schemes. We assume that all wireless channels are independent Rayleigh fading channels with path loss where the path loss exponent α is 2. The distances between the source and the BS, between the BS and the destination, and between the source to the destination are 75 meters, 80 meters and 150 meters, respectively.

Fig. 5.2 shows the rate comparison employing different power adaptation schemes. Suppose $P_r^{(i)}$, the transmission rate at the BS for channel i, ranges from 10dB to 40dB. For the total power constraint case, the source would adapt its own transmission power based on the available BS's transmission power. For the BS power constraint case, the transmission power at the source is set to be 20dB. To illustrate the rate improvement, we also set the capacity of the non-cooperative transmission as a baseline for comparison where the user transmission power is 20dB.

It can be seen that the power adaptation schemes under the total power constraint can achieve higher rate, which is at the expense of higher transmission power at the source. Under the BS power constraint, the channel rate reaches a constant when $P_r^{(i)}$ is large, which is bounded by the limited transmission power at the source.

Secondly, we evaluate our proposed power allocation schemes considering the energy buffer dynamics. The cumulative distribution function (CDF) of energy depletion time

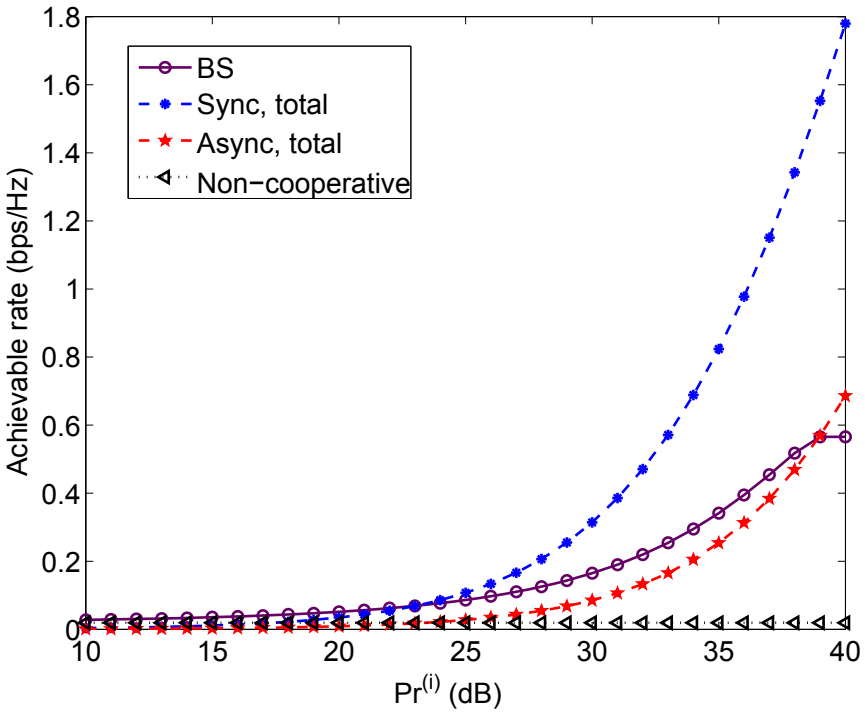

Figure 5.2: Rate comparison for a single-user channel.

is shown in Fig. 5.3 and Fig. 5.4 where Fig. 5.3 illustrates the change with initial buffer storage and Fig. 5.4 depicts the change with discharging rate.

It can be seen from Fig. 5.3 that the CDF curve of the energy depletion time shifts right as the initial buffer energy $Q_0^{(i)}$ grows, which means that the BS is more likely to provide energy output for longer time if $Q_0^{(i)}$ is large. As shown in Fig. 5.4, the CDF curve shifts left as the discharging rate $\mu^{(i)}$ grows, which means that the BS is more likely to deplete its energy soon when the discharging rate increases.

The depletion time expectation $E[D(Q_0^{(i)})]$ of the green energy buffer model shown in Subsection 5.3.1 is depicted in Fig 5.5. The charging rate $\lambda^{(i)}$ is set to be 3.5. It can be seen that $E[D(Q_0^{(i)})]$ decreases with depletion rate $\mu^{(i)}$ and increases with the initial energy

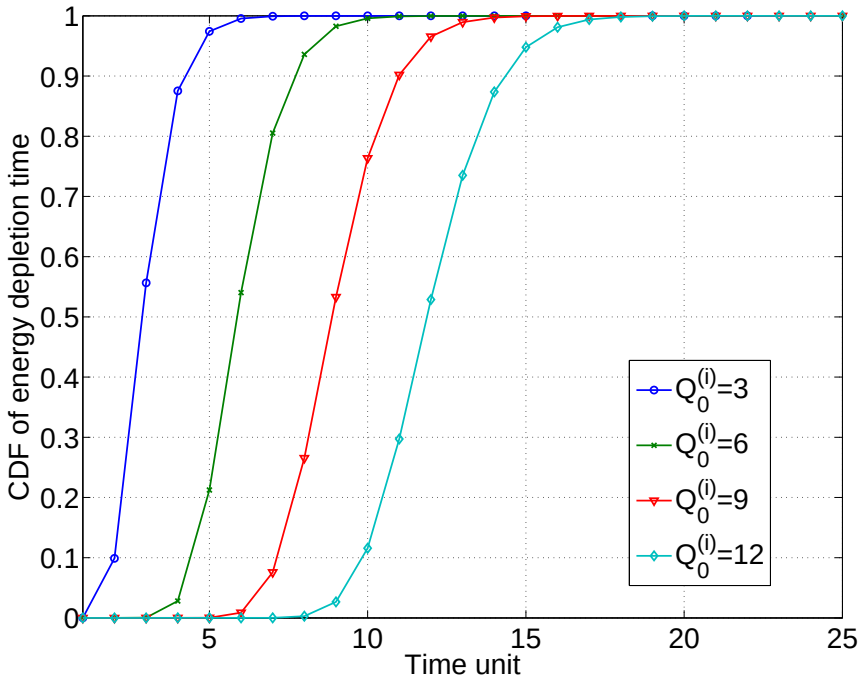

Figure 5.3: CDF of energy depletion time. $\lambda^{(i)} = 3.5$, $\mu^{(i)} = 5.5$.

storage $Q_0^{(i)}$ for both analytical results and simulation results.

Fig. 5.6 and Fig. 5.7 evaluate our proposed power allocation schemes in a practical network containing 20 consecutive transmissions. Each transmission period contains 100 time units. The renewable energy charging rate at the BS during each transmission period is random and time-variant. Suppose that the energy charging rate can be forecasted based on some historical data, e.g. data from the previous day or year. To demonstrate the energy efficiency of our proposed schemes, we compare with a max-sustainability scheme where $P_r^{(i)} = \frac{Q_0^{(i)} - E_0}{T}$ in total power constraint case and $P_r^{(i)} = \min\{\frac{Q_0^{(i)} - E_0}{T}, P_r^{(i)^*}\}$ in BS power constraint case. We calculate both the energy depletion probability and the average transmission rate of all channels according to the reference max-sustainability scheme and

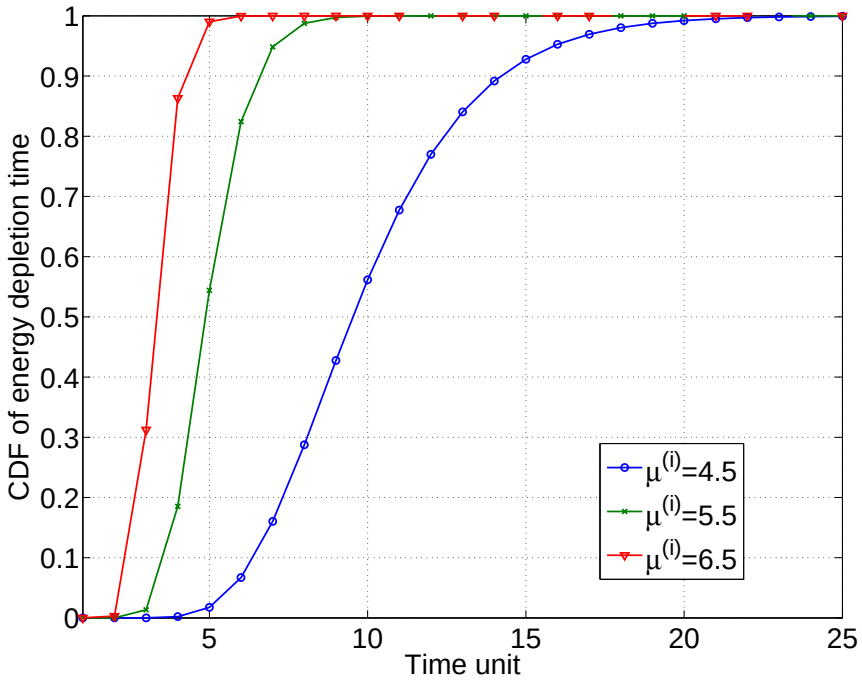

Figure 5.4: CDF of energy depletion time. $Q_0^{(i)} = 10$, $\lambda^{(i)} = 3.5$.

our proposed power allocation schemes in Subsection 5.3.2. The comparison in the total power constraint case is shown in Fig. 5.6 and the result in the BS power constraint case is shown in Fig. 5.7.

It can be observed that our proposed power allocation schemes can improve the average transmission rate by about 36% in the total power constraint case and 16% in the BS power constraint case. The reason is that our schemes exploit the dynamic charging process of the renewable energy to improve the energy efficiency. Compared with the max-sustainability power allocation scheme which has zero energy depletion probability, our proposed method is associated with very low depletion probability.

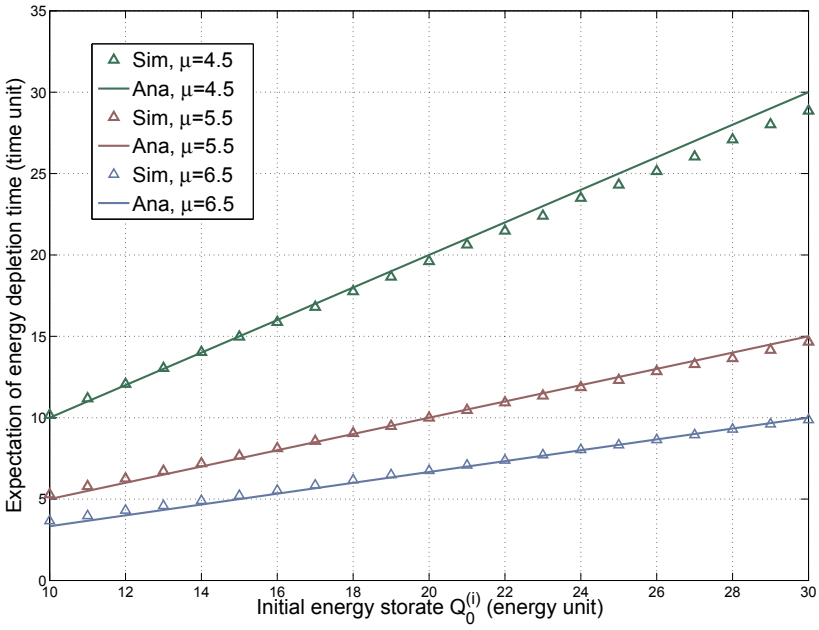

Figure 5.5: Expectation of depletion duration ($\lambda^{(i)} = 3.5$).

5.5 Summary

In this chapter, we have proposed several power allocation schemes to maximize the throughput while maintaining the network sustainability in a device-to-device communication underlaying green cellular network. The results should shed some light on the green wireless network design with energy efficiency and energy sustainability as critical design criteria.

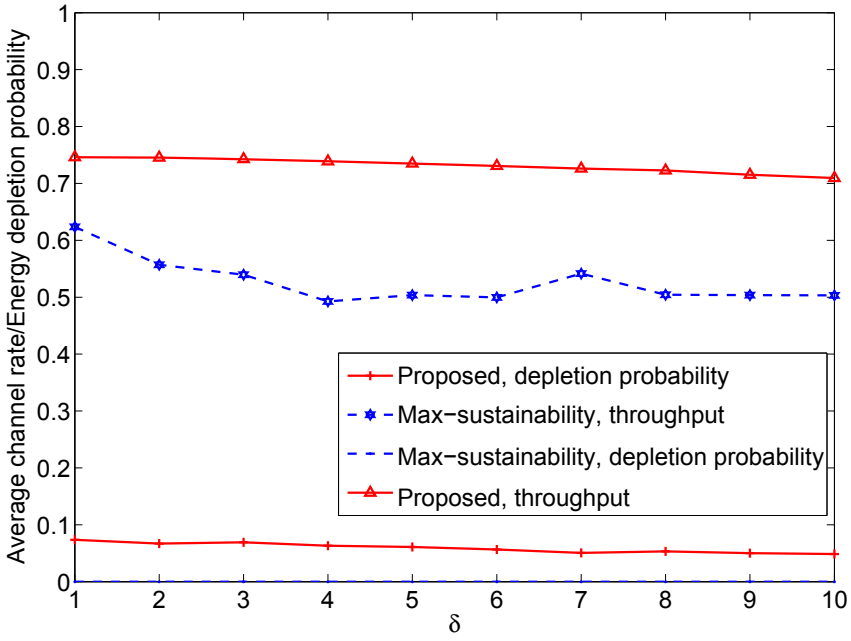

Figure 5.6: Total power constraint case (channel number=20).

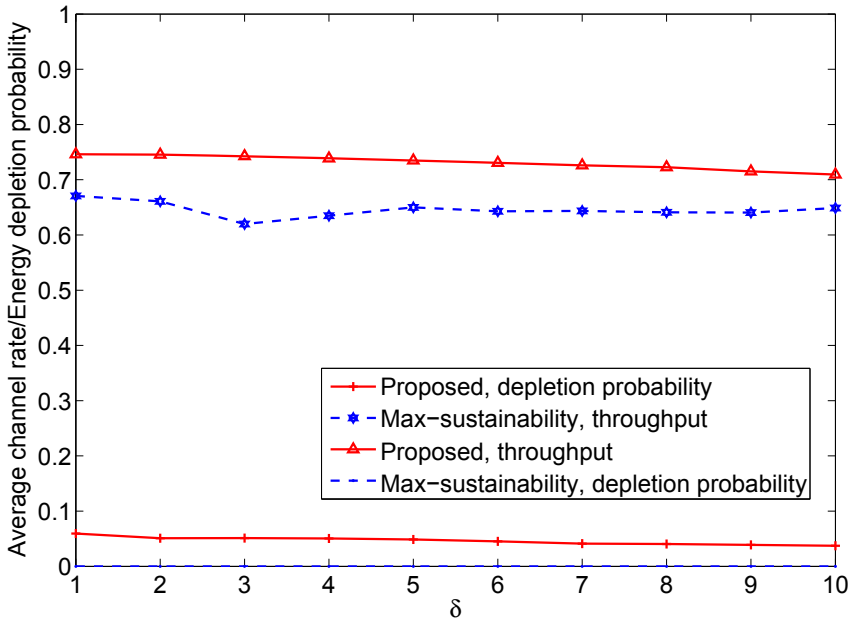

Figure 5.7: BS power constraint case (channel number=20, $P_s = 2$).

Chapter 6

Conclusion and Future Work

In this chapter, we mainly summarize the contributions of this work and propose future research plans.

6.1 Conclusion

As the future-generation wireless cellular networks feature high data rate communication and reduced operational cost, improving the network spectrum efficiency becomes a prominent research issue in cellular networks. In this dissertation, we explore the potential benefits of introducing cooperative relaying in cellular networks and study efficient resource allocation schemes in cooperative cellular networks to enhance the utilization of network resources.

To improve the spectrum efficiency, we first study the resource allocation in LTE-Advanced cellular networks with the deployment of relay stations, from both downlink OFDM and uplink SC-FDMA perspectives. The dedicated relay stations adopt the decode-

and-forward protocol to better exploit the broadcast nature of wireless signals. In the downlink OFDM system, joint efficient subcarrier and power allocation schemes are proposed for overall throughput maximization problem and user fairness maximization problem separately. In the uplink SC-FDMA system, the achievable rate is derived based on the superposition coding. Then, we propose the optimal power allocation schemes to improve the system throughput.

As energy consumption of base stations occupies a significant portion of operational cost in cellular networks, future-generation cellular networks are expected to make use of eco-friendly energy sources at the base station and opportunistic transmission to reduce the cost. Therefore, we further consider the resource allocation in a device-to-device communication underlaying cellular network where the base station is powered by green energy and capable of cooperative relaying. Efficient power adaptation schemes are proposed to enhance both sustainability and efficiency taking the dynamics of the charging and discharging processes into consideration.

6.2 Future Work

In this dissertation, we mainly focus on the resource allocation for cooperative relaying in the cellular network. Along this path, there are several research directions towards a more spectrum and energy efficient cellular networks as listed below.

6.2.1 Joint Resource Allocation and Relay Station Deployment

As introducing relay stations can significantly extend the coverage and improve the transmission rate in cellular networks, a natural question arises: where should the relay stations

be placed? The placement problem is a critical issue for network planning and deployment, which has direct impacts on the subsequent QoS provisioning, especially the date rate and transmission delay. In Chapter 3, we have considered the resource allocation in the downlink OFDM system, which depends on the channel state information of all users. In the future, the research work is to combine resource allocation design and the relay station location planning by taking into consideration the location impact on the channel state information. The objective is to achieve a joint design to further improve the spectrum efficiency of all users in the cellular network.

6.2.2 Resource Allocation in Cellular Networks with Multiple RSs Cooperation

In Chapter 3 and Chapter 4, we consider that a single RS is deployed in each sector and there is no cooperation among adjacent RSs. In the cellular network, each UE is served by at most one relay station to simplify the network scenario. In practical networks, if a UE is located near the sector edge, it might be within the coverage of two adjacent relay stations. This channel can be modeled as a source transmitting to the destination via the help of two parallel relays. Whether this channel can achieve larger transmission rate than single-relay channel and how to allocate resources at the two relays might be a future research direction.

6.2.3 Resource Allocation with Imperfect CSI

In this dissertation, we consider that the channel state information can be accurately estimated at the destination. Based on the perfect CSI, we propose resource allocation schemes which depends on the channel coefficients. In practical cellular networks, the channel state

information is obtained through a feedback channel. However, the perfect CSI assumption is unrealizable, due to bandwidth constraints on the feedback channel as well as the considerable communication overhead cost involved with fast changing wireless environment. Therefore, limited feedback is a practical option that provides quantized CSI at the transmitter. The major drawback of limited feedback is that it suffers from performance degradation due to feedback delay and quantization error. The effect of feedback delay and quantization error on the achievable rate as well as the resource allocation is also a future topic.

6.2.4 Resource Allocation for CoMP Transmission in Cooperative Cellular Networks

The coordinated multipoint transmission (CoMP) is expected to be employed in future-generation cellular networks to utilize the resources more effectively, to enhance the overall system performance, and to improve the end user service quality. CoMP requires dynamic coordination between adjacent eNBs to provide joint scheduling and transmissions as well as joint processing of the received signals. In this way a UE at the edge of a cell is able to be served by two or more eNBs to improve signals reception and transmission and increase the throughput. With the deployment of relay stations, each UE at the cell edge might receive signals from several eNBs and RSs. An efficient design and resource allocation to utilize these signals to achieve both the CoMP transmission cooperation gain and relay channel cooperation gain is necessary.

References

[1] H. Ekstrom, A. Furuskar, J. Karlsson, M. Meyer, S. Parkvall, J. Torsner, and M. Wahlqvist, "Technical solutions for the 3G long-term evolution," *IEEE Communications Magazine*, vol. 44, no. 3, pp. 38–45, 2006.

[2] C. Park, Y. Choi, Y. Han, and H. Seong, "A study on receiving performance improvement of LTE communication network using multi-hop relay techniques," *Future Information Technology*, pp. 323–328, 2011.

[3] X. Huang, F. Ulupinar, P. Agashe, D. Ho, and G. Bao, "LTE relay architecture and its upper layer solutions," in *Proc. of IEEE GLOBECOM*, 2010, pp. 1–6.

[4] 3GPP, "Requirements for Evolved UTRA and Evolved UTRAN," vol. TR 25.913.

[5] ——, "Requirements for further advancements for Evolved Universal Terrestrial Radio Access (E-UTRA)," vol. TR 36.913.

[6] ITU-R, "Requirements related to technical performance for IMT-Addvanced radio interface(s)," Tech. Rep. M.2134, 2008.

[7] A. Ghosh, R. Ratasuk, B. Mondal, N. Mangalvedhe, and T. Thomas, "LTE-Advanced: next-generation wireless broadband technology," *IEEE Transactions on Wireless Communications*, vol. 17, no. 3, pp. 10–22, 2010.

[8] H. Yanikomeroglu, "Cellular multihop communications: infrastructure-based relay network architecture for 4g wireless systems," in *Proc. of Biennial Symposium on Communications*, 2004.

[9] T. Beniero, S. Redana, J. Hamalainen, and B. Raaf, "Effect of relaying on coverage in 3gpp lte-advanced," in *Proc. of IEEE VTC*, 2009, pp. 1–5.

[10] E. Lang, S. Redana, and B. Raaf, "Business impact of relay deployment for coverage extension in 3GPP LTE-Advanced," in *Proc. of IEEE ICC Workshops*, 2009, pp. 1–5.

[11] S. Lee, K. Cho, K. Kim, D. Yoon, and T. Kim, "Performance analysis of lte-advanced system in the downlink spatial channel model," in *IEEE IC-NIDC*, 2009, pp. 169–171.

[12] A. Lo and P. Guan, "Performance of in-band full-duplex amplify-and-forward and decode-and-forward relays with spatial diversity for next-generation wireless broadband," in *Proc. of IEEE ICOIN*, 2011, pp. 290–294.

[13] P. Bhat, S. Nagata, L. Campoy, I. Berberana, T. Derham, G. Liu, X. Shen, P. Zong, and J. Yang, "LTE-Advanced: an operator perspective," *IEEE Communications Magazine*, vol. 50, no. 2, pp. 104–114, 2012.

[14] 3GPP. TS 36.201 Technical Specification Group Radio Access Network; Evolved Universal Terrestrial Radio Access (E-UTRA); Long Term Evolution (LTE) Physical Layer; General Description (Release 8).

[15] H. G. Myung and D. Goodman, *Single Carrier FDMA: a new air interface for long term evolution.* John Wiley & Sons, 2008.

[16] E. Van Der Meulen, "Transmission of information in a T-terminal discrete memoryless channel," Ph.D. dissertation, University of California, Berkeley, CA, 1968.

[17] ——, "Three-terminal communication channels," *Advances in Applied Probability*, vol. 3, no. 01, pp. 120–154, 1971.

[18] T. Cover and A. E. Gamal, "Capacity theorems for the relay channel," *IEEE Transactions on Information Theory*, vol. 25, no. 5, pp. 572–584, 1979.

[19] B. Schein, "Distributed coordination in network information theory," Ph.D. dissertation, Massachusetts Institute of Technology, Dept. of Electrical Engineering and Computer Science, 2001.

[20] G. Kramer, M. Gastpar, and P. Gupta, "Cooperative strategies and capacity theorems for relay networks," *IEEE Transactions on Information Theory*, vol. 51, no. 9, pp. 3037–3063, 2005.

[21] T. M. Cover and J. A. Thomas, *Elements of information theory*. John Wiley & Sons, 2012.

[22] J. Jang and K. Lee, "Transmit power adaptation for multiuser OFDM systems," *IEEE Journal on Selected areas in communications*, vol. 21, no. 2, pp. 171–178, 2003.

[23] W. Rhee and J. Cioffi, "Increase in capacity of multiuser OFDM system using dynamic subchannel allocation," in *Proc. of IEEE VTC*, vol. 2, 2000, pp. 1085–1089.

[24] Z. Shen, J. Andrews, and B. Evans, "Adaptive resource allocation in multiuser OFDM systems with proportional rate constraints," *IEEE Transactions on Wireless Communications*, vol. 4, no. 6, pp. 2726–2737, 2005.

[25] G. Song and Y. Li, "Cross-layer optimization for OFDM wireless networks-part I: theoretical framework," *IEEE Transactions on Wireless Communications*, vol. 4, no. 2, pp. 614–624, 2005.

[26] ——, "Cross-layer optimization for OFDM wireless networks-part II: algorithm development," *IEEE Transactions on Wireless Communications*, vol. 4, no. 2, pp. 625–634, 2005.

[27] M. Mehrjoo, S. Moazeni, and X. Shen, "Resource allocation in OFDMA networks based on interior point methods," *Wireless Communications and Mobile Computing*, vol. 10, no. 11, pp. 1493–1508, 2010.

[28] T. Shi, S. Zhou, and Y. Yao, "Capacity of single carrier systems with frequency-domain equalization," in *Proc. of IEEE Circuits and Systems Symposium on Emerging Technologies: Frontiers of Mobile and Wireless Communication*, 2004, pp. 429–432.

[29] M. Hua, B. Ren, M. Wang, J. Zou, C. Yang, and T. Liu, "Performance analysis of OFDMA and SC-FDMA multiple access techniques for next generation wireless communications," in *Proc. of IEEE VTC*, 2013, pp. 1–4.

[30] T. Liu, C. Yang, and L.-L. Yang, "A low-complexity subcarrier-power allocation scheme for frequency-division multiple-access systems," *IEEE Transactions on Wireless Communications*, vol. 9, no. 5, pp. 1564–1570, 2010.

[31] X. Deng and A. Haimovich, "Power allocation for cooperative relaying in wireless networks," *IEEE Communications Letters*, vol. 9, no. 11, pp. 994–996, 2005.

[32] A. Host-Madsen and J. Zhang, "Capacity bounds and power allocation for wireless relay channels," *IEEE Transactions on Information Theory*, vol. 51, no. 6, pp. 2020–2040, 2005.

[33] A. Sadek, W. Su, and K. Liu, "Multinode cooperative communications in wireless networks," *IEEE Transactions on Signal Processing*, vol. 55, no. 1, pp. 341–355, 2007.

[34] Y. Liang, V. Veeravalli, and H. Poor, "Resource allocation for wireless fading relay channels: max-min solution," *IEEE Transactions on Information Theory*, vol. 53, no. 10, pp. 3432–3453, 2007.

[35] W. Dang, M. Tao, H. Mu, and J. Huang, "Subcarrier-pair based resource allocation for cooperative multi-relay OFDM systems," *IEEE Transactions on Wireless Communications*, vol. 9, no. 5, pp. 1640–1649, 2010.

[36] Y. Li, B. Vucetic, Z. Zhou, and M. Dohler, "Distributed adaptive power allocation for wireless relay networks," *IEEE Transactions on Wireless Communications*, vol. 6, no. 3, pp. 948–958, 2007.

[37] Y. Yao, X. Cai, and G. Giannakis, "On energy efficiency and optimum resource allocation of relay transmissions in the low-power regime," *IEEE Transactions on Wireless Communications*, vol. 4, pp. 2917–2927, 2005.

[38] Y. Liang and V. Veeravalli, "Gaussian orthogonal relay channels: optimal resource allocation and capacity," *IEEE Transactions on Information Theory*, vol. 51, no. 9, pp. 3284–3289, 2005.

[39] T. C.-Y. Ng and W. Yu, "Joint optimization of relay strategies and resource allocations in cooperative cellular networks," *IEEE Journal on Selected Areas in Communications*, vol. 25, no. 2, pp. 328–339, 2007.

[40] T. Wang and L. Vandendorpe, "Sum rate maximized resource allocation in multiple DF relays aided OFDM transmission," *IEEE Journal on Selected Areas in Communications*, vol. 29, no. 8, pp. 1559–1571, 2011.

[41] M. S. Alam, J. W. Mark, and X. Shen, "Relay selection and resource allocation for multi-user cooperative OFDMA networks," *IEEE Transactions on Wireless Communications*, vol. 12, no. 5, pp. 2193–2205, 2013.

[42] H. Kha, H. Tuan, and H. Nguyen, "Joint optimization of source power allocation and cooperative beamforming for SC-FDMA multi-user multi-relay networks," *IEEE Transactions on Communications*, vol. 61, no. 6, pp. 2248–2259, 2013.

[43] J. Zhang, L.-L. Yang, and L. Hanzo, "Energy-efficient channel-dependent cooperative relaying for the multiuser SC-FDMA uplink," *IEEE Transactions on Vehicular Technology*, vol. 60, no. 3, pp. 992–1004, 2011.

[44] ——, "Energy-efficient dynamic resource allocation for opportunistic-relaying-assisted SC-FDMA using turbo-equalizer-aided soft decode-and-forward," *IEEE Transactions on Vehicular Technology*, vol. 62, no. 1, pp. 235–246, 2013.

[45] L.-L. Xie and P. Kumar, "An achievable rate for the multiple-level relay channel," *IEEE Transactions on Information Theory*, vol. 51, no. 4, pp. 1348 –1358, 2005.

[46] X. Zhang, Z. Zheng, J. Liu, X. Shen, and L.-L. Xie, "Optimal power allocation and AP deployment in green wireless cooperative communications," in *Proc. of IEEE GLOBECOM*, 2014, pp. 4000–4005.

[47] 3GPP. TS 36.211 Technical Specification Group Radio Access Network; Evolved Universal Terrestrial Radio Access (E-UTRA); Physical Channels and Modulation (Release 8).

[48] M. Noune and A. Nix, "Performance of SC-FDMA with transmit power allocation and frequency-domain equalization," in *Proc. of PIMRC*, 2010, pp. 852–857.

[49] M.-L. Ku and H.-J. Yeh, "Channel equalization and chunk assignment schemes for LTE SC-FDMA systems in multipath channels," in *Proc. of IEEE ICCT*, 2012, pp. 1166–1171.

[50] 3GPP. TS 36.116 Technical Specification Group Radio Access Network; Evolved Universal Terrestrial Radio Access (E-UTRA); Relay Radio Transmission and Reception (Release 11).

[51] X. Zhang, X. Shen, and L.-L. Xie, "Joint subcarrier and power allocation for cooperative communications in LTE-Advanced networks," *IEEE Transactions on Wireless Communications*, vol. 13, no. 2, pp. 658–668, 2014.

[52] Z. Hasan, H. Boostanimehr, and V. K. Bhargava, "Green cellular networks: A survey, some research issues and challenges," *IEEE Communications Surveys & Tutorials*, vol. 13, no. 4, pp. 524 – 540, 2011.

[53] M. A. Marsan, L. Chiaraviglio, D. Ciullo, and M. Meo, "Optimal energy savings in cellular access networks," in *Proc. of IEEE ICC Workshops*, 2009.

[54] E. Oh, B. Krishnamachari, X. Liu, and Z. Niu, "Toward dynamic energy-efficient operation of cellular network infrastructure," *IEEE Communications Magazine*, vol. 49, pp. 56–61, 2011.

[55] T. H. Luan, L. X. Cai, and X. Shen, "Impact of network dynamics on user's video quality: analytical framework and QoS provision," *IEEE Transactions on Multimedia*, vol. 12, no. 1, pp. 64–78, 2010.

[56] M. Strelec, K. Macek, and A. Abate, "Modeling and simulation of a microgrid as a stochastic hybrid system," in *Proc. of ISGT Europe*, 2012, pp. 1–9.

[57] Q. Zhu and T. Başar, "Multi-resolution large population stochastic differential games and their application to demand response management in the smart grid," *Dynamic Games and Applications*, vol. 3, no. 1, pp. 68–88, 2013.

[58] I. Karatzas and S. E. Shreve, *Brownian Motion and Stochastic Calculus*. Springer, 1991.

[59] S. Denisov, W. Horsthemke, and P. Hänggi, "Generalized Fokker-Planck equation: derivation and exact solutions," *The European Physical Journal B*, vol. 68, no. 4, pp. 567–575, 2009.

[60] S. Peters, A. Panah, K. Truong, and R. Heath, "Relay architectures for 3GPP LTE-Advanced," *EURASIP Journal on Wireless Communications and Networking*, vol. 2009, 2009.

[61] C. Hoymann, W. Chen, J. Montojo, A. Golitschek, C. Koutsimanis, and X. Shen, "Relaying operation in 3GPP LTE: challenges and solutions," *IEEE Communications Magazine*, vol. 50, no. 2, pp. 156–162, 2012.

[62] D. Lee, H. Seo, B. Clerckx, E. Hardouin, D. Mazzarese, S. Nagata, and K. Sayana, "Coordinated multipoint transmission and reception in LTE-Advanced: deployment scenarios and operational challenges," *IEEE Communications Magazine*, vol. 50, no. 2, pp. 148–155, 2012.

[63] Y. Yang, H. Hu, J. Xu, and G. Mao, "Relay technologies for WiMAX and LTE-Advanced mobile systems," *IEEE Communications Magazine*, vol. 47, no. 10, pp. 100–105, 2009.

[64] S. Song, A. Almutairi, and K. Letaief, "Outage-capacity based adaptive relaying in lte-advanced networks," *IEEE Transactions on Wireless Communications*, vol. 12, no. 9, pp. 4778–4787, 2013.

[65] X. Wang and G. B. Giannakis, "Resource allocation for wireless multiuser OFDM networks," *IEEE Transactions on Information Theory*, vol. 57, no. 7, pp. 4359–4372, 2011.

[66] R. Madan, S. P. Boyd, and S. Lall, "Fast algorithms for resource allocation in wireless cellular networks," *IEEE/ACM Transactions on Networking*, vol. 18, no. 3, pp. 973–984, 2010.

[67] R. Aggarwal, M. Assaad, C. E. Koksal, and P. Schniter, "Joint scheduling and resource allocation in the OFDMA downlink: Utility maximization under imperfect channel-state information," *IEEE Transactions on Signal Processing*, vol. 59, no. 11, pp. 5589–5604, 2011.

[68] A. Leith, M.-S. Alouini, D. I. Kim, X. Shen, and Z. Wu, "Flexible proportional-rate scheduling for OFDMA system," *IEEE Transactions on Mobile Computing*, vol. 12, no. 10, pp. 1907–1919, 2013.

[69] J. Huang, V. G. Subramanian, R. Agrawal, and R. A. Berry, "Downlink scheduling and resource allocation for OFDM systems," *IEEE Transactions on Wireless Communications*, vol. 8, no. 1, pp. 288–296, 2009.

[70] I. C. Wong and B. L. Evans, "Optimal downlink OFDMA resource allocation with linear complexity to maximize ergodic rates," *IEEE Transactions on Wireless Communications*, vol. 7, no. 3, pp. 962–971, 2008.

[71] F. He, Y. Sun, L. Xiao, X. Chen, C.-Y. Chi, and S. Zhou, "Capacity region bounds and resource allocation for two-way OFDM relay channels," *IEEE Transactions on Wireless Communications*, vol. 12, no. 6, pp. 2904–2917, 2013.

[72] M. K. Awad, X. Shen, and B. Zogheib, "Ergodic mutual information of OFDMA-based selection-decode-and-forward cooperative relay networks with imperfect CSI," *Physical Communication*, vol. 2, no. 3, pp. 184–193, 2009.

[73] M. K. Awad, V. Mahinthan, M. Mehrjoo, X. Shen, and J. W. Mark, "A dual-decomposition-based resource allocation for OFDMA networks with imperfect CSI," *IEEE Transactions on Vehicular Technology*, vol. 59, no. 5, pp. 2394–2403, 2010.

[74] C.-N. Hsu, H.-J. Su, and P.-H. Lin, "Joint subcarrier pairing and power allocation for OFDM transmission with decode-and-forward relaying," *IEEE Transactions on Signal Processing*, vol. 59, no. 1, pp. 399–414, 2011.

[75] X. Zhang, X. Shen, and L.-L. Xie, "Achievable rates for uplink communications in lte-advanced networks with decode-and-forward relays," in *Proc. of IEEE Global Communications Conference (GLOBECOM)*, 2014, pp. 4168–4173.

[76] ——, "Uplink achievable rate and power allocation in cooperative lte-advanced networks," *IEEE Transactions on Vehicular Technology*, vol. PP, no. 99, pp. 1–1, 2015.

[77] Z. Hasan, H. Boostanimehr, and V. K. Bhargava, "Green cellular networks: A survey, some research issues and challenges," *IEEE Communications Surveys & Tutorials*, vol. 13, no. 4, pp. 524–540, 2011.

[78] G. H. Badawy, A. A. Sayegh, and T. D. Todd, "Energy provisioning in solar-powered wireless mesh networks," *IEEE Transactions on Vehicular Technology*, vol. 59, no. 8, pp. 3859–3871, 2010.

[79] S. Bosio, A. Capone, and M. Cesana, "Radio planning of wireless local area networks," *IEEE/ACM Transactions on Networking*, vol. 15, no. 6, pp. 1414–1427, 2007.

[80] A. Fehske, G. Fettweis, J. Malmodin, and G. Biczok, "The global footprint of mobile communications: the ecological and economic perspective," *IEEE Communications Magazine*, vol. 49, no. 8, pp. 55–62, 2011.

[81] L. X. Cai, Y. Liu, H. T. Luan, X. Shen, J. W. Mark, and H. V. Poor, "Adaptive resource management in sustainable energy powered wireless mesh networks," in *Proc. of IEEE Globecom*, 2011, pp. 1–5.

[82] L. X. Cai, H. Poor, Y. Liu, T. H. Luan, X. Shen, and J. W. Mark, "Dimensioning network deployment and resource management in green mesh networks," *IEEE Wireless Communications*, vol. 18, no. 5, pp. 58–65, 2011.

[83] S. G. Kou and H. Wang, "First passage times of a jump diffusion process," *Applied Probability Trust Advances in applied probability*, vol. 35, no. 2, pp. 504–531, 2003.

[84] H. Kobayashi, "Application of the diffusion approximation to queueing networks I: Equilibrium queue distributions," *Journal of the ACM (JACM)*, vol. 21, no. 2, pp. 316–328, 1974.

[85] A. Farbod and T. D. Todd, "Resource allocation and outage control for solar-powered WLAN mesh networks," *IEEE Transactions on Mobile Computing*, vol. 6, no. 8, pp. 960–970, 2007.

[86] S. Roy, H. Pucha, Z. Zhang, Y. C. Hu, and L. Qiu, "On the placement of infrastructure overlay nodes," *IEEE/ACM Transactions on Networking*, vol. 17, no. 4, pp. 1298–1311, 2009.

[87] S. Saengthong and S. Premrudeepreechacham, "A simple method in sizing related to the reliability supply of small stand-alone photovoltaic systems," in *Proc. of IEEE PVSC*, 2000, pp. 1630–1633.

[88] X. Zhang, Z. Zheng, Q. Shen, J. Liu, X. Shen, and L.-L. Xie, "Optimizing network sustainability and efficiency in green cellular networks," *IEEE Transactions on Wireless Communications*, vol. 13, no. 2, pp. 1129–1139, 2014.

[89] Z. Zheng, X. Zhang, L. X. Cai, R. Zhang, and X. Shen, "Sustainable communication and networking in two-tier green cellular networks," *IEEE Wireless Communications*, vol. 21, no. 4, pp. 47–53, 2014.

[90] Y. Shi, L. Xie, Y. T. Hou, and H. D. Sherali, "On renewable sensor networks with wireless energy transfer," in *Proc. of IEEE INFOCOM*, 2011, pp. 1350–1358.

[91] Z. Zheng, L. X. Cai, R. Zhang, and X. Shen, "RNP-SA: Joint relay placement and subcarrier allocation in green radio communication networks with sustainable energy," *IEEE Transactions on Wireless Communications*, vol. 11, no. 10, pp. 3818 – 3828, 2012.

[92] EARTH. [Online]. Available: https://www.ict-earth.eu/

[93] GREENRADIO. [Online]. Available: http://www.mobilevce.com/green-radio

[94] Global mobile statistics 2013. [Online]. Available: http://mobithinking.com/mobile-marketing-tools/latest-mobile-stats

[95] OPERANET. [Online]. Available: http://www.opera-net.org/default.aspx

[96] A. Sayegh, T. D. Todd, and M. Smadi, "Resource allocation and cost in hybrid solar/wind powered WLAN mesh nodes," *Wireless Mesh Networks: Architectures and Protocols*, pp. 167–189, 2007.

[97] Renewables 2011: Global Status Report. [Online]. Available: http://www.ren21.net/Portals/97/documents/GSR/GSR2011_Master18.pdf

[98] C. Han, T. Harrold, S. Armour, I. Krikidis, S. Videv, P. M. Grant, H. Haas, J. S. Thompson, I. Ku, C. Wang, T. A. Le, M. R. Nakhai, J. Zhang, and L. Hanzo, "Green radio: radio techniques to enable energy-efficient wireless networks," *IEEE Communications Magazine*, vol. 49, no. 6, pp. 46 – 54, 2011.

[99] T. Han and N. Ansari, "On optimizing green energy utilization for cellular networks with hybrid energy supplies," *IEEE Transactions on Wireless Communications*, vol. 12, no. 8, pp. 3872–3882, 2013.

[100] H. Min, W. Seo, J. Lee, S. Park, and D. Hong, "Reliability improvement using receive mode selection in the device-to-device uplink period underlaying cellular networks," *IEEE Transactions on Wireless Communications*, vol. 10, no. 12, pp. 413 – 418, 2011.

[101] K. Doppler, M. Rinne, C. Wijting, C. B. Ribeiro, and K. Hugl, "Device-to-device communication as an underlay to LTE-Advanced networks," *IEEE Communications Magazine*, vol. 47, no. 12, pp. 42 – 49, 2009.

[102] E. Altubaishi and X. Shen, "Performance analysis of spectrally efficient amplify-and-forward opportunistic relaying scheme for adaptive cooperative wireless systems," *Wireless Communications and Mobile Computing (Wiley)*, July 2013.

[103] W. Su, A. Sadek, and K. Liu, "SER performance analysis and optimum power allocation for decode-and-forward cooperation protocol in wireless networks," in *Proc. of IEEE WCNC*, 2005, pp. 984–989.

[104] Y. Zhao, R. Adve, and T. J. Lim, "Improving amplify-and-forward relay networks: optimal power allocation versus selection," in *Proc. of IEEE ISIT*, 2006, pp. 1234–1238.

[105] S. Kadloor and R. Adve, "Relay selection and power allocation in cooperative cellular networks," *IEEE Transactions on Wireless Communications*, vol. 9, no. 5, pp. 1676–1685, 2010.

[106] S. Chen, W. Wang, and X. Zhang, "Performance analysis of multiuser diversity in cooperative multi-relay networks under Rayleigh-fading channels," *IEEE Transactions on Wireless Communications*, vol. 8, no. 7, pp. 3415–3419, 2009.

[107] H. Zhang, P. Hong, and K. Xue, "Mobile-based relay selection schemes for multi-hop cellular networks," *IEEE Journal of Communications and Networks*, vol. 15, no. 1, pp. 45–53, 2013.

[108] S. S. Ikki and M. H. Ahmed, "Performance analysis of adaptive decode-and-forward cooperative diversity networks with best-relay selection," *IEEE Transactions on Communications*, vol. 58, no. 1, pp. 68–72, 2010.

[109] M. Zaeri-Amirani, S. Shahbazpanahi, T. Mirfakhraie, and K. Ozdemir, "Performance tradeoffs in amplify-and-forward bidirectional network beamforming," *IEEE Transactions on Signal Processing*, vol. 60, no. 8, pp. 4196–4209, 2012.